**U.S. Department of Justice**
Federal Bureau of Investigation

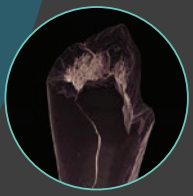

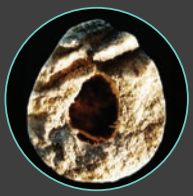

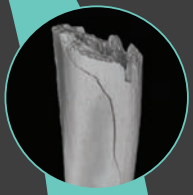

# A GUIDE TO FORENSIC FRACTOGRAPHY OF BONE

# A GUIDE TO FORENSIC FRACTOGRAPHY OF BONE

**AUTHORS:**

**Angi M. Christensen**, PhD, D-ABFA
Federal Bureau of Investigation (FBI) Laboratory

**Mariyam I. Isa**, PhD
Texas Tech University

**Michael A. Smith**, PhD
FBI Laboratory

**Joseph T. Hefner**, PhD, D-ABFA
Michigan State University

**Hugh E. Berryman**, PhD, D-ABFA
Middle Tennessee State University

**Ian S. Saginor**, PhD, PG
FBI Laboratory

**Jodi B. Webb**, MA
FBI Laboratory



**Reprints**
*Printed copies of this guide are available upon request. Please contact Angi Christensen at* amchristensen@fbi.gov.

**Acknowledgements:**
*We would like to thank George Quinn for his assistance reviewing sections of the guide, and for the use of images from his NIST Recommended Practice Guide for Fractography of Ceramics and Glasses, which also served as a model and inspiration for this guide. We are also grateful to Christine Kerrick of the FBI Laboratory's Operational Projects Unit for her assistance with formatting and production. The following individuals contributed figures, other content, or assistance: Mary Holden and Pepperdine University, Mary Mani and Stephanie Hill of the FBI Laboratory, Kaitlyn Fulp of Texas Tech University, Ethan Watrall of the Michigan State University (MSU) Digital Heritage Imaging & Innovation Laboratory, Rhian Dunn of the MSU Forensic Anthropology Laboratory, Todd Fenton of the MSU Forensic Anthropology Laboratory, Rachel Radandt of the MSU Bioarchaeology Laboratory, and Laurel Freas. Finally, many thanks to our other colleagues, friends, and loved ones who provide guidance, feedback, assistance, and moral support.*

Version 1.0, 08 February 2022

# A GUIDE TO FORENSIC FRACTOGRAPHY OF BONE

# 1 Introduction to forensic fractography of bone

Skeletal trauma analysis is an important role of forensic anthropologists in the medicolegal system. Skeletal fracture patterns and features are often examined to assess trauma type (e.g., blunt, sharp, or projectile), as well as other aspects of the traumatic event (such as timing, direction, and magnitude). Traditionally the focus of these analyses centered on the overall fracture pattern of the bone including fragment shape and the intersection of fracture margins, often emphasizing categorization of fractures into discrete types.

Forensic skeletal trauma analysis has experienced a recent shift from emphasizing typological and morphological descriptions to interpretation based on bone's mechanical properties and its response to **force** and different **loading** regimes. One example of this is the recent introduction of the science of fractography to the forensic analysis of skeletal fractures. As a relatively new approach in forensic anthropology, fractography is not yet widely known or understood, and is not commonly taught as part of forensic anthropological educational or training programs. For these reasons, practitioners may feel reluctant to apply fractography in their forensic examinations. This guide will make forensic fractography of bone more accessible to practitioners.

This guide is organized into seven sections. The remainder of Section 1 introduces the science of fractography, how it is used in the analysis of material **failures**, its applications to bone and anthropology, and a brief overview of bone biomechanics and fracture mechanics. Section 2 addresses the origins of fractures, and Section 3 reviews cracking, branching, and fragmentation patterns. Section 4 covers fracture surface features, and how the presence and orientation of these features relate to crack propagation. Section 5 describes the procedures, tools, and equipment that can be used to examine bone fractures. Section 6 discusses possible future research, technologies, and quantified approaches in forensic

fractography, which are intended to challenge and inspire readers to continue research in this area. Section 7 offers some summary guidance as well as some additional case and experimental examples, and a glossary of terms is provided in Section 8. As new knowledge is gained, it is intended that this guide will be continually updated.

### 1.1 Purpose of this guide

The purpose of this guide is to familiarize the user with the science of fractography and how it can be used to examine and interpret skeletal fractures. Moreover, this guide will acquaint readers with the tools and equipment needed to effectively apply fractography to bone. Most of all, this guide aims to demonstrate that with a bit of background information, a few basic tools, and a little practice, fractography can be used to enhance the anthropologist's understanding of trauma events and thereby improve the quality of their forensic products.

### 1.2 Fractography

**Fractography** broadly refers to the study of **cracks** and **fractures** in a material in order to understand the cause of its failure (where a crack is a plane of separation, and a fracture is the separation of the structure into two or more pieces, so a crack might be a fracture in progress). Among the first applications of failure analysis may have been the production of stone tools by controlled fracture, which demonstrates knowledge in selecting stones with favorable fracturing properties, and how to shape them by direct impact and pressure flaking. One of the first documents to discuss macroscopic fractographic techniques was published in 1540 and was used as a quality control practice for ferrous and nonferrous metal working (Biringuiccio 1540). The invention of the optical microscope in 1600 was a significant development for fractography, which became more extensively utilized by metallurgists in the 1700s, notably led by the studies of Réaumur (1722). The term "fractography" was

first used in 1945 for the examination of cleavage fracture surfaces (Zapffe & Clogg 1945). The science of fractography was further revolutionized by the development of the transmission electron microscope (TEM) and scanning electron microscope (SEM) in the 1930s (Lynch & Moutsos 2006), leading to a large number of fractography studies in the 1960s and 1970s.

### *1.2.1 Fractography definitions and uses*

The American Society for Testing and Materials (ASTM) defines fractography as *the means and methods for characterizing fractured specimens or components* (ASTM Standard 1322, 2015). Fractography can also be defined as *the study of fragments and their interpretation in terms of material properties and conditions leading to fracture* (Fréchette 1990). Although some define fractography more narrowly as *the study of fracture surface morphology and its relationship to crack propagation* (Hull 1999), others consider fractography more broadly as *the study of all evidence of material failure, including those relating to the fracture surface as well as fragment size, shape, and breakage patterns* (Quinn 2016), or *the study of fractures in materials, components, and structures* (Quinn 2020).

In practical terms, fractography is a tool for studying material failure. A principal tenet of fractography is that the analysis of cracks and fractures can reveal information about how, why, and where a failure occurred and a crack traveled. In brittle materials, a crack usually originates at a discontinuity or flaw. The stress that creates and drives a discontinuity to propagate may be thermal, chemical, or mechanical (Fréchette 1990). Fractography can help determine the point of **origin** of a fracture, and can help identify the presence of flaws, regions of localized stress concentrations, and even deliberate damage, providing insight into the causes of failure (Hull 1999). Fractography is often applied in studies of failure of engineering structures and products, which can help to ensure future reliability and safety of materials (Hull 1999).

Identification of the type of fracture and the micromechanics involved also gives an indication of the types and magnitudes of the stresses that accompanied the failure and the overall nature of the failure. Fractography can also reveal details of crack growth rate and environmental conditions (such as temperature) and identify material limitations. The path of fracture propagation is dependent on the material's microstructure, so studying the fractured surface of a material can reveal information about the microstructure and mechanical properties of the material.

### *1.2.2 Forensic fractography*

Fractography is used in a wide range of forensic applications as well. Commonly examined materials in forensic contexts include glass, ceramics, metals, and plastics. Analysis of fractured window glass provides information on the nature and order of a series of impacts to the windows. For example, it is possible to determine the order and direction of a series of bullet impacts on a windshield by studying the intersections of cracks from different events and other properties of the impact sites. Toolmark examiners may compare the correspondence of fracture features on two items to determine whether they are pieces of the same item.

Fractography can be incredibly informative in failure analysis and forensic engineering. Material scientists at the National Transportation Safety Board (NTSB) use fractography to investigate transportation disasters such as plane crashes. Examination of a fracture surface can provide evidence as to whether fracture was rapid (e.g., from overload) or occurred over a prolonged period of time (e.g., fatigue, creep), whether corrosion and/or elevated temperature was significantly involved, whether fracture was hastened by a design flaw (e.g., improperly radiused notch), or improper usage. Fractography and failure analysis also feature prominently in civil litigation involving product liability suits for all manner of consumer products from gas cans to hip implants.

Similar types of fractographic analysis are performed in criminal investigations as well. The practice has a prominent place in industry worldwide and is essential to prevent further failures and protect against economic losses.

Forensic fractography of bone is still in its infancy, but as will be demonstrated in this guide, it can provide incredibly useful information to the practicing forensic anthropologist.

### *1.2.3 Fractography resources*

Although primarily issuing from an engineering perspective, there are several helpful resources available for forensic practitioners interested in learning more about fractography. Fréchette's *Failure Analysis of Brittle Materials* (1990) is an excellent reference focusing on both theory and practice of assessing crack propagation. The *NIST Recommended Practice Guide: Fractography of Ceramics and Glasses* (Quinn 2007, 2016, 2020) is a comprehensive work focusing on ceramic and glass, which also includes an extensive bibliography. The American Society of Materials (ASM) *Handbook on Failure Analysis and Prevention* (2002) introduces failure analysis with an emphasis on root cause analysis and failure prevention and includes a summary of the most important research that had been conducted at the time of its publication. Although these references do not emphasize crack propagation in bone, they will give the reader a more thorough understanding of the study of failure in brittle materials.

## 1.3 Bone fractography

The application of the science of fractography to the study of bone is not new. Several studies of human and non-human bone have used fractography to learn more about bone's biomechanical properties and how bone fails (e.g., Braidotti et al. 2000; Corondan & Haworth 1986; Kimura et al. 1977; Martens et al. 1986; Pope & Outwater 1972; Vashishth et al. 2000; Wise et al. 2007). Fractographic studies of bone can also be found in relation

to surgical implants and other clinical matters (e.g., James et al. 1992; Topoleski et al. 1990). Anthropological and odontological applications of fractography are also not new. Fractography has been used in the study of stone and bone tool manufacture (Johnson 1985; Tsirk 2010; Tsirk & Parry 2000) and has also been used in the study of failure of dental tissues (Bajaj & Arola 2009; Bajaj et al. 2010; Quinn 2005) and dental restorative materials (Øilo et al. 2014; Scherrer et al. 2008, 2009; Thompson et al. 1994).

### *1.3.1 Fracture surfaces and the postmortem interval*

Studies have examined fracture surface differences in wet versus dry bone and changes associated with increasing postmortem interval. Macroscopic differences in fracture surface topography have been noted in fresh versus dry bone (Johnson 1985; Symes et al. 2014). In another study, geographic information systems (GIS) were used to examine relative fracture surface relief on pig bones fractured in perimortem and various postmortem timeframes, finding that fresher bones exhibited greater surface topography than bones broken later (Hentschel & Wescott 2015). In one study involving wet and dry bovine femoral head samples in tensile loading, scanning electron microscope (SEM) micrographs showed that wet bone behaves more like a ductile material, while dry samples were more like brittle composites (Braidotti et al. 2000). These differences can likely be attributed to the loss of organic material as bone dries and becomes more brittle. The relationship of fracture surface roughness to material toughness has been documented in several studies (Piekarski 1970; Saha & Hayes 1977; Vashishth et al. 2000; Wise et al. 2007), and changes as the bone becomes drier.

### *1.3.2 Fracture surfaces and the propagating crack front*

Changes in fracture surface morphology across an individual fracture surface have also been noted in the anthropological literature. Tensile surfaces of fracture initiation regions have

been described as "mottled," "billowy," "wavy," or "smooth," while compression surfaces appear more "jagged," "splintery," "sharp," or "saw-toothed," with "peaks and valleys" (Emanovsky 2015; Galloway & Zephro 2005; Isa et al. 2018; L'Abbé et al. 2019; Rainwater et al. 2019; Symes et al. 2012). The transverse sections of butterfly fractures were observed to be smoother than those surfaces after the bifurcation, which was attributed to higher energy (Martens et al. 1986). The roughness of bone fracture surfaces was found to correlate with crack propagation speed (Behiri & Bonfield 1980). While not described as such at the time, these observations were a form of bone fractography.

### *1.3.3 Fractography and forensic anthropological examinations*

Forensic questions related to skeletal fractures might include: How did this bone break? Why did it break? What type of force was applied? How was the force applied? Where (anatomically) was force applied to bone? How much force was applied to the bone? From which direction did the force originate? In the case of multiples fractures, in what order did they occur? The way force is applied to bone is often referred to by forensic anthropologists as the **trauma mechanism**. Trauma mechanism is typically categorized as being blunt, sharp, high-velocity, or thermal. Although these categories can be descriptive and helpful to understanding the trauma event, the forces that produce skeletal trauma occur along a continuum and not in discrete categories (Spatola 2015). Two important variables relevant to trauma mechanism are the surface area of the load and the loading rate. For example, the difference between what anthropologists refer to as "blunt" and "sharp" trauma is the surface over which the load is applied. Sharp trauma results from a load applied by a tool with very small surface area (e.g., the blade of a knife), while blunt trauma results from loads applied over larger surface areas. The difference between "high velocity projectile" and other categories of trauma is the loading rate and impact surface

area. High velocity projectile trauma results from a force applied by an object moving at a very high rate of speed and impacting a small surface area (e.g., gunshot or explosive-related impacts). At their extremes, trauma mechanisms are often more apparent, but they can sometimes be difficult to discern. These categorizations also do not always fully consider the mechanics of how the bone actually failed.

Fractography can help provide a better understanding of bone failure from an engineering perspective. Recently, consideration has been given to applying the principles of fractography to forensic anthropological questions. Importantly, bone is a structurally complex, naturally occurring, composite material and its fracture behavior is more nuanced than that of many standard engineering materials; however, the principles of fractography still apply. Several studies have demonstrated the utility of fractography for interpreting aspects of skeletal fractures, specifically crack propagation direction (which can inform how and where the load was applied). In an assessment of femora fractured experimentally in 3-point bending, anthropologists and fractographers analyzed the presence and orientation of fracture surface features and found them to be reliable indicators of fracture initiation and propagation, as well as finding very strong agreement between assessors (Christensen et al. 2018a). This study also investigated optimal examination conditions for fractographic analysis of bone, some of which are discussed in Section 5. In a review of an autopsy sample of blunt trauma cases, fractographic features were found to correlate well with autopsy soft tissue and radiologic findings, as well as with traditional forensic anthropological skeletal trauma analyses (Love & Christensen 2018). A study of complex fractures found fractography features to support fracture propagation ground truth as documented through high-speed video (Isa et al. 2020). It has also been shown that some fractographic features can be seen in CT scans (Christensen & Hatch 2019; Christensen

& Decker 2020; Machin et al. 2021), suggesting that fractography may be applicable to a broader scope of contexts than dry bones. Most studies have focused on fractures resulting from blunt trauma, but some fracture surface features have also been noted in association with American Civil War projectile traumas (Lillard & Christensen 2020), and projectile impact fracture mechanisms have been elucidated through the use of high-speed video and micro-CT (Rickman & Shackel 2019a; 2019b). Although there is much more to be learned about forensic fractography of bone, this guide will draw upon these findings as well as the wealth of information related to fractography of other materials.

## 1.4 Bone biomechanics and fractures

Applying fractography requires a working knowledge of the microstructure of the subject material, as well as some knowledge of **fracture mechanics**, a discipline within mechanical engineering dealing with how cracks respond to loads. Cracks that are studied as part of a fractographic analysis initiate and propagate in response to stresses and strains, so it is helpful to have a good understanding of mechanics generally and bone **biomechanics** specifically. A thorough review of fracture mechanics is beyond the scope of this guide, but some basic principles will be discussed as they apply to bone. Readers interested in a more in-depth study of fracture mechanics are directed to sources such as *Fracture Mechanics: Fundamentals and Applications* (Anderson 2005) or *Guide to Fractography of Ceramics and Glasses* (Quinn 2020). More technical aspects of bone biomechanics can also be found in sources such as *The Bone Biomechanics Handbook* (Cowin 2001), *Bones: Structure and Mechanics* (Currey 2013), *Skeletal Tissue Mechanics* (Martin et al. 1998), *Biomechanics of Hard Tissues* (Öchner & Ahmed 2011), and *Mechanical Properties of Bone* (Evans 1973).

### *1.4.1 Stress and strain*

In forensic analysis of bone, the failures of interest are typically fractures resulting from mechanical stress in the form of trauma.

Skeletal trauma results from the application of some type of force to the bone. The relationship between force and deformation is one of the primary principles in understanding bone fracture mechanics. Materials can be categorized based on their ability to undergo deformation and absorb energy before failure. Brittle materials undergo little plastic (permanent) deformation and have low energy absorption before failure. Ductile materials have high energy absorption before failure and may experience extensive plastic deformation before fracture. The distinction between brittle and ductile materials is not always clear, and external factors such as the ambient pressure, temperature, and speed of deformation can affect a material's behavior. For example, many materials exhibit more ductile behavior when subjected to high temperatures, high pressures, and low strain rates, while low temperatures, low pressures, and high strain rates may encourage more brittle behavior.

A material's reaction to **loading** can be visualized as a load-deformation curve, showing a material's response to force as a function of **stress** and **strain**, where stress is the load per unit area, and strain is the change in dimension (relative deformation, i.e., a change in length compared to an initial length) of a loaded body (Martin et al., 1998), while the slope of the line represents the elastic modulus. Figure 1.1 shows the stress-strain curve for a typical brittle material, a typical ductile material, and bone. The linear portion of the curve largely represents **elastic** (transient) **deformation** that is recovered when the object is unloaded. Figure 1.2 shows a more detailed stress-strain curve for bone including elastic and plastic deformation zones. Because bone is composed of both a brittle material (hydroxyapatite mineral) and ductile material (collagen), it behaves somewhere between a brittle and ductile material. Cortical bone, like most materials, is more brittle at higher strain rates (Morgan et al. 2018). Strain in bone has been reported to rarely exceed about 3% (Currey, 1970).

*Figure 1.1:*
*Stress-strain curves for typical brittle materials (left), ductile materials (middle), and bone (right)*

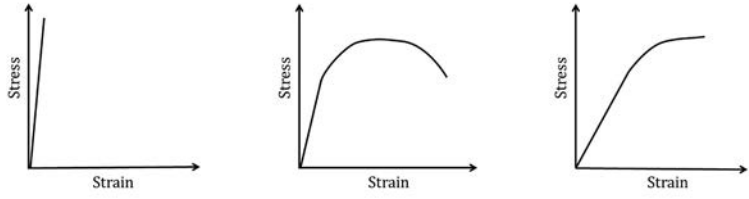


*Figure 1.2:*
*Stress-strain curve for bone [from Christensen et al. 2019]*

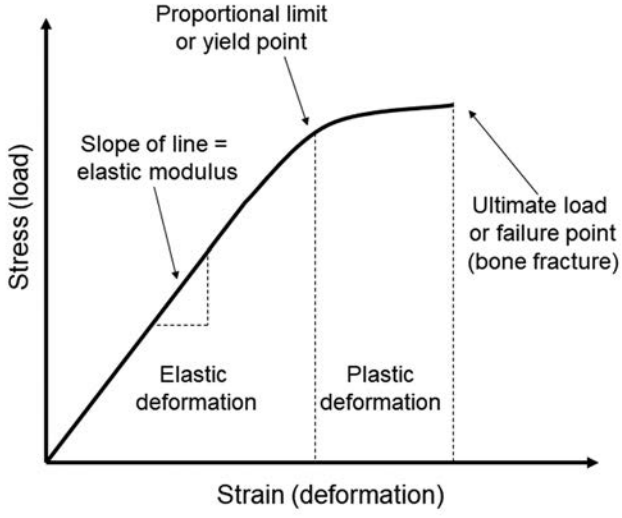


Load and deformation are linearly proportional for materials such as metals, plastics, and bone, until the yield point is reached, at which point the slope is reduced. The yield point designates the load at which appreciable, permanent (plastic) deformation begins. Very brittle materials such as ceramics and glasses do not yield

before fracture and their stress-strain curves are therefore linear. More ductile materials such as metals and bone will be linearly elastic until the yield point. Elastic deformation is a temporary, recoverable deformation; when the force is no longer applied, the material will go back to its original shape. When loaded beyond the yield point, the material will respond through plastic deformation, which causes a permanent change to the material structure. With increasing load, the ultimate load or failure point is eventually reached, and it is at this point that fracture occurs. The load at the failure is used to calculate a material's tensile **strength**. The area under the curve is a measure of the amount of total energy needed to cause a fracture and corresponds to the material's energy absorption or **toughness**. Toughness is an important bone biomechanical property because a tough bone is more resistant to fracture. Factors including water content, subject age, and drug use have been shown to reduce bone toughness (Nazari et al. 2009; Nyman et al. 2013; Park et al. 2019; Wang et al. 2002). Bone is also a **viscoelastic** material that is stiffer when loaded rapidly than when loaded slowly. It therefore deforms less when loaded at higher velocities.

**Residual stress** refers to internal stress remaining present in a material after an original stress has been removed. Residual stresses can be involved in impacts, where cracks appear at unloading, driven by residual tensile stresses that remain locked in the elastic-plastic structure after the load is removed; prior to full unloading, tensile stress is partially neutralized by compressive stress induced by contact pressure (Kadin et al. 2019). Residual stress can cause warping or distortion in a structure. Residual stress can also be created when there are thermal differentials in portions of a structure or the interior versus exterior of a structure. There can also be residual stresses at the microstructural level, such as between grain boundaries or between an inclusion and the matrix. Residual stress may be either beneficial or harmful to a structure depending upon circumstances and can be highly variable within that structure.

Residual stresses may influence the appearance of fracture features and patterns allowing their presence to be inferred.

### *1.4.2 Bone microstructure*

Once a fracture has initiated, crack propagation is highly dependent on the material's microstructure (Corondan & Haworth 1986; Hull 1999; Kimura et al. 1977). Many principles of fractography have been developed from the study of glass, which is considered an ideal medium for study of brittle materials because it is uncomplicated by directional cracking behavior (Fréchette, 1990). The same cracking principles also apply to more structurally complex materials but may be more difficult to identify and interpret.

Bone has a very complex microstructure. Unlike many manufactured materials, bone is a highly hierarchical composite (Olszta et al. 2007, Weiner & Wagner 1998), consisting primarily of hydroxyapatite and collagen. The constituents of bone are organized into primary lamellar bone and osteons. Bone is an **anisotropic** material and therefore has different mechanical properties in different directions. Osteonal bone is considered transversely **isotropic** because it has the same properties in transverse directions but has different properties in the longitudinal direction (Reilly & Burstein 1975). Bone toughness is strongly related to this arrangement of lamellae and osteons (Currey 1962; Evans & Riolo 1970; Evans 1973; Kimura et al. 1977). The alignment of osteons in cortical bone provides anisotropic toughening such that a crack propagating transversely (perpendicular to osteons) is more likely to twist and deflect than a longitudinal crack (parallel to the osteons) (Morgan et al. 2018). This configuration also results in bone behaving mechanically like a fiber-reinforced composite, where lamellar bone represents the "matrix" and osteons represent the "fibers" (Burr et al. 1988; Corondan & Haworth 1986). Bone is somewhat different in that fiber-reinforced composites do not

have connections between the different constituents, whereas in bone the fibers and matrix are interconnected and composed of the same material (Corondan & Haworth 1986). Bone fractures, however, have been noted to share features with other composites such as fiber (osteon) "pull-out" (Behiri & Bonfield 1980; Martens et al. 1986; Pope & Outwater 1972).

Once initiated, cracks will propagate in order to dissipate **strain energy** by creating new surfaces (Griffith 1920), eventually stopping through deceleration, often due to changes in the stress fields, intersecting another crack, or venting at a structure's edge. Cracks will propagate along weak interfaces when they provide a lower energy fracture path than the surrounding material (Hull 1999). Some materials, including bone, will therefore tend to fracture along grain boundaries. Bone's "grain" is well understood from fractography and other studies of bone architecture (e.g., Benninghof 1925; Dempster 1967). The interfaces between lamellae in bone are weak (Piekarski 1970) and there is a preference for cracks to propagate between lamellae (Pope & Outwater 1972). This explains why bone often cracks longitudinally when drying. In forensic contexts, transverse fractures resulting from trauma are more commonly observed, and these require the application of large forces since bone is considerably tougher transversely.

Bone's microstructural arrangement has several features that enhance resistance to failure. Although the weak interfaces between lamellae facilitate longitudinal fracture, they actually serve as a crack-stopping mechanism transversely (Piekarski 1970; Koester 2008). The cement line, which represents the boundary between an osteon and the surrounding bone, may impede crack growth by providing a relatively ductile, energy absorbing interface with the surrounding bone matrix (a desirable feature in fiber-reinforced composites subjected to repeated loading) (Burr et al. 1988). The interfaces may also act to redirect crack propagation. Discontinuities

in bone are therefore generally seen to enhance fracture resistance characteristics rather than impair them (Piekarski et al. 1970; Pope & Outwater 1972). Low strain rates produce fractures that tend to preferentially follow interlamellar boundaries, with fractures moving up the side of fibers; with increased strain the crack moves fairly indiscriminately across all constituents (Pope & Outwater 1972).

### *1.4.3 Loading regimes*

Fracture initiation and propagation are related to the force applied to or load experienced by the material (while there are slight differences in the purest sense, the terms "force" and "load" are often used interchangeably). There are five different types of loads that can act on a structure including a bone (Figure 1.3). **Tension** is a result of opposing forces acting to stretch a structure apart or lengthen it. **Compression** is a result of opposing forces acting to squeeze or compress a structure. **Shear** loading results from adjacent forces in opposite directions. **Bending** creates a stress gradient with maximum tension at the convex surface, maximum compression on the opposite (concave) surface, and zero stress somewhere in the middle (the **neutral axis**, where tensile stresses are balanced by the compression stresses on the opposite side). **Torsion** involves rotation or twisting. Bending and torsion involve **moments of force**, resulting from force applied to a rotational system at a distance from the axis of rotation. A material's strength typically varies by the type of load. Many materials, including bone, have high compressive and relatively lower tensile strengths, and typically fail under tension. In the longitudinal direction, human femoral cortical bone is strongest under compression, moderately strong under tension, and weakest under shear loading; in the transverse direction, bone is strongest under compression and weakest under tension (Morgan et al. 2018). Forces do not always occur in isolation, and traumatic events affecting bones may involve various loading types. In addition to trauma-related loads, bones are continually subjected to a variety of forces arising from gravity,

body movements, impacts, and other forces exerted on the skeleton by the viscera (Evans 1973), which may also affect failure. During normal physical activities, bone is subjected to strains of 0.1-1.0%; during impact loading strains can be more than 10 times this rate (Morgan et al. 2018).

*Figure 1.3:*
*Loading regimes [modified from Christensen et al. 2019]*

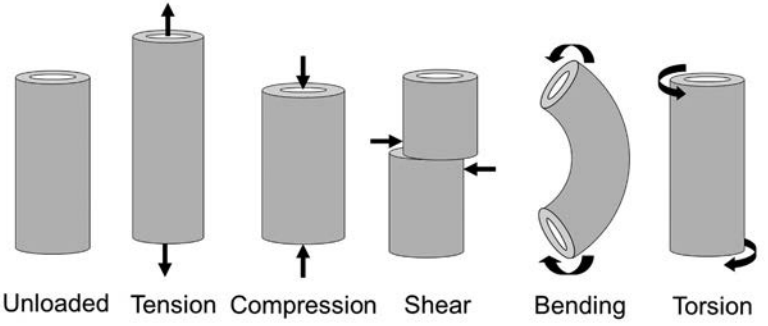


Stress is relevant to loading regimes and is commonly used to describe the severity of the loading on the material since it takes into account the size and geometry of the structure. Stresses and strains are affected by structure geometry and cross-sectional area and vary with different loading regimes. In the simplest loading regimes of tension, compression, and shear as pictured in Figure 1.3, the stresses are constant through the structure due to the simple, uniform loading condition. For uniform tension, stress is calculated as the applied force divided by the cross-sectional area. Consider a force of 1000 pounds applied to two different sized rods. If one rod has a cross sectional area of 1 $in^2$, the force creates a stress of 1000 $lbs/in^2$ = 1,000 psi (pounds per square inch). If the same force is applied to a rod with a cross sectional area of 0.1 $in^2$, the stress is 1000 lbs/0.1 $in^2$ = 10,000 psi, and the rod will be more likely to break depending upon its absolute strength. Stresses and strains can also vary with location in a structure. In bending, for

example, one side of the structure is in tension while the other side is compressed. The magnitude of these stresses depends upon the distance from the neutral axis. Many structures are weaker in tension and therefore typically fail on the side under tension. Failure originating from true compression (in bone as well as other materials) is rare and usually involves preexisting flaws/inclusions (Quinn 2020).

Fractures are also affected by the amount and rate of the applied force. **Magnitude** refers to the amount of force applied. Greater forces result in higher stresses, and the material may be unable to dissipate the energy through a single crack and the crack may therefore branch. When large magnitude forces are applied to bone, fracture severity typically increases and may result in **comminution** or fragmentation from multiple branching events. The surface area over which the force is applied will affect how the material responds. Deformation is easier to resist if the same load is applied over a large surface area versus a small surface area; the greater the surface to which a given load is applied, the less force per unit area (stress) that is applied to the structure. Loading rate also affects failure. **Dynamic loads** are applied suddenly and at relatively high rates of speed. This type of loading is most often responsible for fractures examined in forensic contexts. **Static loads** are constant with time; **quasi-static** loads are from forces applied slowly. Static and quasi-static loading are often used in experiments aimed at testing material properties. Bone can resist deformation to greater load before failure if the load is applied slowly rather than rapidly because it has more time to absorb the energy associated with the loading (Evans 1973).

### *1.4.4 Crack growth and fracture toughness*

Although a thorough discussion of fracture mechanics is beyond the scope of this guide, a brief overview of cracks and crack growth is warranted. Fractures in bones and other brittle materials involve

cracks. These cracks--which may be macroscopic and visible, or microscopic in nature--may already exist, or they may develop under loading. If there is a preexisting crack in a structure, the larger that crack is, the weaker the structure is likely to be. Fracture is often a matter of the application of enough force to cause a crack to propagate. If a structure has a crack but there is no stress acting on it, it will not fracture; if the structure experiences high loads but the cracks are very small, they may not propagate. For all classes of materials, fracture may be the result of a single event that creates and propagates a crack causing breakage, or it may be a series of events involving the introduction of a crack and then subsequent loading(s) that causes it to propagate.

**Fracture toughness** refers to the critical condition for the onset of rapid crack propagation. The greater the fracture toughness, the more resistant the material is to crack growth. In some materials this property has a specific value, for example, 0.75 $MN/m^{1.5}$ for glass, 3 to 12 $MN/m^{1.5}$ for ceramics, 0.5 to 3 $MN/m^{1.5}$ for polymers, and 30 $MN/m^{1.5}$ or more for some types of cast iron (Ashby 2011). For many materials crack growth resistance is also dependent on the environment, for example, the fracture toughness of glasses is lower in the presence of water, even in the form of humidity in air. The fracture toughness of bone is a complex calculation since bone is anisotropic, but reported values for the fracture toughness of cortical bone range from 1.8 to 2.3 $MN/m^{1.5}$ (Bajaj 2009; Nalla et al. 2005a,b; Vashishth et al. 1997) to as high as 2 to 5 $MN/m^{1.5}$ (Ritchie et al. 2008). The fracture toughness of human tooth enamel varies with location through the enamel thickness and is reportedly from 0.67 to 2.0 $MN/m^{1.5}$ (Bajaj et al. 2010; Bajaj & Arola 2009), with tooth dentin varying from 1.3 to 1.7 $MN/m^{1.5}$ (Bajaj & Arola 2009).

A plot of crack growth resistance is referred to as an **R-curve** and can be discussed in terms of **stress intensity factors**. The plain stress, stress intensity (denoted as $K_I$) is used to describe the stresses ahead of the tip of a crack that is being pulled open

in tension (Figure 1.4). Stress intensity is a function of the stress, the crack size, and geometry factors. A crack will grow when any combination of these factors causes the stress intensity at a crack tip to reach the critical value greater than the fracture toughness of the material (denoted as $K_{IC}$).

*Figure 1.4:*
*Loading conditions and the crack front; a load P is applied to an object creating stresses; the stress flields are shown immediately in front of the crack tip*

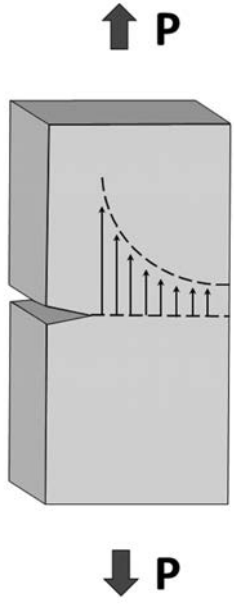


In many materials (including bone) there is a rising R-curve effect whereby as a crack propagates, the resistance to further crack propagation increases, and it requires higher and higher applied energetic gain to achieve further crack extension. Rising R curves are caused by a crack interacting with a material's microstructure resulting in localized plasticity. These interactions can impede crack propagation, but eventually they reach a limit, called the R-curve

plateau, and no further toughening occurs. Once a crack reaches the material's critical stress intensity, $K_{IC}$, it will grow, become unstable, and cause fracture.

### 1.5 Summary

Fractography is a tool for studying and understanding material failure. Bone is a material that obeys physical laws, and we can therefore use fractography, fracture mechanics, and other engineering principles to better understand the fracture event. A thorough knowledge of bone's microstructure and responses to loading will enhance this understanding.

The complexity of the composition of bone makes it challenging from an engineering perspective. Many common stress solutions for structures have been derived assuming the material is homogeneous and isotropic. The analysis of stresses and strains in a structure like bone can therefore be complex. Many of the engineering concepts in this guide are simplified in the interest of addressing more practical applications in forensic anthropological contexts. However, even a basic understanding of these principles can improve a practitioner's understanding of the trauma event. For complex problems and loading conditions, consultation with an engineer may be beneficial.

Importantly for the examination of bone fractures (and unlike many manufactured materials), biological variation can result in differences in bone's biomechanical properties and therefore patterns of failure. There are differences in bone composition and geometry between sexes, across populations, with age, as well as in association with pathological conditions and individual loading regimes. While many studies have informed our knowledge of biomechanics of bone as a tissue generally, individual variation should be considered in any comprehensive analysis of fractures in a forensic context.

# Fracture Origins

## 2 Fracture origins

A **fracture origin** refers to the point where a fracture begins. This location is a localized weak point or **flaw** in the material. The term "flaw" does not necessarily refer to something negative or improper –brittle materials are imperfect and contain irregularities and inhomogeneities. These can behave as flaws that represent a fracture origin. This section addresses the causes and relative locations of the origins of fractures.

Fractures originate from a variety of sources. Flaws, either on the interior or surface, may consist of inclusions of another material type, or irregularities or voids within the structure. They can result from temperature differentials or be produced by impacts with sharp, blunt, or fast-moving objects. Fracture origins can be time-dependent, with slow crack growth from preexisting flaws, or may occur from repetitive, subcritical loads causing **fatigue failure**. In any case, the fracture origin will be the site with the most vulnerable combination of tensile stress and flaw severity (Quinn 2020).

In brittle materials like ceramics and glass, preexisting flaws from manufacture and processing can act as fracture origins. Flaws can be due to **manufacturing defects**, machining, corrosion, or wear, or there may be contact damage cracks on the surface from a variety of external sources. In bone, microstructural variabilities can act as origins for time- or cyclical-related crack formation. Alternatively, fractures can be large cracks introduced by sudden, unstable, and catastrophic external events such as trauma. In forensic contexts, skeletal fractures generally originate due to sudden impacts (for example, with blunt objects, the ground, a bullet, or a blade). This guide will therefore primarily focus on fracture origins related to impacts. Thermal origins are also briefly addressed.

### 2.1 Fracture origins from impacts

Cracks can be caused by impact or contact between objects causing dynamic crack initiation and propagation. The failure modes operative during impact-related fracture are complex and

depend upon a variety of intrinsic factors (target and impacting material characteristics including elastic properties, geometry, and density) and extrinsic factors (including projectile velocity, mass, striking-surface area, and design) (Fenton et al. 2021; Zukas 1982). Bone presents a particularly complex material for failure analyses due to its hierarchical structure, in which failure can occur on multiple scales (Currey 2013). Despite this microstructural complexity, bone typically exhibits brittle, ceramic-type behavior at high strain rates. Many of the fractography principles involved in failure of ceramics and other brittle materials are therefore informative and relevant to impact failure in bone (see for example, Quinn 2020). Important to understanding impact-related failure, most fractures involve uniaxial or biaxial stress states (or stresses in either one or two dimensions). Impacts, however, involve a triaxial stress state, with stresses in all three directions (Figure 2.1). Impact loading can create single or multiple origins. There can be localized residual stresses at the site of sharp impacts or contact damage (Quinn 2020).

*Figure 2.1:*
*Cross-section of impact site showing triaxial stresses and zone of tension [from Christensen et al. 2021]*

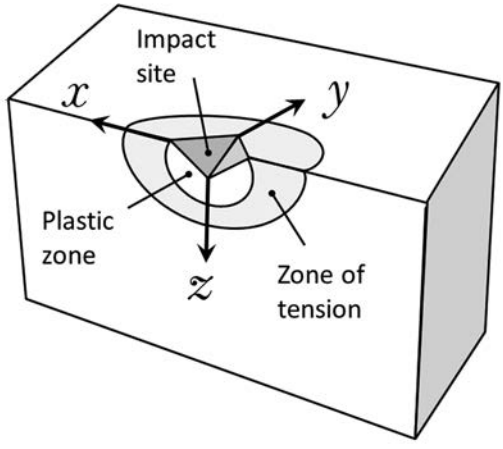

Traumatic impacts to bone are typically categorized as being blunt, sharp, or high velocity in nature. Blunt skeletal trauma is defined as a relatively slow load applied over a relatively large surface area (Berryman & Symes 1998; Passalacqua & Fenton 2012). It may result from a blow from an object (such as a club, hammer, or fist), but also includes deceleration impacts such as transportation accidents or falls from heights. Sharp skeletal trauma is defined as being created by impacts from a tool that focuses stress onto a smaller surface area. These impacts are typically associated with knives and saws but may also include other pointed or beveled tools (DiMaio & DiMaio 2001; Spitz 1993; Symes et al. 1998, 2002). High velocity projectile trauma is characterized by a very rapid application of force over a relatively small surface area, usually supplied by a bullet from a firearm (Berryman & Symes 1998; DiMaio 1993), but could also be from shrapnel from a blast or another very fast-moving small object. As discussed in Section 1 of this guide, these categories can be useful in describing the likely scenario involved in the cause of the fracture, but the loading that creates these traumas occurs along a continuum rather than as discrete types and levels of force, with the appearance of the resulting fracture depending on the force as well as surface area of the impacting interface (Berryman et al. 2017; Kroman 2007).

In forensic assessments of skeletal trauma, fracture origins are typically of interest in understanding the location where a bone was impacted (i.e., from where the force originated). Much work has focused on the relationship between fracture patterns and impact location, such as whether fracture origins are at the location of impact or elsewhere (e.g., Fenton et al. 2021; Gurdjian et al. 1947, 1950; Isa et al. 2018; 2019; Kroman et al. 2011; Powell et al. 2012). The relationship, however, is somewhat more complex. The location of the fracture origin will typically depend on where the tensile stresses are greatest, and therefore is related to a number of factors in addition to impact location including loading regime,

surface area of loading, nature of the two impacting materials, stress concentrators, and structural geometry.

Although it may represent just one part of a fractographic analysis, identification of the fracture origin is a relevant and informative part of the investigation into material failure, often being critical to understanding the cause of failure. Fracture origins can be identified using a number of approaches and by examining several features of the fractured structure. In some materials, the shape of the broken fragments may provide clues about the fracture origin. For example, in fractured tempered glass, it is often possible to find the two fragments adjacent to the origin based on their larger size and distinctive morphology (Figure 2.2). Tempered glass owes its impact resistance to manufacturing treatments that leave its outer surfaces in compression and the interior in tension. When failure in tempered glass is triggered by an impact, a surface crack is driven through the surface compression temper zone and into the interior tensile zone. The glass then catastrophically fractures into many small fragments as the stress differential between the surface and interior of the glass is released. The glass at the origin site cracks with branches forming adjacent polyhedrons that are larger and have a greater number of sides (usually >4) than the other fragments. Fracture origins from impacts may also be evidenced by localized damage and the location of stress concentrators. These will be discussed in the following parts of this section. Other features that can be assessed to identify fracture origins include cracking and branching patterns (see Section 3) as well as the morphology of the fracture surface (see Section 4).

*Figure 2.2:*
*Fracture origin in tempered glass; the right image shows an enlargement of the boxed area on the left, with the polyhedral outlines highlighted, and the arrow indicating the fracture origin [from Christensen et al. 2021].*

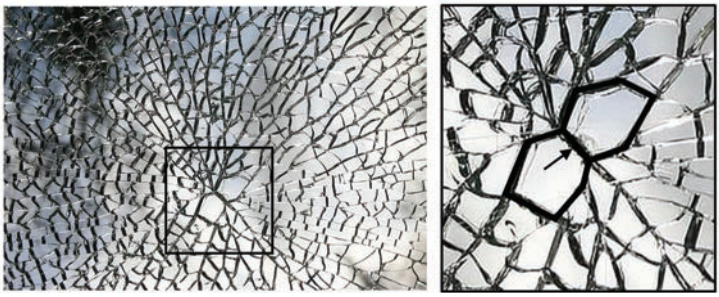

### *2.1.1 Impact site damage*

Impacts can create localized damage at the impact site, and this damage may aid in identification of the fracture. This damage depends on the properties of the two impacting materials as well as the nature of the loading imparted during impact, and may include crushing, chips, patterned marks, and missing fragments. The term **witness mark** is used to refer to evidence of contact with a foreign body for glass and ceramics.

Pecks and dings refer to small indented regions where sharp objects impact glass and ceramics. With increased magnitude of loading, an impact site may be pulverized or crushed. Sharp impacts in particular may produce heavy damage and missing fragments. Sharp impacts to bone, such as those associated with knives and saws, leave localized alterations including incisions, punctures, gouges, **kerfs**, or clefts. These may also produce nearby fractures, if the incision causes sufficient tensile stresses within the bone (Figure 2.3).

*Figure 2.3:*
*Os coxa with multiple sharp alterations (black arrows); the incision in the iliac crest caused tensile stresses in the bone resulting in a fracture initiating from the apex of the incision (white arrow)*

Blunt or sharp impacts or contact loading can cause a chip. **Chipping** refers to the fracture of a small piece of material from the edge of a structure, usually resulting from concentrated loads near an edge. The shape of a chip depends on the loading angle and

can reveal information about the direction of force that caused the chip. In skeletal trauma, chipping may be seen in cases of sharp impact, especially where the force is applied obliquely to the bone. Chipping has also been reported in blunt force impacts at the point of fracture origin, with the size of the chip fragment increasing with increasing impact energy (Cohen et al. 2016, 2017). Note that for glasses and ceramics, edge chips are commonly secondary fractures that have nothing to do with the original failure event and can occur from impact with other fragments during breakage or subsequent handling (Quinn 2020). Care should be taken in interpreting bone chipping to determine whether the chip is related to the original failure event or a secondary event such as handling or contact between fragments.

Contacts may produce **microcracks** that penetrate beneath the impact site and are not visible to the unaided eye. These cracks may occur in the absence of other impact site damage, and their extent may not necessarily be correlated with surface damage (Quinn 2020). Suspected impact sites (even in the absence of other apparent impact damage) should therefore be examined for microcracks that may have been produced below the surface. Lighting, fingerprint powder, staining, or radiology may be useful in visualizing microcracks in bone (see Section 5).

In some cases, the impact site damage may have a **pattern** such that that the impacted structure retains an impression reflecting the size, shape, or other properties of the impacting object. These are often referred to as **tool impressions** in forensic contexts. These may be macroscopic as in the case of a hammer head impression, or microscopic as in the case of striations left by a knife or saw (Figure 2.4).

*Figure 2.4:*
*Tool impressions on bone created by a reciprocating saw*

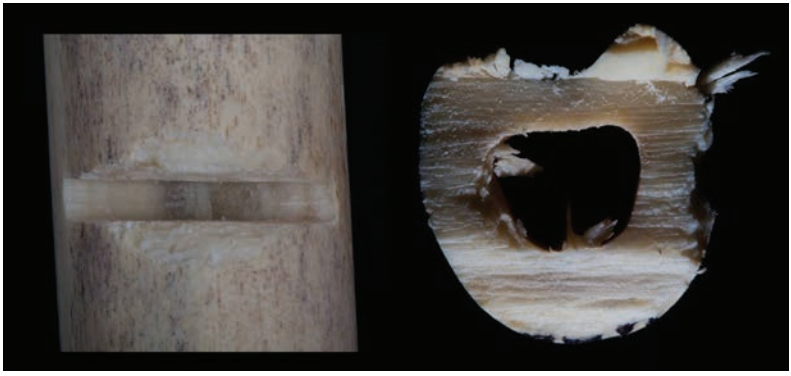

The impact event may transfer intervening materials into the impacted structure, or the impacted structure may retain fragments of the impacting object. Impact sites may therefore be evidenced by inclusions of debris such as hair, metal fragments, paint, or other materials (Figures 2.5 and 2.6). This material itself may be valuable evidence in forensic contexts, especially if it can provide a possible link to the impacting object class. For example, lead or other remnants may confirm contact with a high-velocity projectile or gunshot primer (Berryman et al. 2010; Brogdon & Messmer 2011), or other metallic residues may indicate sharp impact (Gibelli et al. 2012). Care should be taken in forensic analyses to ensure that this foreign material in fact resulted from the impact leading to the fracture and is not from subsequent contamination.

*Figure 2.5:*
*Hair and green-colored substance adhering to an internal bone surface at the site of a blunt impact.*

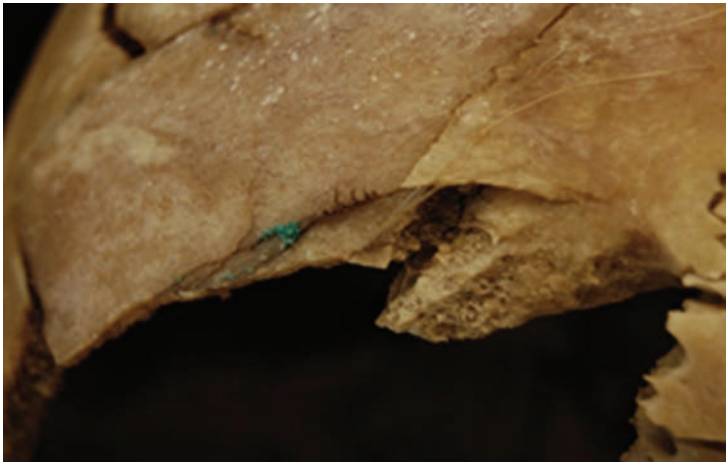

*Figure 2.6:*
*Microphotograph illustrating paint transfer from saw blade (hacksaw) to bone (cut surface)*

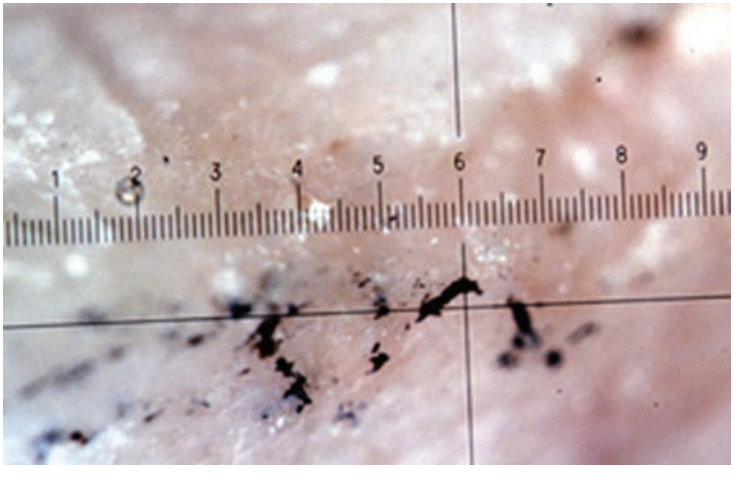

### *2.1.2 Remote origins*

In bone (and other materials) cracks will typically initiate where the tensile stresses are greatest. This may be in the vicinity of the impact site, but impacts can impose stress distributions such that the fracture initiates in areas of high tensile stress elsewhere in the impacted structure. If stress concentrators (see Section 2.4) are located in the stress field created by an impactor, the crack will likely originate at that location. For blunt objects impacting glass plates, for example, the impact can create bending forces such that the crack originates from a flaw at the edge of the plate, with the crack running back to the impact site, then radiating and branching outward. Similar crack initiation and propagation has been observed in blunt cranial impacts (Fenton et al. 2015, 2021; Gurdjian et al. 1947, 1950; Isa et al. 2019) (Figure 2.7). Bone morphology and geometry can also have a significant influence on fracture origins. Different regions of the human skull, for example, exhibit different thicknesses, **buttressing**, strengths and elastic properties (Jaslow 1990; Maloul et al. 2013; Peterson & Dechow 2003, Yoganandan et al. 1995), which may affect remote cracking. Sutures may also serve as stress concentrators where a remote fracture may originate (Fenton et al. 2021). In tubular bones, impacts can impose bending stresses (such as the bumper of a car impacting a tibia), creating tension on the side of the bone opposite the impact, which is where the fracture originates (Figure 2.8).

*Figure 2.7:*
*Remote crack origin in a cranium from an experimental cranial impact with a 1.125-inch diameter aluminum implement; a linear fracture originates in the inferior temporal (A) and propagates toward the impact site (B) [Modified from Isa et al. 2019]*

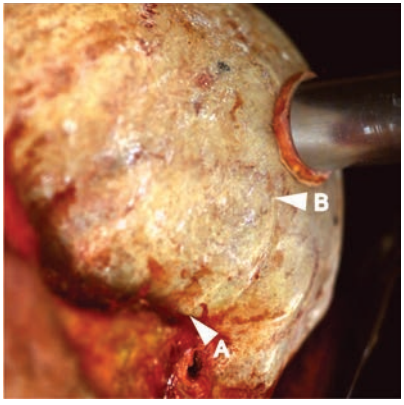


*Figure 2.8.*
*Fracture origin in bent bone from a combined loading experiment (3-point bending with compressive axial loading) performed on a human femur; the impact anvil was applied posteriorly at the midshaft, and it can be seen that fracture initiation is not directly opposite the impact location [Modified from Isa et al. 2018]*

## 2.2 Thermal origins

Thermal fractures originate due to differential strains when portions of the structure begin to stretch or contract but are constrained by other portions at different temperatures. These strain differentials can be between different portions of the structure, or between the surface and interior of the structure. In center-heated glass plates, for example, if a heat source is directed towards the center of a glass plate, the warmer glass expands relative to the glass at the edge. This thermal differential causes compression in the middle and tension on the edges, creating differential strains and stresses (Quinn 2020). The differential stresses can create and propagate cracks originating at the edge of the glass and traveling inward until the stress differential is eliminated.

Many materials are not affected by gradual temperature gradients but are more vulnerable to failure with sudden temperature changes referred to as **thermal shock**. Ceramics and glasses are susceptible to sudden cool down thermal stress, since tensile stresses are created at the surface, which cools quickly and tries to contract, but is constrained by the warmer interior, creating tensile strains on the exterior. Many thermal cracks are low-energy fractures and therefore typically lack branching (see Section 3) or surface markings (see Section 4) (Quinn 2020).

Although it is well understood that bone fractures in response to thermal stress, the fractography of burned bone is not yet well understood. Thermal cracking in bone will often be evident due to other changes associated with thermal exposure (including color change), but more work is needed to better understand how fractography can be applied to burned bone.

## 2.3 Pressure fractures

Pressure fractures result from internal pressure that causes the structure to burst. Such fractures can be experienced, for example, by a carbonated beverage bottle or medicinal vial. Although

unlikely to occur in bone (which has many paths for fluids to escape and lower the internal pressure), it is worth understanding this type of failure, which can place the entirety of the outside surface of a vessel into tension.

In an internally pressurized bottle, its curvature gives rise to both **hoop stress** (acting circumferentially) and **axial stress** (acting in the lengthwise direction). The hoop tensile stresses are double the axial stresses, so the initial crack will be vertical (Figure 2.9), starting on the outside of the structure and propagating inward. The fracture then typically branches in a symmetrical pattern about the structure's vertical axis, with the number of branches being proportional to the stress in the glass (Quinn 2020). This pattern can be important in differentiating between a structure that burst and one that fractured from an impact.

*Figure 2.9:*
*Pressure fracture in a burst glass bottle; the initial crack is in the bottle's vertical axis (right, arrow and solid line), then branches about its vertical axis (right, dashed lines) [image courtesy of Mary K. Holden and Pepperdine University]*

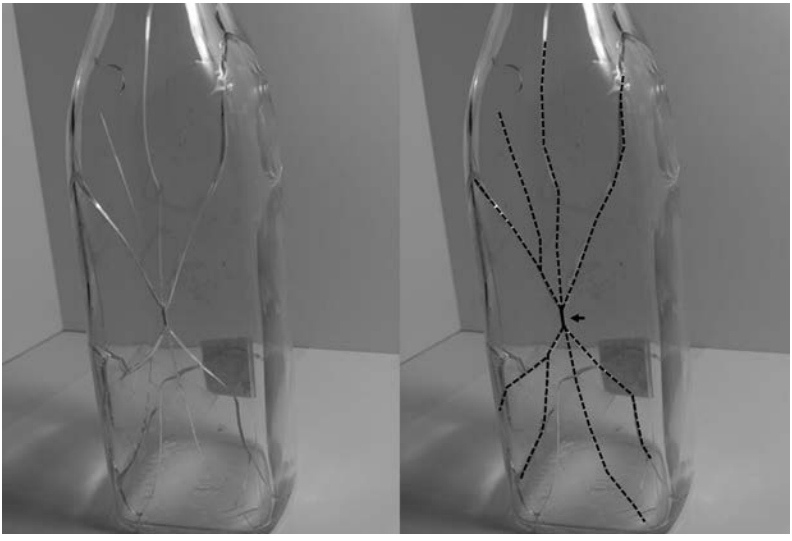

## 2.4 Strength limiting flaws and features

Irregularities or shape changes in an object can act as **strength limiting flaws** by becoming **stress concentrators**. Strength limiting flaws are important considerations because they may behave as a crack origin in an area not otherwise predicted or expected based on overall material properties, geometry, or even the type of loading. Strength limiting flaws generally include voids and cavities, inclusions, compositional irregularities, and microdamage.

### *2.4.1 Voids and cavities*

In glasses and ceramics, pores and bubbles are common and easily identified flaws, usually appearing as discrete, smooth, round cavities (Figure 2.10). Large internal pores can be relatively harmless and may not act as fracture origins, but they can be significant stress concentrators if they contact each other or are near the material's surface (Quinn 2020). In bone, the opening of a nutrient foramen is a pore that can act as a stress concentrator. Indeed, cracks have been noted to originate at nutrient foramina in tests of impacted bone (Christensen et al. 2018a, Rickman & Shackel 2019a) (Figure 2.11). Other foramina in bones and even openings in cranial sutures may also act as stress concentrators as do pathological features, such as abscesses and cysts.

*Figure 2.10:*
*The fracture origin in a cordierite glass ceramic bend bar at the site of an internal spherical pore from a bubble in the original material; the black arrows indicate the direction of crack propagation [modified from Quinn 2020]*

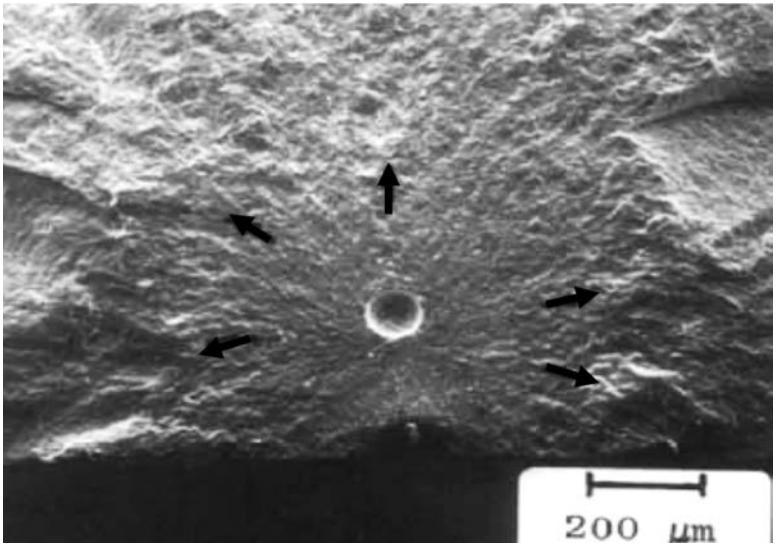

*Figure 2.11:*
*Crack origin at the site of a nutrient foramen opening in a photograph (left) and CT scan (right) of the same bone; solid arrows indicate the nutrient foramen opening on a posterior human femur and the dashed arrows indicate the direction of crack propagation*

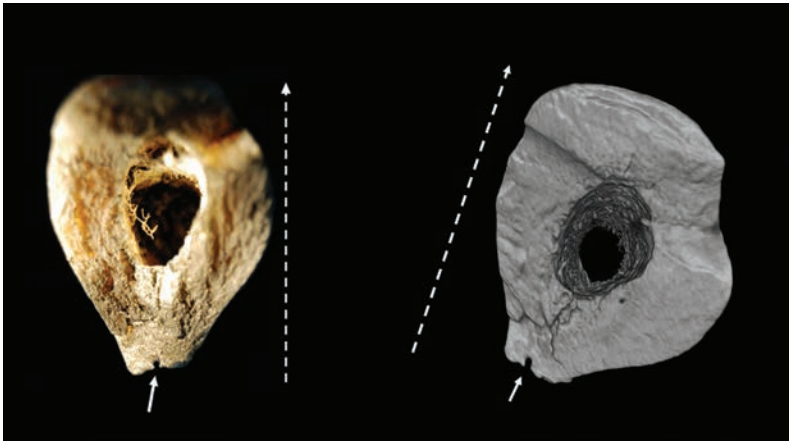

### *2.4.2 Inclusions*

**Inclusions** refer to volume distributed flaws that represent a foreign body with a composition different than that of the rest of the structure. In glass and ceramics, inclusions are often easy to identify by color or reflectivity differences compared to the surrounding matrix (Figure 2.12). The effect of an inclusion depends on how closely its elastic and thermal properties match those of the matrix. Inclusions may cause cracking, may themselves crack, or may detach and pull away from the matrix creating a void.

*Figure 2.12:*
*An inclusion (indicated by the arrow) in a tempered glass window that caused the window to fracture [Image courtesy of Mary K. Holden] (This example is further reviewed in Section 7)*

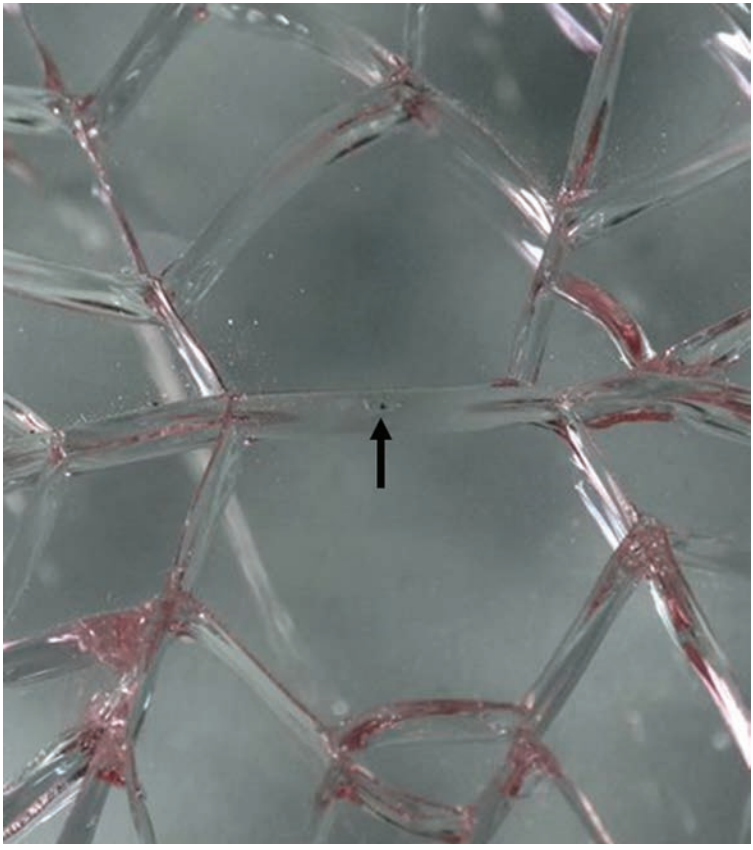

In bone, inclusions would be rare but may include surgically implanted devices (if they are on the interior of the bone), or remnants of a previous trauma where metal or other foreign fragments remain embedded in the bone. Dental fillings in teeth may also be considered inclusions.

### *2.4.3 Compositional irregularities*

Compositional irregularities refer to nonuniform distribution of microstructural constituents. There are many types of irregularities that can act as strength-limiting flaws. **Grain boundaries** can be vulnerable areas in coarse grained materials. Grain boundary cracking sometimes occurs from internal strains from differential contractions in anisotropic grains. In bone, grain boundaries and discontinuities such as lamellar interfaces and cement lines between osteons and surrounding bone can be stress concentrators. However, these may also serve as a crack stopping mechanism (Burr et al. 1988; Piekarski 1970; Pope & Outwater 1972).

### *2.4.4 Damage and microdamage*

Weakened areas of a material may also be strength limiting. In many materials, these may result from corrosion or oxidation, causing pits, bubbles, or blisters that weaken a structure and make it susceptible to fracture. In bone, weakened areas may include regions of a previous fracture, woven bone, grafted bone, inflammation due to infection, or areas with poorly organized or compromised bone (Figure 2.13). Decay and accompanying cavities may represent weakened areas of teeth.

*Figure 2.13:*
*Weakened areas of bone, such as the periostitis on this tibial midshaft, may cause fractures to preferentially originate in this area [from Christensen et al. 2019]*

**Microdamage** from normal physiological loading may also be strength limiting. Microdamage can manifest as debonding of hydroxyapatite aggregates and non-collagenous proteins, or as slippage of lamellae along one another or along cement lines (Jepsen et al. 1999; Poundarik et al. 2012; Varvani-Farahani & Najmi 2010). Microdamage, like grain boundaries, may also increase resistance to crack growth, particularly if linear microcracks are ahead of a larger crack (Nalla et al. 2005a,b; Vashishth et al. 2000).

Aging and disease can also significantly affect the mechanical properties of bone and increase strength limiting features. Age- and disease-related changes can include the accumulation of microdamage and increased porosity, both of which can increase susceptibility to failure. Cortical bone strength under both compression and tension has been noted to decline approximately 2% per decade beginning in the third decade of life (Morgan et al. 2018), with fracture toughness decreasing approximately 4% per decade (Burstein et al. 1976; Koester et al. 2011; Nalla et al. 2004). Bone porosity is inversely correlated with bone toughness and strength (Morgan et al. 2018). More porous bone (such as that associated with osteoporosis) is more susceptible to having microdamage lead to fracture than areas with higher mineral content.

## 2.5 Summary

In forensic contexts, fractures typically originate due to sudden impact or stresses induced by thermal changes. Impacts may produce contact damage at the impact site that may indicate fracture origins and potentially even reflect characteristics or properties of the impacting object. Impacts may also produce high tensile stresses at a location distant to the impact site, resulting in remote fracture origins. Strength limiting flaws may behave as stress concentrators and thereby influence the specific location of the fracture origin. This may help explain different fracture patterns produced in different specimens exposed to similar loading regimes (i.e., as has been documented in experimental trauma studies).

# Cracking and Breakage Patterns

## 3 Cracking and breakage patterns

Once a fracture initiates at the origin (see Section 2), the fracture will extend and propagate under differential stress conditions. The initial fracture often begins as a single crack, but its path depends on a number of intrinsic and extrinsic factors. Where the crack initiated, it will be straight and propagate **normal** (perpendicular) to the direction of maximum local principal tension (Fréchette 1990; Quinn 2020), usually normal to the structure's free surface. As the crack propagates, minor deviations in the direction of local principal tension can modify the plane and direction of cracking. If stresses are too great to be dissipated through a single crack, multiple cracks may be created. These deviations and the need to dissipate stress affect the paths of the fractures. Fracture paths are not random but occur in patterns that are related to stress conditions and material properties. These patterns can indicate the location of the fracture origin, as well as provide information about the cause of the fracture, the energy of the fracture, and the stress state (Quinn 2020). This section addresses cracking patterns, including those surrounding the impact site, as well as crack branching and fragmentation patterns.

### 3.1 Impact site crack patterns

As discussed in Section 2, impacts can create localized damage to the impact site, including microcracks in the immediate vicinity of the impact site. At higher velocities, there are often cracks that emanate from or are directly associated with these impact sites. Such cracks may include radial cracks, circumferential cracks, and cone cracks.

#### *3.1.1 Radial cracks*

**Radial cracks** may be generated from the impact site, originating from within the zone of the contact and propagating outward. These tend to be easy to interpret, as the cracks fan out away from the impact site such that the radiating crack pattern leads back to

the origin in the middle (Figure 3.1). Similar to glass and ceramics, radiating fractures from a blunt or projectile impact to a cranium can point back to an origin at their center (Figure 3.2). If the impacting object has a large surface area, the radial cracks may not lead directly back to a central location/point but will still lead back to the impact region. For remote origins (as discussed in Section 2), the linear fracture may initiate at a location other than the impact location and radiate back toward the impact site.

*Figure 3.1:*
*Radiating fracture pattern in a fractured borosilicate crown glass disk; the fracture origin is in the middle of the disk where the radial cracks meet [from Quinn 2016]*

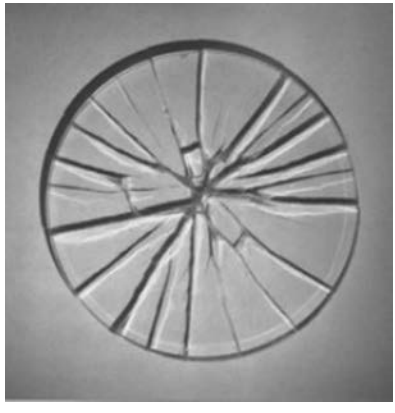

*Figure 3.2:*
*Radial cracks from a projectile impact on a cranium; the projectile impacted and penetrated the left temporal squama, with radial fractures extending anteriorly and posteriorly (black arrows); the extension of the fractures is more easily visualized in the CT scan (right), in part due to the staining on the bone; in the CT scan, radiodense debris is also noted on the anterior aspect of the entrance defect (white arrow)*

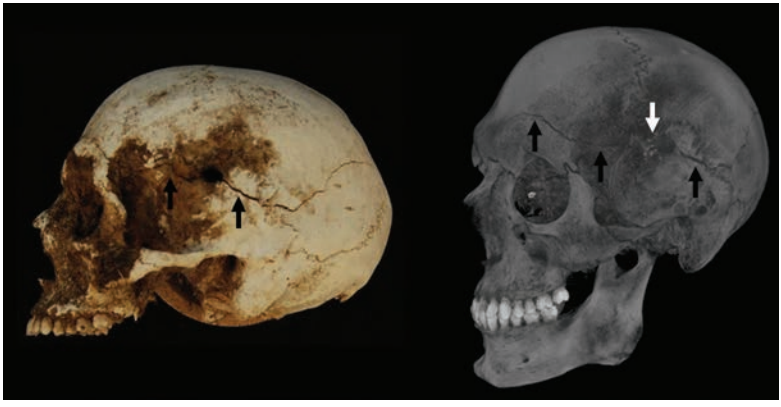

Impacts involving less force or objects with large surface areas may not necessarily initiate radial cracking on the impacted side of a structure. Bending from an impact can create tension and initiate cracking on the opposite side that travels through the material toward the point of impact (see Section 2). For example, blunt impact to the exterior of a cranium can create tension on the endocranial surface, with radiating cracks initiating endocranially (Figure 3.3). These fractures may not necessarily propagate all the way through to the ectocranial surface. If blunt trauma is suspected in the absence of ectocranial fractures, the endocranial surface should be examined carefully for fractures.

*Figure 3.3:*
*Blunt impact to a cranium; tension is experienced on the endocranial surface where radiating fractures will initiate*

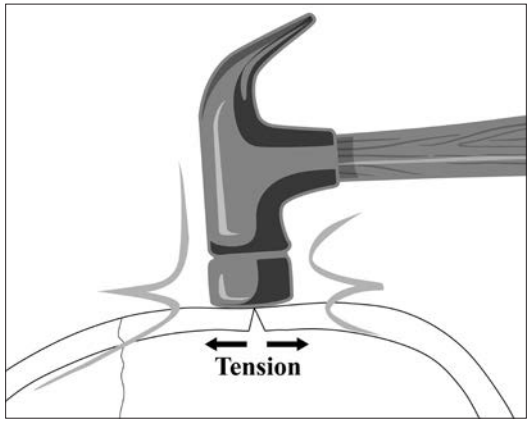


In addition to pointing towards the impact location, radiating fractures in other brittle materials also have relationships to other intrinsic and extrinsic factors. In indentation testing, the sums of the lengths of surface cracks emanating from an impact are related to the load and material toughness (Palmqvist 1957). The morphology and size of cracks associated with indentation are dependent on material properties, indenter geometry, and the applied indentation load (Chiang et al. 1982; Johanns et al. 2014; Lankford 1982; Lawn & Wilshaw 1975). More research is needed to understand the implications for skeletal trauma analysis, but further investigation of radial cracks in bone from a fractography perspective may reveal that these cracks can provide more information about the trauma event than just the impact location (this is discussed further in Section 6).

### *3.1.2 Circumferential cracks*

If the structure is continually loaded, the radially-fractured segments can bend inward, causing them to fracture in bending, leading to circumferential secondary cracking (Figure 3.4). These

**circumferential fractures**, which are roughly circular, semi-circular, or arc-shaped, are often offset by the radial fractures, which also confirms that the radial cracks came first (see Section 3.4 on intersecting cracks). While radial cracks initiate on the side opposite the impact, in these secondary fractures, the maximum tension is on the impacted side of the material and the fracture therefore initiates on this surface. This can be confirmed by examination of the fracture surfaces (see Section 4). In lower velocity impacts to crania, the maximum tension is on the impacted surface and the circumferential fracture therefore initiates ectocranially, propagating toward the endocranial surface. With high-velocity perforating impacts to crania (because the cranium is an enclosed structure), the segments produced by radial fractures may be pushed outward due to the temporary cavity created by energy transfer from the projectile, resulting in circumferential fractures that initiate on the endocranial surface. In both instances, the circumferential fractures will tend to angle/bevel from the impact surface as it advances toward the more fixed end of the bone plate defined by the radiating fractures.

*Figure 3.4:*
*Circumferential fractures on human cranium [modified from Christensen et al. 2019]*

Note that the term **concentric fracture** traditionally has been used interchangeably with the term circumferential fracture by anthropologists and others to refer to this fracture pattern. Technically, circumferential refers to fractures at the periphery or relating to the circumference of a structure, whereas concentric refers to multiple generations of arc-shaped fractures sharing a common center (Figure 3.5). Concentric fractures are less common but occasionally seen in high-velocity impacts to bone (Figure 3.6). A case study involving concentric fractures in bone from blunt trauma is also shown in Section 7.

*Figure 3.5:*
*Circumferential (left) versus concentric (right) fractures.*

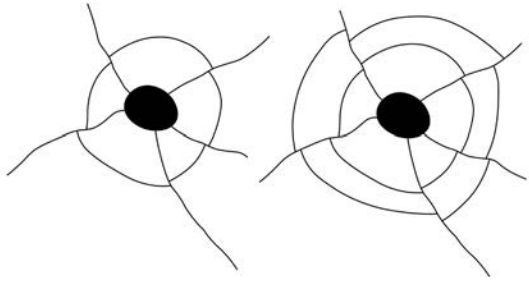

*Figure 3.6:*
*Gunshot trauma to a cranium (left), showing radial (R) and concentric (C) fractures (right) [from Christensen et al. 2021]*

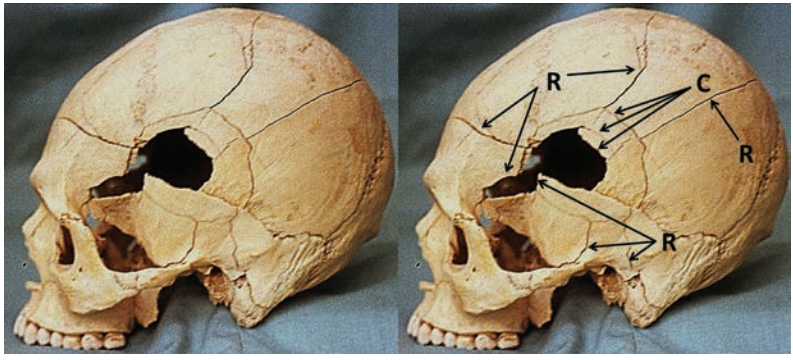

### *3.1.3 Cone cracks*

Impacts or contact loadings at higher velocities can produce a **cone crack** (Figure 3.7), which is a conoidal fracture that results when an object impacts or passes through a brittle material, first described by Hertz (1896) and therefore sometimes referred to as Hertzian cone cracks. When the applied load reaches a critical value (dependent on the elastic properties of the two contacting materials), a **ring crack** forms due to tensile stresses on the impacted surface of the structure. This circular ring crack is concentric with and just outside of the area of the two contacting bodies. For contact with a spherical indenter that does not involve penetration of the structure by the object, there is a relationship between the size of the projectile and the ring crack, such that the contacting object is almost always larger than the ring crack on the contacting surface (Quinn 2020). On the surface, the first principal stress is tensile, with a maximum value at the edge of the area of contact between the impactor and impact surface and is responsible for the formation of the initial shallow ring crack. The initial ring crack propagates normal to the free surface of the structure for a very short distance. The ring depth is approximately uniform around the circumference, and at this point the stresses are axi-symmetric (Warren et al. 1995).

*Figure 3.7:*
*Hertzian cone crack [from Christensen et al. 2021]*

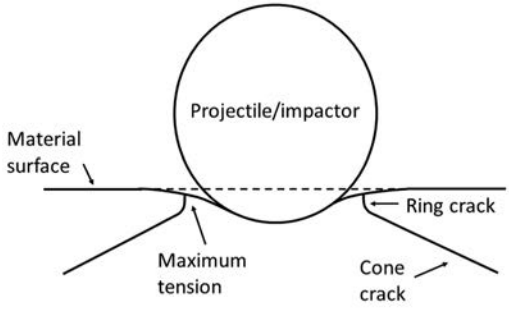

With increasing load, the crack tip **stress intensity factor** around the ring crack increases until a critical value is reached, at which point the crack will propagate outward for a distance related to the load (Lawn 1998; Warren et al. 1995). As with other fractures, a cone crack will propagate along paths that maximize strain energy release, typically normal to the greatest tensile stresses, with in-plane shear stress influencing crack growth direction. The angle of the cone crack depends on the material's Poisson's ratio as well as shear stresses, structure thickness, and method of support (Fischer-Cripps 2007). Propagation of a cone crack through the full thickness of a structure results in the formation of a conoid (cone-shaped piece) of material (which may remain intact for lower impact velocities) and leaves behind a conoidal void. This conoid typically undergoes comminution (breaks up into smaller pieces) if the impact is ultimately a perforation event (Kaufmann et al. 2003; Zaera & Sánchez-Gálvez 1998). The conoidal morphology of the void created is commonly referred to as **beveling** in forensic contexts. Cone cracking is well understood to be the mechanism responsible for bevel production in other brittle materials such as glass, for example when a bullet passes through a window (Figure 3.8), and unsurprisingly this morphology bears a striking resemblance to high velocity projectile traumas in bone (Figures 3.9 to 3.11). Cone cracking has also been recently shown experimentally to be the mechanism responsible for this pattern in bone (Christensen et al. 2021; Rickman & Shackel 2019a,b,). This beveling pattern is commonly reported in forensic literature to be distinctive to high-velocity projectile impacts, but cone cracking is also associated with blunt impacts and low velocity projectiles (Quatrehomme et al. 2016; Rickman & Shackel 2019; Spatola 2015; Vermeij et al. 2012).

*Figure 3.8:*
*Cone crack and conoidal bevel (as well as radial and circumferential cracks) in glass from a projectile; left: view from projectile entrance with the bevel away from the viewer; middle and right: two oblique views of the exit with the bevel toward the viewer [from Christensen et al. 2021]*

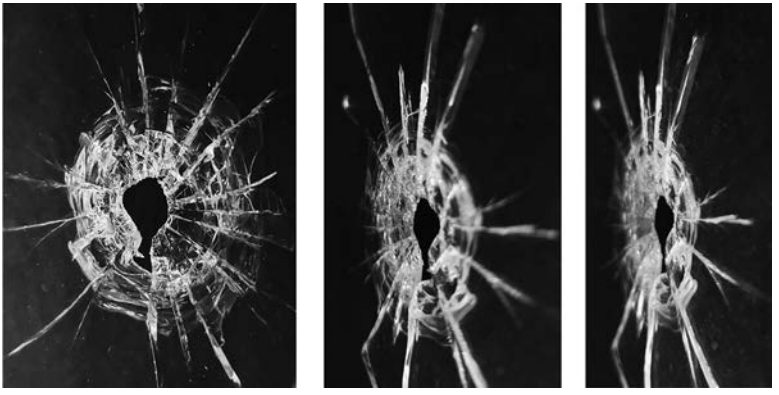

*Figure 3.9:*
*Conoid bevel in bone from a projectile exit, viewed from the endocranial surface (left) and ectocranial surface (right); radial cracks are also associated with the impact [modified from Christensen & Passalacqua 2018]*

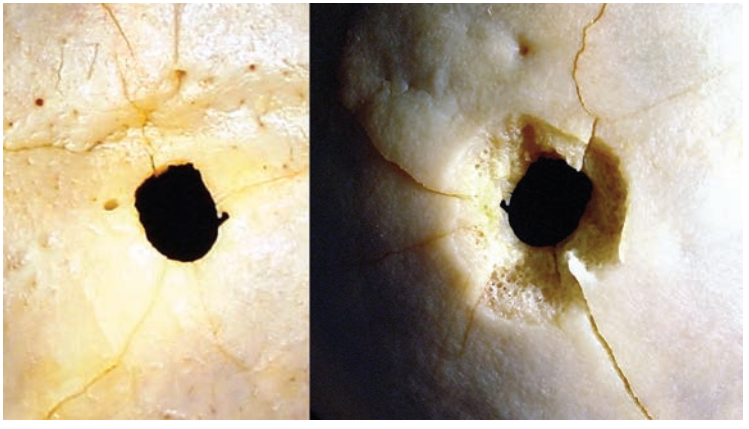

*Figure 3.10:*
*Cone crack in adult porcine scapula Left: View of exit side of impact with bevel and fragments of the cortical floor of the conoid still in situ and nearly fully covering the bevel; Right: µCT transverse-section of the same beveled fracture showing the entry cortical fracture edge (a), the trabecular fracture margin (b), the exit cortical fracture edge (c), and the bevel present behind the lower left fragment (d) [from Christensen et al. 2021]*

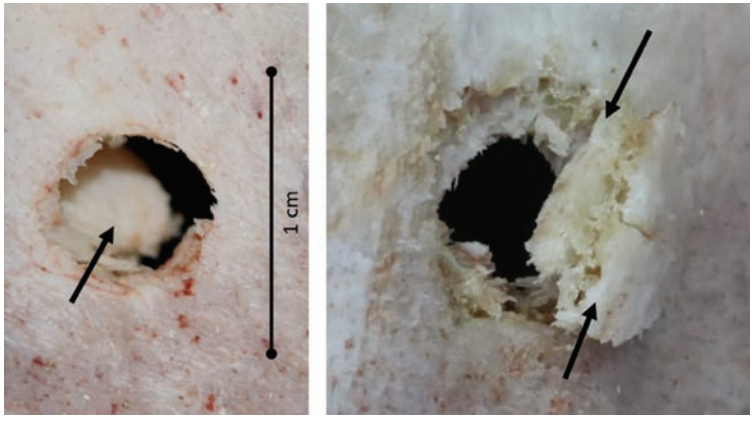

*Figure 3.11:*
*Cone crack in a human cranium imaged with high-resolution CT scanning; reconstructed cranium (top left), a sliced plane view of the beveled bone edge (bottom left and right), and close-up view of beveled portion (bottom right)*

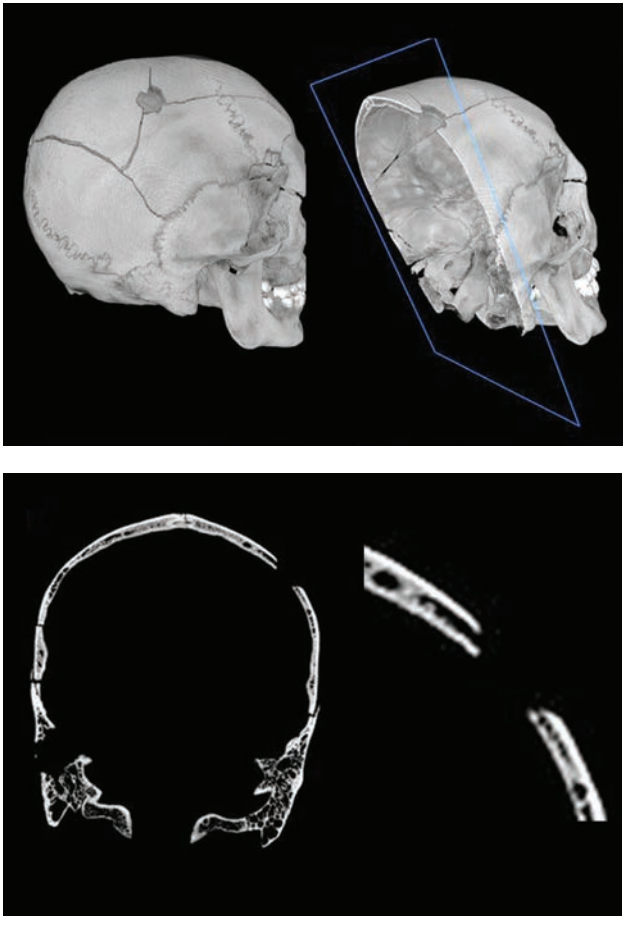

In glass and synthetic brittle materials, cone crack angle (measured as the half-angle of the cone) is known to decrease with increasing impact velocity (Chaudhri 2015; Knight et al. 1977),

resulting in less flared cones at higher velocity. This relationship has been successfully utilized in glass to estimate projectile impact velocity from the cone angle (Miyamoto & Murakami 2000). Cone crack angle is also known to vary with specimen thickness (Miyamoto & Murakami 2000) and angle of impact (Chaudhri 2015). Impact trajectories are reported to affect cone angle in ceramics (Kocer & Collins 1998). Preliminary work on the angle of the entry cortical fracture edge has revealed considerable variation between specimens and even within specimens around the circumference of the cortical entry (Rickman & Shackel 2019a). Further experimental work is needed on the angle of beveled fractures in bone to establish the intrinsic and extrinsic factors that influence bevel geometry. Importantly, failure and fracture patterns are strongly influenced by structure geometry, and within the human skeleton there is significant variation in bone shape and configuration. Therefore, the response of each bone or bone type to certain loading conditions will vary, and measurements of cone angle should not be used to estimate impact velocity in bone without further research. Much of the experimental work has focused on bones with **sandwich structures** (having stiff faces separated by a lightweight core, such as the cranium). Cone cracks, however, have also been documented in long bones (Kieser et al. 2011) so they are not limited to sandwich structured bones. Additional research on different loading and impacting regimes may clarify the creation and appearance of cone cracks and other fracture patterns on various bone types.

### 3.2 Crack branching

As fracture speed increases from the origin, the crack reaches a limiting (terminal) velocity and may split into two cracks, or **branch**, in order to dissipate strain energy (Fréchette 1990), also sometimes referred to as **velocity branching**. Although the initial fracture propagates normal to the maximum tensile stresses, these branches may be at non-normal angles to the far-field (remote) stress

direction. Crack propagation and branching can be affected as a crack moves from one type of stress field to another (for example, tensile to compressive), and may be evidenced by a sudden change in crack propagation direction. Low energy fractures, including many thermal fractures, may not branch. Even with high local stresses precipitating initial crack propagation, stress levels may be low in other portions of the structure. Branching may not occur at all if the failure stresses are low, if the stresses decrease in the direction of crack propagation, or if the stresses are relieved.

### *3.2.1 Branching patterns*

Crack branching patterns are a valuable aid in determining the direction of crack propagation. Crack branching pattens can lead back to the fracture origin as well as provide information about the stress state and stress magnitude. For example, a pair of branches in opposite directions typically bracket the fracture origin (Figure 3.12). Because the crack is branching to dissipate energy, higher energy impacts will cause a greater number of branching events (see Section 3.3). Cracks also typically propagate normal to the origin surface for a short period, so often, locating the fracture origin can be accomplished by examining branching patterns and tracing them back to the region of the first (flat/normal) fracture (Figure 3.12).

*Figure 3.12:*
*Branching can be used to determine the direction of crack propagation and traced back to the fracture origin; dashed arrows indicate the direction of crack propagation*

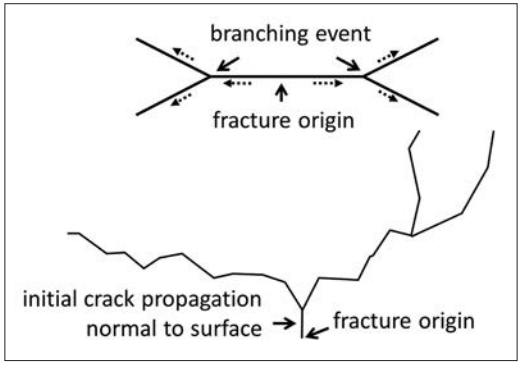


Branching patterns are addressed in only limited and broad terms in forensic anthropological contexts. General categories are typically used to describe fracture shapes and patterns such as buckle, greenstick, transverse, oblique, or spiral (e.g., Carter & Spengler 1978; Galloway 1999; Gozna 1982), with little consideration for branching and crack propagation. The so-called "butterfly" or wedge fractures is a branching fracture pattern in bone that has received considerable attention (e.g., Christensen & Smith 2013; Daegling et al. 2008; Emrith et al. 2020; Passalacqua & Fenton 2012; Reber & Simmons 2015; Wheatley 2008). The causes of these fracture types, however, tend to be oversimplified (or in some cases misinterpreted), often including broad claims of force directionality in relation to fracture patterns.

Wedge fractures occur in tubular or linear structures that fail in bending. The wedge-shaped piece opposite the fracture origin may be useful in interpreting the overall stress and loading state, but will never have the fracture origin on it, which will be on the two matching pieces nearer the tensile stresses surface (Figure 3.13). The fragment may also be useful in reconstruction.

*Figure 3.13:*
*Wedge fracture on a bone that failed in bending; while the wedge fragment may be useful in reconstructing the bone and understanding the failure event, the fracture origin is on the complementary fragment surfaces indicated with white arrows, and not on the wedge fragment (which is marked "c")*

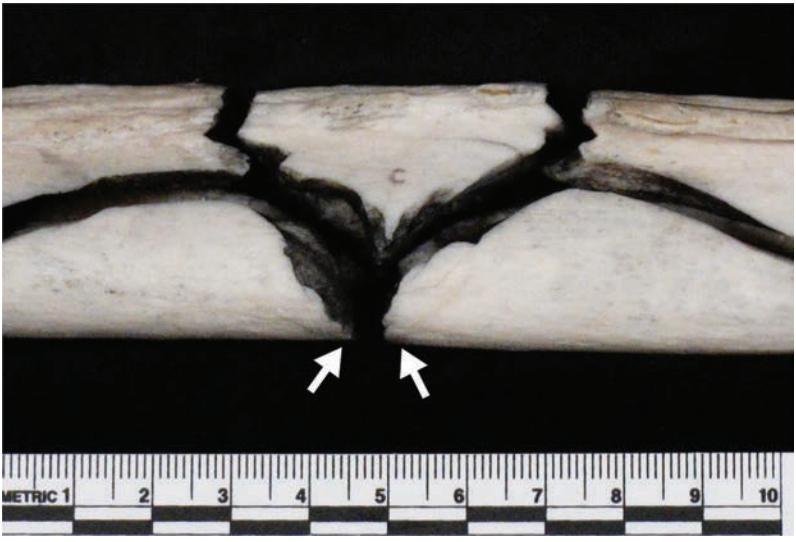


In relation to fracture surface features (Section 4), the mirror and hackle regions will precede a branching event since in these regions the crack has not yet reached terminal velocity. In femora experimentally fractured in bending, branching has been documented occurring after the mirror region and with the onset of arrest ridges (Figure 3.14), which also represents where the primary stress has changed from tension to compression.

*Figure 3.14:*
*CT scans of femora fractured in bending; crack branching (indicated with solid arrows) is seen to occur after the mirror regions and just prior to the onset of arrest ridge; dashed arrows mark the fracture origin*

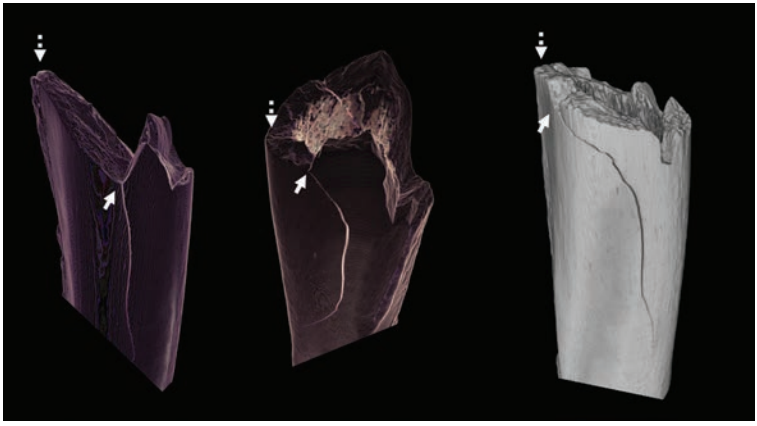

### *3.2.2 Branching distances and angles*

The distance a crack travels before branching is related to the stresses and stored energy of the structure; the greater the stored energy, the shorter the distance to branching (Quinn 2020). The angle of the branching can also provide useful information about the fracture event. The angle of the branching varies with the stress state. In glass, uniaxial stress (such as direct tension) tends to produce forks of around 45°, while equibiaxial stress (such as a uniformly loaded thick window with an origin near the center) may cause a fork of as much as 180°, circumferential hoop stresses (such as a pressurized bottle) fork at around 90°, and torsion fractures have very small forking angles (Preston 1935; Quinn 2020). Moderate to high strength structures tend to branch around 30-45° (Quinn 2020). Others have noted greater variation and branching angles, and the exact angle of the branch is likely dependent on the shape of the structure, the loading configuration, the number of branching events, the stress level, and possibly material properties (Bullock & Kaae 1979; Quinn 2020).

In a study involving pig rib fractures produced in a blast event and in manual 4-point bending, branching angles were noted to be more acute in those from the blast event, and also to have longer normal cracks prior to the branching event (Figure 3.15), likely due to the greater magnitude of force and shorter loading duration (Christensen & Smith 2013).

*Figure 3.15:*
*Rib fractures in pigs from a blast event (top) and manual 4-point bending (bottom); note the more acute branching angle and longer pre-branching normal crack in the blast specimens; the black lines show the crack prior to branching and the white lines show branching angles [modified from Christensen & Smith 2013]*

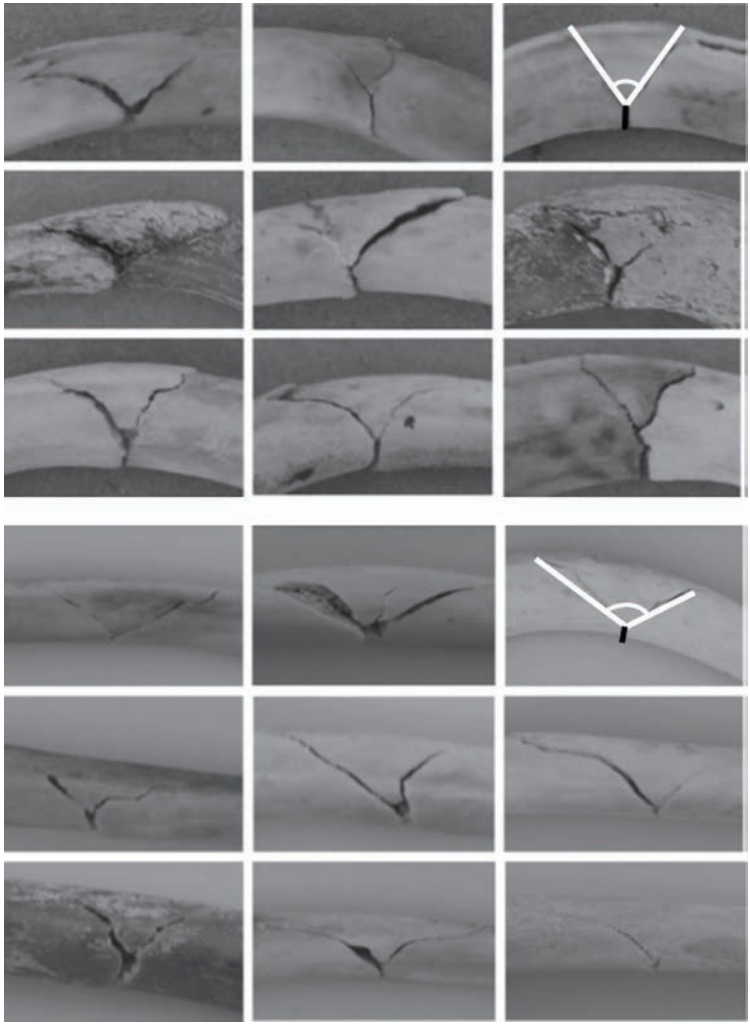

Torsional loading can produce fractures that are at an angle to the structure length. Torsion usually does not induce a special failure mode, and the fracture still starts as a crack propagating normal to the shear stress direction. Many parts that fail in torsional loading also have a bending component. Fracture surfaces may also display twist hackle (Section 4).

In ceramics, the angle does not necessarily stay constant and may curve, resulting in an increase to the angle (Rice 1984). Branching patterns appear to split the broken structures into regions of approximately similar area, implying that the cracks partition the structure into pieces with comparable areas and strain energies (Quinn 2020; Rice 1984). As a crack progressively branches, it may begin to interact with other branching cracks (Quinn 2020). Branching angles also diminish with progressive branching (Bullock & Kaae 1979). There are a number of factors that may affect branching angles including material properties and structure shape, and quantification can be complicated. They can, however, provide at least a qualitative indication of the stress state.

There is little consensus on how to measure branching angles, with some recommending the angle be measured close to the point of branching (Fréchette 1990, Preston 1935), while others suggest it is better to measure the angle once it has stabilized (Quinn 2020). Branching angles tend to start small, and then increase to its stable configuration (Quinn 1999, 2020). Branching angles also vary within a structure, usually due to spatial variations of the stresses. As previously noted, bone is a very complex structure in terms of both its composition and geometry. Certain parts of the skeleton have areas that are more reinforced or buttressed, which helps redirect forces and dissipate stress and may therefore affect fracture angle. Little is currently known about branching angles in bone attesting to the need for more research to better understand crack branching distances and angles in bone (see Section 6).

### 3.3 Fragmentation patterns

The extent of fragmentation (i.e., number of fragments produced by branching events) depends on the stress state of the structure and the total energy available for fracture (Quinn 2020). Low energy fractures create less branching and therefore fewer fragments. High energy fractures can create extensive fragmentation (often called **comminution** when the fractured material is bone). In such cases, information may still be gained from reconstruction of some of the branching patterns, or from the fracture surfaces (see Section 4).

When fragments are present, they will likely need to be reconstructed prior to assessment of the crack patterns (see Section 5), although examination of fracture surfaces (see Section 4) may need to occur first. Sometimes in forensic contexts not all of the fragments will be present at the time of analysis (due, for example, to an incomplete recovery); however, even if the fragment(s) with the fracture origin are not present, valuable information about the fracture event can still be present in the other fragments (Quinn 2020).

### 3.4 Intersecting cracks

The location and pattern of intersecting cracks can also facilitate fracture interpretation. The first crack will pass through the material undisturbed, perhaps branching. Assuming the first crack completely cleaves the material, a second crack that intersects the first crack will stop, since the energy is dissipated through the discontinuity and the tensile stresses will not be able to carry across the first crack (Figure 3.16). Many forensic practitioners may be familiar with this concept in the form of Puppe's Rule, which states that the sequence of cranial injuries can be determined based on cracks terminating into preexisting cracks (Puppe 1903). Although this and many other articles describe this pattern with specific reference to bone fractures (e.g., Kranioti 2015; Madea & Staak 1988; Viel et al. 2009) the crack intersection principle applies to all brittle materials.

*Figure 3.16:*
*Intersecting cracks on a cranium; the fractures indicated by the white arrows preceded those indicated by the black arrows as evidenced by their termination into the first*

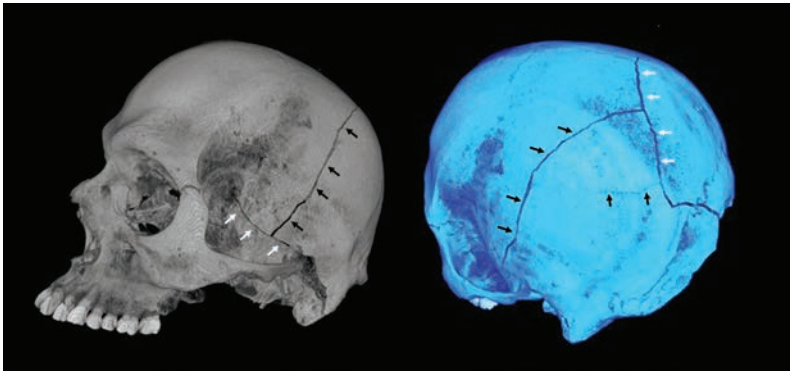

This interpretation of crack sequence can be corroborated by looking at the fracture surfaces (see Section 4). Fracture surface features for the first crack plane will be continuous and connected on each side of the intersection (Quinn 2020). In cases where an existing crack does not completely cleave the material, a subsequent crack may be able to traverse it. For example, in a bending fracture where the crack does not go all the way through the compression side, a remnant interface of unbroken material provides a path for a second crack to cross the first. The fracture surface features of the first crack will be continuous on both sides of the intersection. The second crack, however, will have a change in the crack plane, often a jog or hook to complete the fracture on the other side of the first crack. Similarly, in the cranium, fractures often terminate in cranial sutures which dissipate the fracture energy. If a fracture appears to cross a suture, then the suture was not completely open, and there was some bridging of bone that allowed the fracture to continue through the suture.

In projectile impacts, radiating cracks can travel more quickly than the projectile. In the case of a projectile impacting and

penetrating a cranium, these cracks can reach the other side of the cranium before the projectile (Berryman & Symes 1998) (Figure 3.17). Radiating cracks from the projectile exit may therefore terminate into radiating cracks created from the entrance impact (see case example in Section 7). This type of intersection can be used to deduce or confirm the entrance versus exit in addition to interpreting the sequence of multiple impacts (either blunt or projectile).

*Figure 3.17:*
*Intersecting cracks on bone; the fracture indicated by the white arrows preceded the fracture indicated by the black arrows demonstrating that the projectile exit defect occurred after the projectile entrance defect that produced the fracture with white arrows*

Intersecting cracks can also be used to differentiate between cone cracks and circumferential cracks. Although both are curved in nature, in many cases it will be possible to differentiate them based on whether the curved crack or the radial cracks are continuous versus terminating into previous cracks (Figure 3.18). In the case of circumferential cracks from inward bending of segments, the radial cracks will appear first and will be continuous, while the circumferential cracks (which appear later) will terminate into them and be discontinuous. In the case of ring cracking, the ring appears first and will be continuous, while the radial cracks (which appear later) will terminate into the cone crack and be discontinuous.

*Figure 3.18:*
*Radial and circumferential cracks (left) compared to radial and ring cracks (right); grey areas indicated impact location/region, solid lines indicate primary cracking, and dashed lines represent secondary cracking*

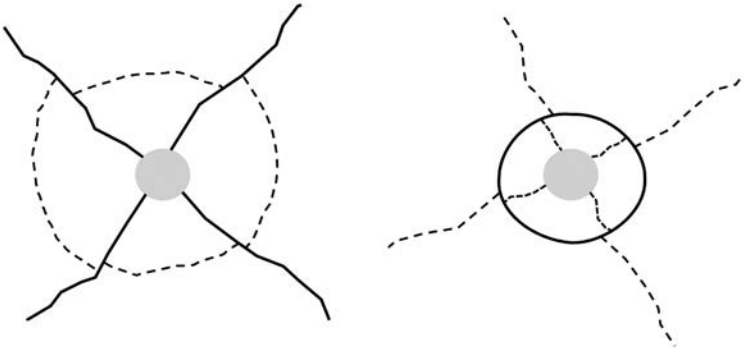

## 3.5 Summary

Cracks may initiate from an impact site or remote to that impact site, as determined by intrinsic and extrinsic properties. Crack branching pattern is a valuable observation in establishing crack propagation. Depending on the stress conditions, cracks may branch as they travel away from their origin and this pattern of crack branching can help indicate the location of the fracture

origin. Moreover, branching patterns can provide information about the cause of the fracture, the energy involved, and the stress state experienced by the structure. Cone cracks can form from high velocity impacts or low velocity impacts that may or may not penetrate. Velocity of the impactor may be reflected in the cone crack angle with the angle decreasing as velocity increases. Crack intersections can provide information about the sequence in which cracks occurred as well as the stress state.

# Fracture Surface Features

# 4 Fracture surface features

The fracture surface refers to the surface created by the separation of two portions of a material as a result of a propagating crack front. Fracture surfaces can reveal information about mechanical properties of a material, the mechanism of failure, and origin and propagation direction of the fracture (Hull 1999). Fracture surfaces (particularly of brittle materials) display features related to the fracture origin, as well as the speed and stability of the propagating crack, which can be seen as arrangements of ridges and lines with specific orientations relative to the moving crack front.

## 4.1 Fracture surfaces

A number of macroscopic and microscopic markings or features may characterize a fracture surface. These features can be used to identify the location of fracture origin and the direction of crack propagation, to identify the cause of the failure, and to estimate the stress level at failure (Bradt 2011). The greater the stress in the fracture, the more stored energy, and the more prominent the fracture markings (Quinn 2020). Very weak structures with low stored energy often break into pieces with relatively featureless fracture surfaces and can be difficult to interpret (Quinn 2020). Very strong structures have so much stored elastic energy that excessive fragmentation can occur, making the fracture origin difficult to locate (Quinn 2020). Very porous or coarse-grained materials can also mask fracture surface markings (Quinn 2020).

Because of its very fine (i.e., amorphous) microstructure, glass shows many fracture surface features very well and is therefore a useful introductory example. Although there are many features that may be apparent on a fractured glass surface, three in particular are well-documented and easy to identify: the mirror, mist, and hackle regions (Figure 4.1).

*Figure 4.1:*
*Mirror, mist, and hackle regions of a fractured 5mm glass rod [from Christensen et al. 2018a]*

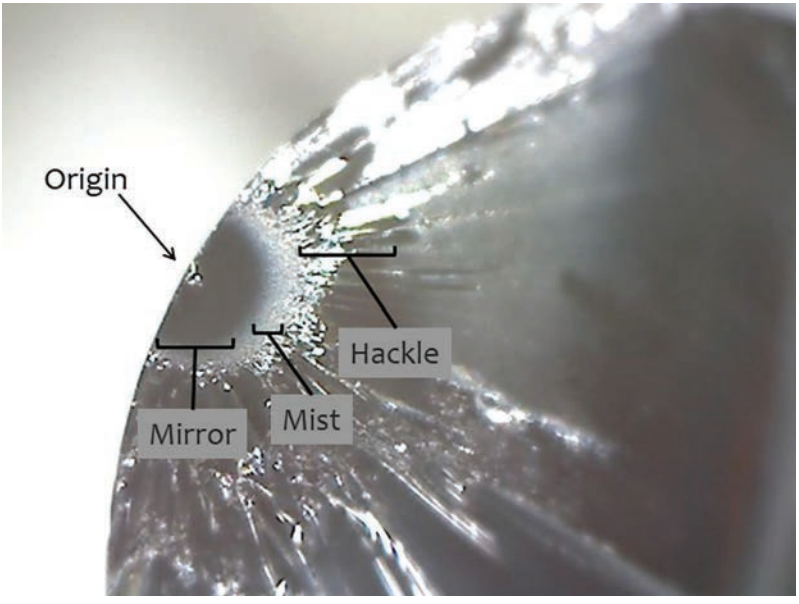


All fractures in brittle material start at a single origin point and then accelerate outwards forming a propagation front. As this propagation front expands, the speed of the fracture increases rapidly. This increasing fracture speed is reflected in the changing pattern of markings left behind on the fracture surface. The region closest to the fracture origin site is often associated with a **mirror** zone, which is a smooth region surrounding and centered on the fracture origin (Quinn 2020) that is indicative of planar crack growth radiating rapidly outward from the origin. Adjacent to the mirror zone, a **mist** region marks where micro-steps begin to develop in the crack front due to its rapid motion. As the crack accelerates away from the origin, local deviations (twists and tilts from the main fracture plane) occur, and these deviations become optically discernible in the mist region (Quinn 2016). As the crack advances,

these deviations increase and oscillate, forming larger rough steps referred to as **hackle** (Quinn 2020). The rough hackle region of a fracture surface is characterized by angled ridges and valleys resulting from increasing crack speed and increasing dynamic instability (Bradt 2011). Hackle ridges and valleys are oriented in the direction of the fracture origin and can be used to locate the origin of the fracture. The relative macroscopic "roughness" of a fracture surface can therefore indicate the direction of fracture propagation, with the smoother surface being adjacent to the crack nucleation site, becoming progressively rougher as the crack accelerates.

The terminology used to refer to fracture surface features is somewhat standard but varies to some extent between material types because of differences in the appearance of fracture surface features. In 2018, Christensen et al. developed terminology specific to the assessment of bone, noting that this would be beneficial because fractographic features of bone appear somewhat differently from previously described features in other materials in both quality and degree of expression. The terminology used here reflects those recommendations along with terminology used in other areas of fractography. Features seen in other materials and not previously observed in bone are also described here. This is partly to facilitate understanding of crack propagation behavior and also because it is recognized that just because some of these features have not been previously observed on bone does not mean that future practitioners may not encounter them.

All available fracture surfaces should be examined, as features may be easier or more reliably observed on some fragments versus others. Fracture surface examination may not be possible in cases of incomplete fractures that do not result in fragmentation; in these cases, the fractographic analysis may be limited to cracking and branching patterns (see Section 3). In theory, for a simple fracture that produces a single non-branching crack, the two fracture surfaces

should be complements: a ridge on one surface will correspond to a valley on the other. In practice, fractures are often more complex, fragments may be missing, and surfaces can be contaminated or damaged in a way that precludes a thorough fractographic analysis. A very useful feature of fractography, however, is that each fracture surface (even for small fragments) may have features that reveal information about the fracture event.

## 4.2 Mirror

As noted previously for glass, the mirror zone is a smooth region surrounding a fracture origin. Fracture mirror in glass is very distinctive and easy to identify because of the virtual lack of any other microstructural surface features (Figure 4.1) and can usually be recognized even by novice fractographers. The term derives from the fact that the region is so smooth that it reflects light like a mirror. Mirror represents the region where the crack initiated and radiated outward from a flaw at the fracture origin. Usually there is only one mirror corresponding to a single fracture origin; however, occasionally there can be multiple simultaneously activated origins that produce more than one mirror region (Quinn 2020). In some instances, a fracture mirror may not be located.

### *4.2.1 Changes within the mirror zone*

Within the mirror region, the crack accelerates from near zero to terminal velocity (700-2500 m/s in glass) which occurs in microseconds (Field 1971; Quinn 2020; Richter & Kerkhof 1994). Although not yet optically discernible, a gradual progression of localized deviations from the main crack plane are formed in the mirror region and have been observed using transmission electron microscope images (Figure 4.2). These deviations occur as the crack accelerates away from the origin, and micro portions of the crack front experience slight twists and tilts from the main fracture plane (Beauchamp1996; Fréchette 1990; Quinn 2020). These twists and tilts are momentary, since the crack plane deviations are restricted

by the energetic costs of creating an additional crack surface, and the variations therefore quickly rejoin the main propagating crack plane. As these local deviations increase in scale, they eventually become optically discernable as the mist region, and as the crack plane advances, eventually as hackle (Beauchamp1996; Fréchette 1990; Quinn 2020).

*Figure 4.2:*
*Transmission electron microscope images from a fracture mirror in tempered soda lime glass with arrows showing the direction of crack propagation: (a) smooth mirror area near origin with some round bumps; (b) approximately 1/3 of the way to the mirror/mist boundary with ridges elongated in the direction of crack propagation; (c) near the mist boundary, with ridges becoming longer and wider; and (d) in the mist region, with similar increasing ridges which are now optically detectable [modified from Quinn 2020, from Beauchamp 1971, 1996]*

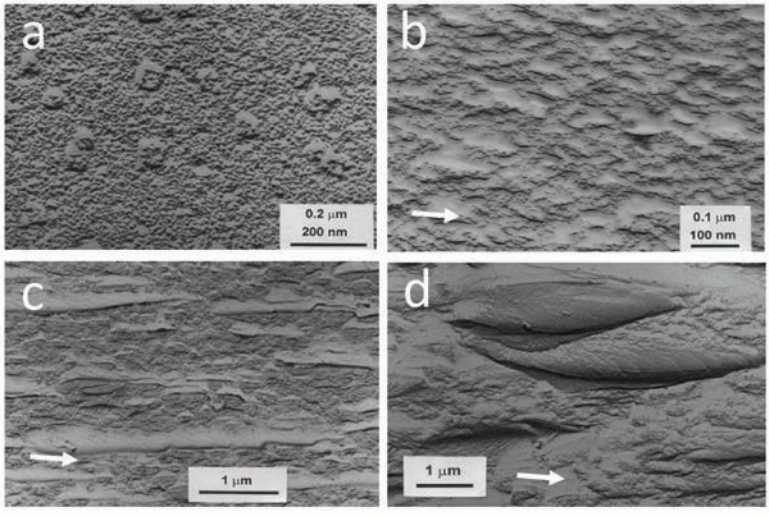


### *4.2.2 Mirror shape*

In strong specimens with much stored elastic energy, the mirror is typically circular or semicircular in shape, but deviations may also occur, for example due to surface irregularities (Quinn 2020). When fractures originate on the interior of a structure, they are usually

circular; fractures with surface origins (such as those resulting from bending loading), may have flared or elongated mirrors (Quinn 2020). As the crack accelerates from the surface origin (which was experiencing tension), it progresses through a diminishing stress field toward the neutral axis, slowing down the crack and elongating the mirror.

### *4.2.3 Mirror in ceramics*

Mirror is also seen in more structurally complex materials such as ceramics (Figure 4.3) but is less smooth than in glass because the fine detail of the fracture mirror is obscured by the larger microstructure. Mirror also does not look as smooth in composites due to their directional cracking properties and larger microstructure. For these more structurally complex materials, the mirror is identified as a region that is relatively smooth compared to the rest of the fracture surface. Mirror markings in these materials may be affected by the mode of crack propagation (i.e., whether the crack propagates along grain boundaries or directly through grains) (Quinn 2020). Mirrors may not be detectable in coarse grained materials or those with more than 10% porosity (Quinn 2020) and may be more detectable in strong versus weak structures (Rice 1973).

*Figure 4.3:*
*Mirror in zirconia polycrystal ceramic; SEM image (left) and stereomicroscopic image (right); the brackets indicate the mirror regions, and the arrows indicate the direction of crack propagation [modified from Quinn 2020]*

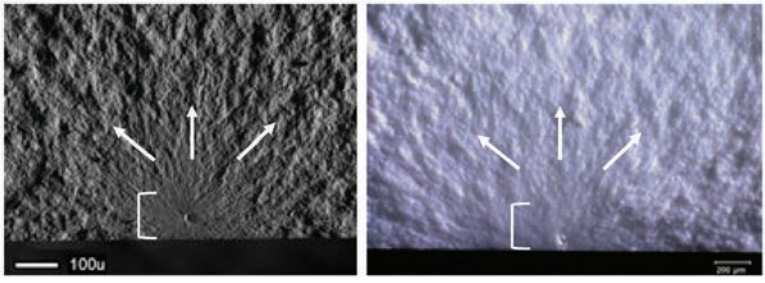

### *4.2.4 Bone mirror*

**Bone mirror** is a region at the fracture origin that is relatively flat compared to the rest of the fracture surface (Figure 4.4). As with other structurally-complex materials, bone mirror will never be as flat and smooth as in glass, and may not even be detectable due to bone's high porosity and large microstructure. But bone mirror may be identified as the most featureless portion of the fracture surface, prior to tilts and deviations from the original fracture plane. The bone mirror region indicates the location where the fracture initiated. The mirror region in bone may not be circular but may more commonly appear irregular. This is due in part to frequent failure in bending, as well as the bone mirror encountering the medullary cavity.

*Figure 4.4:*
*Examples of bone mirror identified with brackets; arrows indicate the direction of crack propagation [modified from Christensen et al. 2018a]*

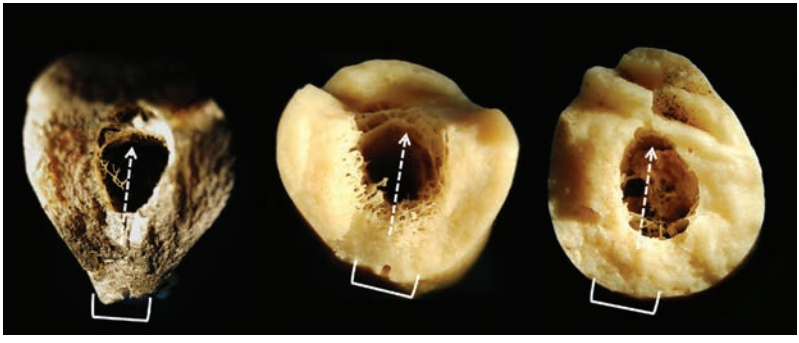

## 4.3 Hackle

**Hackle** is a broad category of surface features that includes any line on the surface of a fracture running in the local direction of cracking (Fréchette 1990; Quinn 2020), although there are many variations in degree and type.

### *4.3.1 Mist, velocity, and microstructural hackle*

In glass, mist or **mist hackle** (Figures 4.1 and 4.2) refers to the markings on the surface of an accelerating crack, observable as a misty appearance (Quinn 2020). Mist hackle is often considered a component of the mirror region in glass and is rarely observed in other materials. **Velocity hackle** refers to hackle markings formed on the surface of a crack that is propagating at close to its terminal velocity and is identified as discrete elongated steps aligned in the direction of cracking (Quinn 2020). This hackle region represents the precursor to branching since this is the region where the crack reaches terminal velocity (Bradt 2011). **Microstructural hackle** refers to broad lines that form from non-specific sources and are attributed to microstructural or geometric irregularity (Quinn 2020). This form of hackle typically occurs in porous materials, and is aligned in the direction of crack propagation (Quinn 2020). The porous microstructure or some geometric irregularity causes portions of the crack to advance on non-coplanar regions separated by rounded ridges as opposed to sharp steps (Quinn 2020) (Figure 4.5).

*Figure 4.5:*
*Microstructural hackle in ceramics: hackle lines in a coarse-grained zirconia (top) and ceramic membrane (bottom); in the top image, black arrows indicate the hackle lines and the white arrow indicates the fracture origin, in the bottom image, white arrows indicate the hackle lines and the black arrow indicates the fracture origin [from Quinn 2020]*

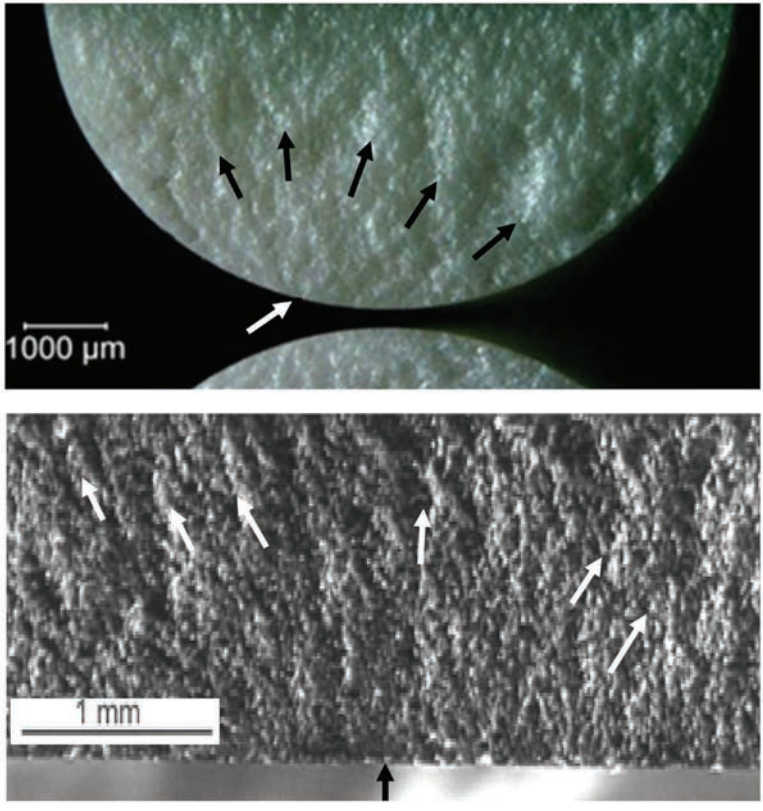


### *4.3.2 Bone hackle*

**Bone hackle** is a type of coarse hackle, appearing as angular or rounded ridges resulting from an increase in crack speed and instability. In bone, differentiating microstructural hackle from

velocity hackle may be difficult (Christensen et al. 2018a). Due to the coarse and porous nature of bone, bone hackle more closely resembles the microstructural hackle seen in ceramics than the velocity hackle seen in glass. Bone hackle may sometimes be sharp or angular, while other times it is more rounded (Figure 4.6). With either form, the ridges are aligned in the direction of crack propagation.

*Figure 4.6:*
*Bone hackle, indicated with solid white arrows; dashed arrows indicate the direction of crack propagation [modified from Christensen et al. 2018a]*

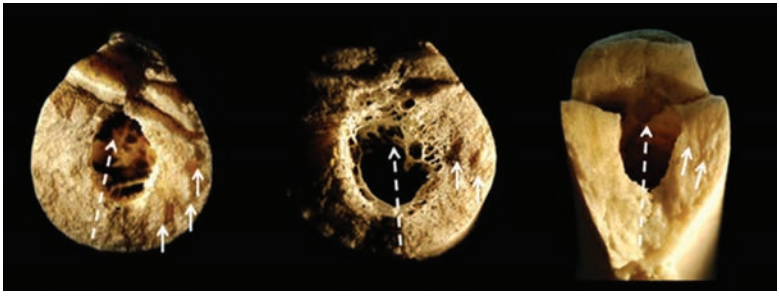

### *4.3.3 Twist hackle*

**Twist hackle** (also called delta patterns, river deltas, or lances) results when the crack passes a microstructural or geometric feature that causes a localized, lateral rotation of the principle tensile force such that a portion of the crack front twists away from the main crack propagation direction (Fréchette 1990). It is characterized by a localized series of roughly parallel ridges radiating at an angle to the main crack front (Figure 4.7). These ridges point in the direction of the localized crack propagation. Twist hackle is observed in granular materials such as silicon carbide as well as in polycrystalline ceramics. In coarse grained materials such as bone (Figure 4.8), twist hackle may not all line up the same way, as the crack takes detours through the microstructure in response to local conditions (Quinn 2020).

*Figure 4.7:*
*Twist hackle in glass indicated with black arrows; the large concentric features are arrest lines (see Section 4.5), which the twist hackle crosses perpendicularly.*

*Figure 4.8:*
*Twist hackle in bone indicated with boxes*

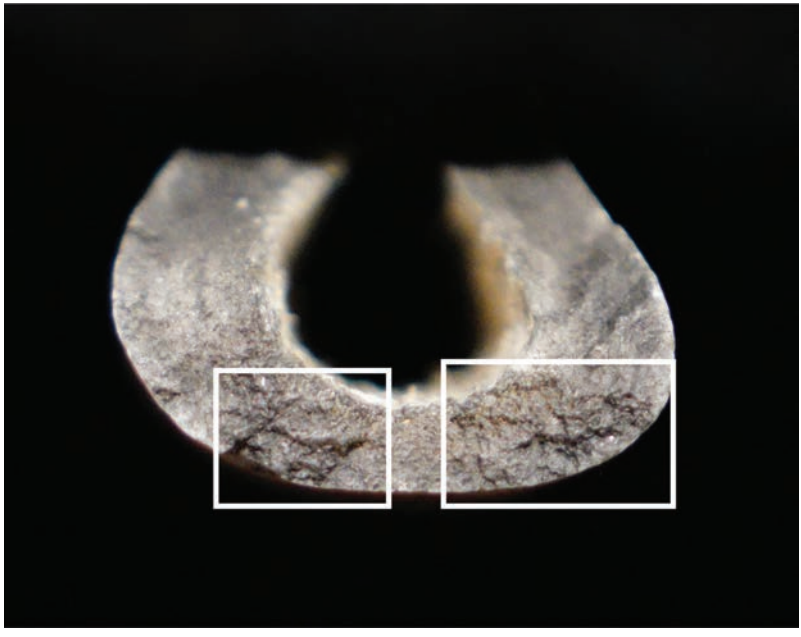

## 4.4 Wallner lines

**Wallner lines** (also called "rib marks") are curved lines on a crack surface, which are concave in the direction the crack is propagating (Fréchette 1990), marking successive positions in the advancing crack front. Wallner lines result from the intersection of the expanding crack front and an expanding elastic wave, causing the crack to ripple out of the plane like a wave on a pond surface (Quinn 2020) (Figure 4.9). Wallner lines are categorized as primary, secondary, or tertiary depending on the source of the elastic wave. Although Wallner lines have not previously been documented in bone, they can be seen in other coarse-grained materials (Figure 4.10), so it is possible they may be observed in bone. If observed, Wallner lines in bone will be expressed with the concave side facing the fracture origin and would likely require at least low-power microscopy for visualization.

*Figure 4.9:*
*Wallner lines in glass; the arrow indicates the direction of crack propagation [from Christensen et al. 2021]*

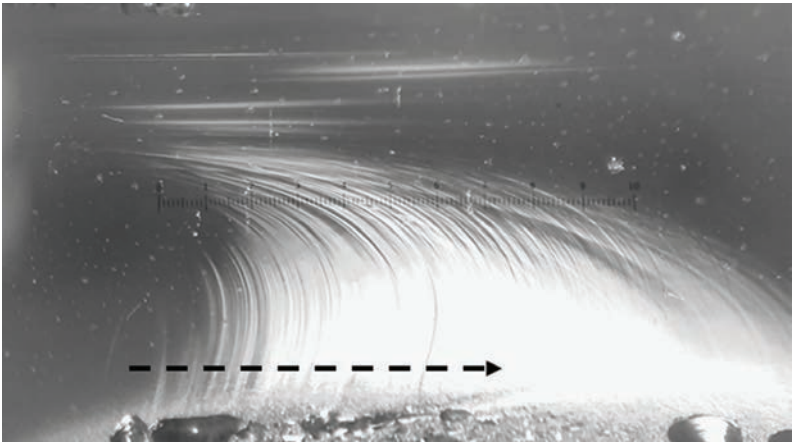

*Figure 4.10:*
*Wallner lines in a polycrystalline ceramic; the dotted line highlights a Wallner line and the arrow indicates the direction of crack propagation [modified from Quinn 2020]*

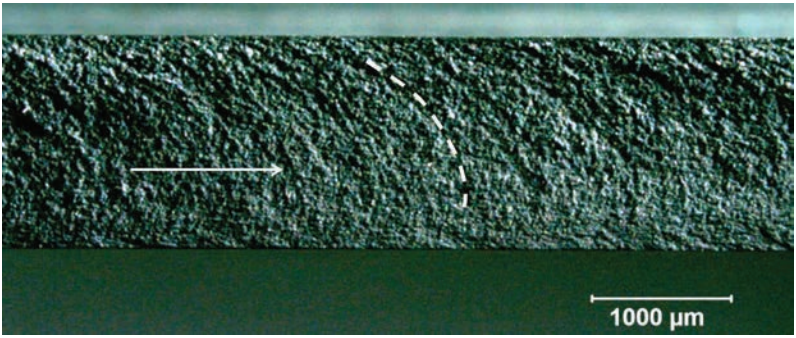


## 4.5 Arrest lines

**Arrest lines** are sharp lines on a fracture surface resulting from an arrested (or momentarily hesitated) crack prior to resumption of crack propagation under an altered stress configuration (Quinn 2020). These lines are sharper than Wallner lines and represent stepwise crack propagation (Figure 4.11). It is not necessary for the crack to come to a complete stop; the arrest lines occur because the crack progresses along a different plane, usually in response to a change in the axis of principle tension (Quinn 2020). Arrest lines may be curved or straight (Quinn 2020). Arrest lines are somewhat different from **fatigue striations** resulting from repetitive loading. These lines are produced by stepwise crack growth due to loading and unloading. These striations are not generally seen in glasses and fine-grained ceramics, but are more commonly seen in metals, with each arc-like band corresponding to a loading cycle during which a damage process occurs, with the crack jumping forward and then arresting (Quinn 2020).

*Figure 4.11:*
*Concentric arrest lines from cyclic loading of a glass plate in bending [from Quinn 2020]*

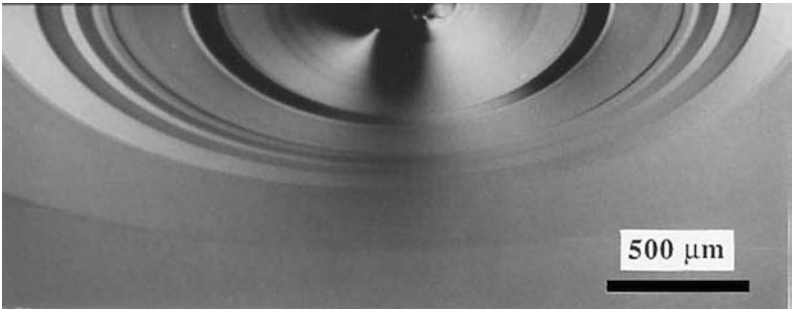


### *4.5.1 Arrest ridges*

In bone that fails in bending, there is not a distinct halt in crack propagation, but as the crack reaches the compressive side of a bending fracture, drastic changes in crack propagation velocity are experienced (cracks slow down very rapidly once they reach the compressively-loaded portion of a structure), resulting in pronounced ridges or peaks (Figure 4.12). These peaks are referred to as **arrest ridges**. Arrest ridges in bone are typically very prominent and easy to identify. They will be aligned approximately perpendicular to the direction of crack propagation.

*Figure 4.12:*
*Arrest ridges in bone; solid arrows point to the ridges and dashed arrows indicate the direction of crack propagation [modified from Christensen et al. 2018a]*

### 4.6 Wake hackle

**Wake hackle** is a line resulting from a split crack front passing an obstacle such as an inclusion or pore. It is caused by slight shifts in the angle of the propagating crack wave as it reaches the other side of the inclusion and may occur at any area along the fracture surface. The two fronts of the propagating crack wave end up slightly out of sync on the following side of the inclusion, creating a marking that is aligned with the direction of crack propagation (Quinn 2020) (Figure 4.13). Wake hackle can even be identified in more complex and porous materials where few other fracture surface features are present. In bone, wake hackle has been noted in association with nutrient foramina or other small pores (Figure 4.14).

*Figure 4.13: Wake hackle in glass; solid arrow points to a wake hackle line and the dashed arrow indicates the direction of crack propagation*

*Figure 4.14:*
*Wake hackle in bone; the solid arrows point to wake hackle lines and the dashed arrows indicate the direction of crack propagation [modified from Christensen et al. 2018a].*

### *4.6.1 Wake features*

In most materials, wake hackle is observed as a singularity (a line) in association with a small inclusion or pore around which the crack propagates. The medullary cavity of tubular bones represents a special case of an "inclusion." This large inclusion results in relatively larger differences in crack wave alignment as it reaches the other side of the cavity. This can be seen as the offset alignment of features such as arrest ridges on the following side of the medullary cavity (Figure 4.15). Both the singular line and the offset ridges are a function of the crack wave propagating out of sync or plane around an inclusion. This offset alignment of features on the following side of a large inclusion are referred to as **wake features**.

*Figure 4.15:*
*Wake feature in bone; the circle shows the central region of offset arrest ridges, and the dashed line shows the offset ridges in the direction of crack propagation [modified from Christensen et al. 2018a]*

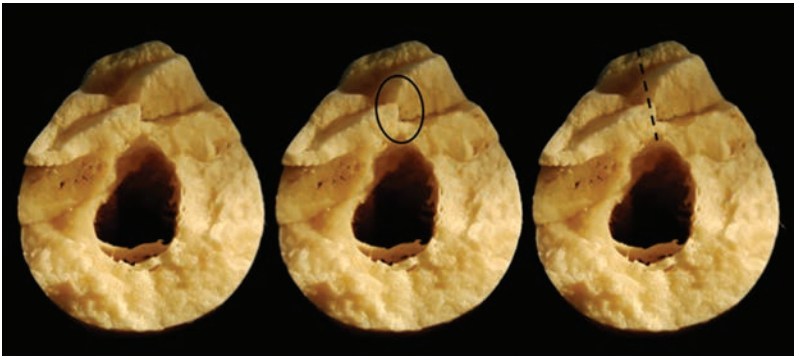

## 4.7 Cantilever curl

**Cantilever curl** (also called compression curl) is a curved lip just before terminal fracture of a body loaded in bending (the positive portion of which is sometimes referred to in earlier anthropological literature as a "breakaway spur") (Figure 4.16). After the crack propagates from the tensile side to the compression side, it experiences a deceleration in velocity and changes in direction. Cantilever curl is formed late in the fracture sequence, often due to elastic wave reverberations interacting with the slowly moving crack in its final stages of breakthrough (Kolsky 1976).

*Figure 4.16:*
*Cantilever curl on a fused silica rod fractured in bending; the solid arrow points to the cantilever curl and the dashed arrow indicates the direction of crack propagation [modified from Quinn 2020]*

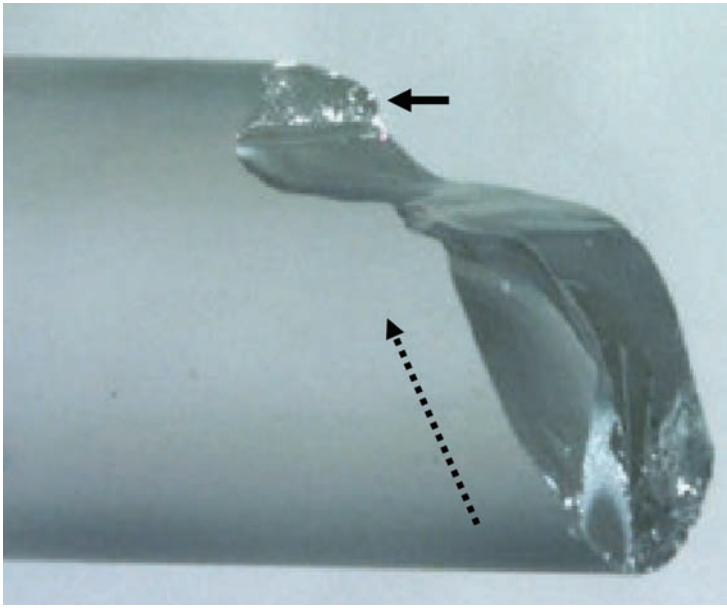

Cantilever curl is often easily identified on the compressive side of fractured bone (Figure 4.17), occurring just before terminal fracture and representing the final feature of the fracture event. In cases where branching occurs (such as in a wedge fracture of a long bone), there may be two or more cantilever curls. Cantilever curl is a feature associated with a bending fracture or a load with a strong bending component. The presence or absence of compression curl can therefore be important for interpretation of structural failures. It can indicate the location where the fracture ended (and conversely, tells you that the fracture initiated directly opposite this location), and also indicates that the bone was loaded primarily in bending. In bone, it is often the most easily identifiable and sometimes the only identifiable fracture feature.

*Figure 4.17:*
*Cantilever curl on bone; the solid arrow points to the cantilever curl and the dashed line indicates the direction of crack propagation [modified from Christensen et al. 2018a]*

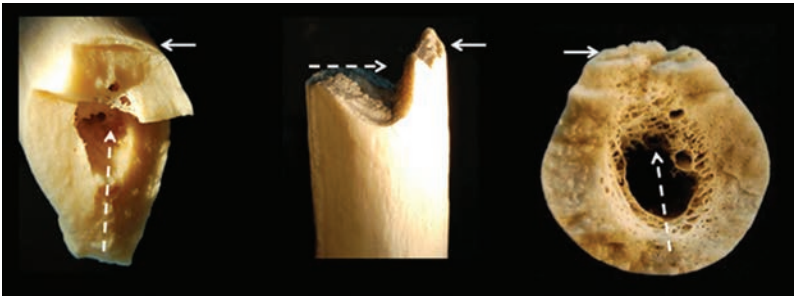

## 4.8 Other surface features

There are various other well-documented features often observed in glass, but not seen in other coarse-grained materials, that are considered unlikely to be found in bone. They will be briefly described here; readers interested in more information are directed to Quinn (2020).

**Shear hackle** is a variant of twist hackle that may appear in a hollow specimen and has been noted to have little significance in reconstructing a failure event (Fréchette 1990). **Corner hackle** is a fan-like array of hackle that is created when a crack goes around a curve (Quinn 2020). **Step hackle** is a form of twist hackle that occurs as a single arc-shaped line as a result of bending and twisting (Quinn 2020). **Scarps** are curved lines caused by the interaction of a propagating crack and a liquid, marking sudden changes in velocity due to interactions of the crack with the liquid (Quinn 2020).

## 4.9 Crack propagation direction versus force direction

Importantly, the fracture surface features described here are indicative of the direction of crack propagation, but this is not the same as (and in fact, may be directly opposite of) the direction of applied force (Figure 4.18). Many bones (particularly tubular/

limb bones) fail in bending, where the force is applied to one side of the bone causing the bone to fail in tension on the opposite side, with the crack propagating back toward the side of force application. Fracture surface features are, in themselves, insufficient for determining the direction of force application. Additional information about the fracture may be needed from fracture patterns (Section 3), or other bony or contextual evidence.

*Figure 4.18:*
*Fractured femur showing the direction of applied force, which is opposite the direction of crack propagation*

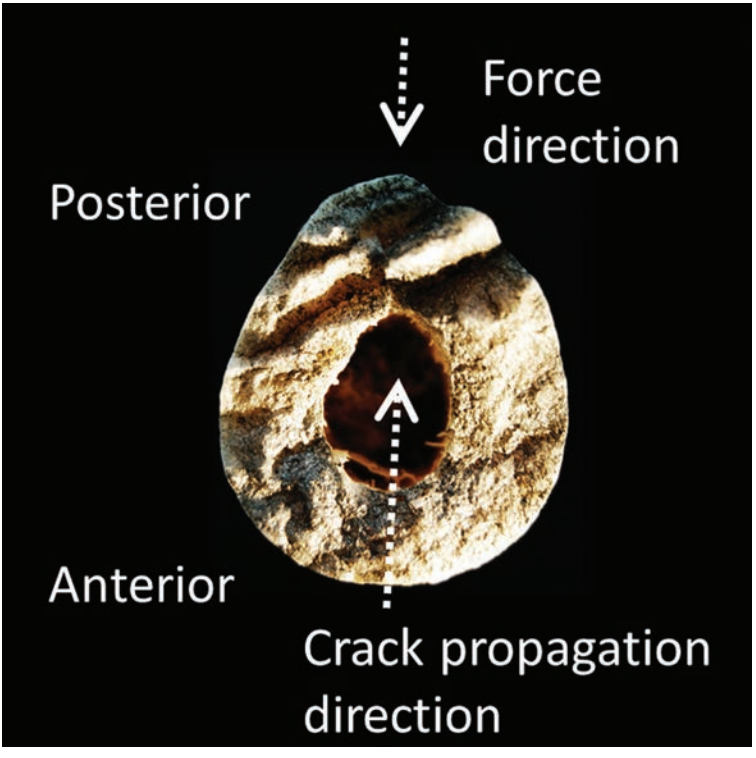

## 4.10 Summary

The fracture surfaces of a broken structure, including bone, can reveal information about where a fracture initiated and the direction the crack traveled (Figure 4.19). Certain features (such as cantilever curl) can even provide insight into the loading experienced. It is important to examine the surfaces of all available fragments to get a full picture of the fracture surface features.

*Figure 4.19:*
*Multiple fracture surface features of a femur broken in bending; solid lines and arrows point out features, and the dashed arrow indicates the direction of crack propagation*

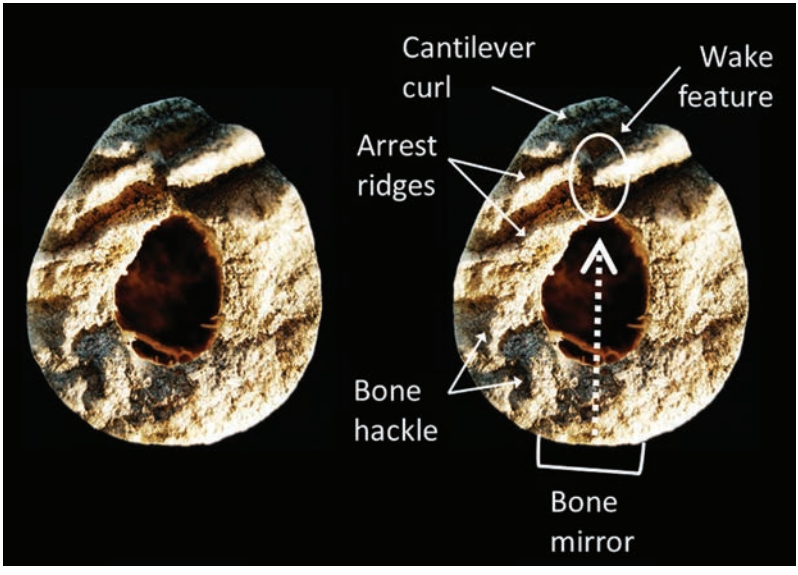

# Procedures, Tools and Equipment

## 5 Procedures, tools, and equipment

This section describes procedures, tools, and equipment used in the fractographic analysis of bone. Examination should take place on a large, clean surface with appropriate lighting and workspace. Analysis begins with a visual examination of the overall fracture pattern and fracture surfaces. Fractography can involve examination of detail at all levels of magnification from the unaided eye to the atomic level (Hull 1999). Many fractographic features in bone are visible with the unaided eye, but depending on the needs of the analysis and features of interest, examination can proceed at higher magnifications. Documentation should take place throughout the examination, including before and after processing and reconstruction. There are many sophisticated tools available to aid with visualization and documentation of fractures. Fractography, however, can be applied to bone in most cases using easily accessible equipment. The following procedures are intended as a guide to techniques that may increase the likelihood of locating and identifying certain features or patterns, with the understanding that individual cases and practitioner needs will vary, and that practitioners may find other effective approaches based on available resources.

### 5.1 Sample preparation

Broken bones should be examined and documented both before and after processing. Fragile, fragmented bone is susceptible to further damage during processing and analysis. Initial documentation with notes and photos helps to establish whether defects were present prior to the examination (Galloway et al. 2014). Fractured bones may also have inclusions or adherents that may provide clues about the fracture event specifically or the death event more broadly. Examples include the presence of hairs embedded in the bone from crushing or incision, discoloration/staining from a hematoma, differential staining that may indicate fracture timing (perimortem versus postmortem), and metal debris

or soot associated with a projectile. These materials should be documented and, if necessary, sampled prior to processing and analysis. In cases of suspected projectile trauma, remains should be radiographed prior to processing to locate and document projectile fragments. Typically, the bone (including all fracture surfaces) should be carefully cleaned prior to fractographic examination to remove any surface debris or other contaminant that may impede the analysis. The examination space should be arranged so that the bone (or portions thereof) can be completely rotated and viewed from different angles to ensure the entire structure can be observed, as well as be held steady, during the analysis.

### *5.1.1 Cleaning and processing*

Cleaning and processing are often required to remove adhering tissue, soil, floral debris, or other material from bone and expose fracture patterns and surfaces. Processing approaches should involve consideration for avoiding or minimizing alterations to bone dimensions, deterioration, production of postmortem damage to the bone, changes in bone structure, and commingling. Consideration should also be given to the fragility of the bone (e.g., burned, osteoporotic, fetal bone), and any examinations that may be performed on the bones following anthropological examination. A common principle is to apply the minimum amount of cleaning required to visualize the anatomy or features of interest (Galloway et al. 2014).

Light brushing with a dry or wet nylon brush may be sufficient to clean skeletonized remains. Dry, skeletonized bones should not be soaked in water because the drying process can create additional cracks (Galloway et al. 2014). When significant soft tissue is present, further processing is typically needed. The first step is to mechanically remove as much soft tissue as possible (sometimes with the aid of a scalpel or knife) without damaging the underlying bone. Before discarding soft tissue, it should be carefully searched for bone fragments or other potential evidence.

Many methods of debris removal can be used, and the selection of processing method may depend on the type of adhering material, the analysis being conducted, and any long-term storage or curation plans. Methods may include manual removal, cold or warm water bacterial maceration, cooking (i.e., the application of additional heat via boiling, simmering, incubating, and/or microwaving), the use of chemicals or enzymes, and processing using invertebrates such as dermestid beetles (King & Birch 2015; Steadman et al. 2006). Processing methods vary in the amount of time required, the ease of acquiring materials, the potential for damage to bone and DNA, and the suitability for long-term storage and handling. Careful research and the identification of case-specific goals will inform the choice of processing method(s).

For fresh, decomposing, mummified, skeletonized, and formalin-fixed remains, a fast and effective method of soft tissue removal involves macerating bones in a solution of water, detergent, and sodium carbonate over low heat (Fenton et al. 2003). For more fragile remains, such as subadult bones in suspected abuse cases, the use of an incubator is recommended to maintain even bath temperature without creating hotspots (Love & Sanchez 2009). Out of several maceration techniques tested, microwaving was reported to be most effective at preserving cutmarks in bone (King & Birch 2015); however, even this method was shown to alter the size and appearance of sharp force defects (Komo & Grassberger 2018).

After processing, it may be desirable to degrease specimens that will be curated or used for teaching or courtroom presentation, although this step is not necessary in most forensic cases. A warm bath of mild ammonia can help to reduce grease (Fenton et al. 2003). Other chemicals that can be used for degreasing include acetone, hydrogen peroxide, benzene, and gasoline (Steadman 2006). Bleaching methods (including oxidizers like hydrogen peroxide) should be avoided in forensic cases as they are likely to damage bone and nuclear DNA (Steadman 2006). Following

processing, skeletal material should be allowed to dry on racks or towels prior to analysis, avoiding the use of heat or moving air to dry bones, which can introduce drying-related cracks.

### *5.1.2 Specimen holders*

Activities such as notetaking, photography, using handheld magnifiers, and adjusting light sources require frequent use of one or both hands. Specimen holders can be used to position a sample during analysis, freeing the hands for these activities. Consideration should be given to the size, shape, and fragility of the specimen under investigation when choosing an appropriate holder. Examples of holders that pose a low risk of damaging bone include cork rings, bean bags, slotted foam blocks, small sandboxes, and clay. Polymer clays can be very useful for holding small specimens in position (Figure 5.1), and can usually easily be removed manually or with solvents such as ethanol or acetone (Quinn 2020). In contrast, conventional clays can blend into fracture features and are more difficult to remove.

*Figure 5.1:*
*Bone fragment held in position for examination using polymer clay*

### *5.1.3 Labeling*

A good practice is to label pieces of a broken bone using a logical system (e.g., letters or numbers proceeding in one anatomical direction, such as proximal to distal). Labels reduce the amount of time spent refitting fragments during analysis and are also useful for referencing specific fragments in notes, photos, sketches, and reports. Felt tip pens with water-soluble ink that is easily removed with alcohol or acetone are commonly used in fractography of glass and ceramics (Quinn 2020). Fine-tipped permanent ink pens have also been recommended for labeling bone (Meadows Jantz 2017), but bone is porous, and inks tend to absorb into fine cracks. If specimens will be curated or retained for further analysis, a more permanent labeling method may be necessary. One recommended approach to labeling objects in archaeological collections is a "sandwich" technique. This involves first placing a thin coat of clear reversible lacquer on the labeling area, then writing the label on top of the base coat using permanent water- or pigment-based paint, and finally applying a topcoat of clear varnish (National Park Service 2020).

## 5.2 Visual assessment

Fracture features may be observed at all levels of magnification ranging from the unaided eye to the atomic level (Hull 1999). The level of magnification applied during an analysis depends on the purpose of the examination and the type of information of interest. Questions relevant to forensic trauma analysis (e.g., directionality of force application, location of fracture initiation) may not require high levels of magnification although some level of magnification will often reveal additional features or information.

In general, fractographic assessment proceeds from lower to higher magnification and should begin with an unaided visual examination (Christensen et al. 2018a; Fréchette 1990; Quinn 2020). Examination using low-power magnifiers or with more

powerful microscopes can follow depending on the needs of the analysis. The purpose of this section is to briefly explain the tools available to assist with visual assessment and how they can aid fractographic analysis.

### *5.2.1 Unaided eye*

Analysis begins with a simple, visual assessment of fractures with the unaided eye, and should include examination of each of the broken pieces, overall crack and breakage patterns (see Section 3), and fracture surfaces (Section 4). During this stage, the initial goal is to become acquainted with the overall fracture pattern and orient the components. Many fractographic features in bone can be observed with the unaided eye, including bone mirror, wake features, bone hackle, arrest ridges, and cantilever curl (Christensen et al. 2018a; Isa 2020; Love & Christensen 2018). These features are easily visible when fracture surfaces extend across large cortical areas, such as in the femoral midshaft, but may not be apparent in elements with thinner cortical bone (Love & Christensen 2018).

## 5.3 Low-power magnifiers

Low-power magnifiers may enhance visualization of bone fracture features of interest (Christensen et al. 2018a, Love & Christensen 2018). While stereo microscopes (discussed in the next section) can also be used for this purpose, other types of magnifiers are less expensive and offer more flexibility to the user. Several types of low-power magnifiers are available. The choice of which to use will depend on various factors including the duration of the task, the level of magnification desired, and whether measurements will be taken.

The size and construction of the lens or lenses are two important factors to consider. Lens size affects magnifying power (how much larger an object appears) and field of view (visible area). Smaller diameter lenses are more curved and therefore offer higher magnifying power, but smaller fields of view. In contrast, larger diameter lenses offer larger fields of view but lower magnifying

power. Lens size also affects working distance (the distance between the object and lens required to keep the object in focus) and depth of field (the distance between the closest and farthest part of an object in focus). Larger lenses typically have longer working distances and longer depths of field than smaller lenses, making them easier and more convenient to use over long periods of time. Singlet lenses are typically less expensive than doublet or triplet lenses. With multiple lenses it is possible to achieve greater magnification and correct for spherical aberrations (incompletely focused images) and color aberrations (distorted colors at the edges of objects).

### *5.3.1 Handheld magnifiers*

Handheld magnifiers are portable, relatively inexpensive, and available in a variety of magnifications up to 30x. Typically, the magnifier is held in one hand and the specimen under analysis is manipulated with the other. A magnifying glass is one example of a handheld magnifier, comprising a convex lens mounted in a frame with a handle. The highest magnifying power is achieved when the lens is held close to the eye, but magnifying glasses can also be used at further distances. Magnifying glasses usually consist of a single, uncorrected lens. They have low magnifying power (2x-6x) and therefore do not provide significantly more information than can be obtained with the unaided eye. They may, however, make analysis more comfortable by aiding visualization while allowing for long depths of field and working distances.

### *5.3.2 Loupes*

A loupe is another type of handheld magnifier designed to be held close to the eye (Figure 5.2). Loupes typically consist of a single lens or multiple lenses mounted in a cylindrical holder without a handle. Start with the loupe positioned approximately 1 inch from your eye. With the other hand, move the specimen toward the loupe to bring it into focus, while holding the position of the loupe steady. Resting a finger or the back of the hand holding the loupe

against the face can help stabilize it. Loupes are used in a variety of settings including biology, geology, and jewelry and watch-making. Jeweler's or watchmaker's loupes consist of lenses mounted in plastic eye cup cells. The user holds the cell in place by squinting the muscles around the eye socket. An advantage of the hands-free nature of this tool is that it allows the analyst to hold the specimen in one hand and take notes with the other. Biologists and geologists often use magnifications in the range of 10x-20x to examine details of small organisms or trace minerals and grain surfaces. Loupes with singlet lenses offer magnification power from 5x-10x. Triplet lenses, such as Hastings triplets, can achieve magnifications up to 20x without significant aberration. For most applications, a 20X loupe is not recommended, because it has a narrow depth of field making it difficult to use. A 10X loupe is almost always preferable. In addition, investing in a Hastings triplet will significantly improve performance at a relatively low cost. A pocket comparator consists of a loupe equipped with an etched scale and can be used to take measurements on flat surfaces.

*Figure 5.2:*
*A loupe used to examine a bone fragment*

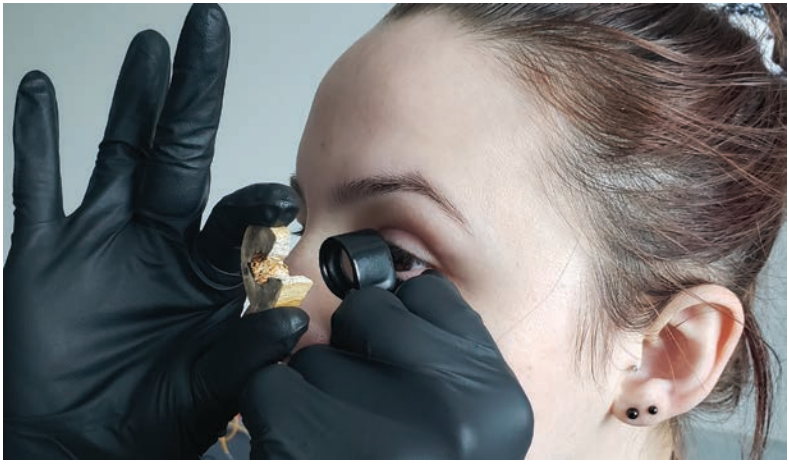

## 5.4 Microscopy

Microscopes offer higher magnification power than the previously discussed magnifying tools. Selection of an appropriate microscope to use in analysis will depend on the size of the features of interest, the level of magnification desired, and the equipment available. This section discusses different types of microscopes and the type of information they provide. Many microscopes also have photographic capabilities, which is discussed in section 5.7.3.3.

### *5.4.1 Stereo microscopes*

Stereo microscopes, also called dissecting microscopes, are low-power optical microscopes used to enlarge images of samples visible to the unaided eye. In fractography of bone, they are useful for examination of fracture surfaces between 2x and 4x magnification (e.g., Christensen et al. 2018a, Love & Christensen 2018).

Stereo microscopes use light reflected from an object's surface, making it possible to view solid objects and surfaces. Stereo microscopes (Figure 5.3) employ two eyepieces, each with its own objective lens. The offset axes of the eyepieces create depth perception and allow for magnified, 3-dimensional views. Stereo microscopes produce upright, laterally correct images that are easily correlated with specimens under observation. They have relatively long working distances that allow for examination of small or large objects, and those with pronounced topography. Placing a stereo microscope on a long mounting post makes it possible to accommodate larger bone fragments. Auxiliary attachment lenses can also be used to increase working distance. Contact between the specimen and the objective lens should be avoided, or both could be damaged.

*Figure 5.3:*
*Stereo microscope used to examine a bone fragment; polymer clay (section 5.1.2) and fiberoptic lights (section 5.6.2) are also used here.*


Different types of stereo microscope systems are available including fixed and zoom magnification systems. Fixed systems use paired sets of objective lenses with a fixed degree of magnification. In zoom systems, users can increase or decrease the degree of magnification continuously over a set range.

### *5.4.2 Compound microscopes*

Compound microscopes are high-power optical microscopes. They employ multiple lenses to achieve higher levels of magnification than stereo microscopes. The ocular lens is located in the eyepiece, while the objective lens is located close to the sample. The total magnification is the product of the magnifications of the objective and ocular lenses. Compound microscopes usually have multiple exchangeable objective lenses that can be rotated into place to adjust the magnification. Compound microscopy uses light transmitted through a sample and therefore requires larger objects such as bone to be sliced into thin sections (Figure 5.4). This type of microscopy is useful for examining the relationship between fractures and bone microstructures (e.g., Pechníková et al. 2011, 2015). Unlike stereo microscopes, which provide upright and unreversed 3-dimensional images, compound microscopes provide inverted, 2-dimensional images. This makes it more cumbersome to correlate an image with the specimen being observed.

*Figure 5.4:*
*Compound microscope being used to examine a thin section of bone*

### *5.4.3 USB microscopes*

USB microscopes are low-power digital microscopes that connect to a computer via a USB port (Figure 5.5). Whereas optical microscopes use lenses to magnify the object of interest, digital microscopes are more like web cams with high-powered macro camera lenses. They do not have eye pieces because images are displayed directly on a computer monitor. USB microscopes rely on incident light from LED lights located next to the lens. They typically include software with the ability to capture still and/or video images, as well as measurement and annotation tools (Figure 5.6). Most are sensitive enough to function without additional light sources, though fiberoptic lights may be useful for enhancing features of interest (see section 5.6.2 below).

*Figure 5.5:*
*USB microscope being used to examine a fractured bone surface*

*Figure 5.6:*
*Images taken using a USB microscope and annotated using the proprietary software, highlighting bone mirror and the initiation of bone hackle (left), and cantilever curl (right)*

Compared to optical microscopes, digital microscopes offer similar magnifications but larger depths of field, making them useful for examining 3-dimensional specimens. Typically, these devices offer actual magnification up to 25-30x; this magnification is determined by the working distance between the camera and the object. Higher magnification is achieved by increasing the image size; therefore, the maximum magnification depends on the resolution of the camera.

A major advantage of digital microscopes is that they make it easy to record, store, and manipulate (e.g., rotate or annotate) digital images. These can be useful in publications, case reports, and in the courtroom during testimony.

### *5.4.4 Scanning electron microscopes (SEM)*

Scanning electron microscopy (SEM) uses a focused beam of electrons to scan the surface of an object (Figure 5.7). The interaction between electrons and atoms at various depths produce signals that communicate information about the 3-dimensional topography and composition of the sample surface. With SEM it possible to achieve high magnifications and high resolutions, even at the nanoscale (Shah et al. 2019). SEM usually requires nonreversible preparation

of samples. Therefore, conducting SEM analysis on replicas of areas of interest is recommended (see section 5.8). Samples must be cut to a size small enough to fit in the SEM chamber. Conventional SEM units operate using high vacuum conditions and require the use of clean, dry, and electrically conductive samples (Shah et al. 2019). Bone is not naturally conductive, therefore the application of gold, gold palladium, platinum, or carbon sputter coat (see section 5.5.4) is necessary to render bone samples conductive. In contrast, environmental SEMs (ESEMs) operate using a low vacuum that does not require modification such as desiccation or sputter coating (Shah et al. 2019), and therefore can be applied to image bone surfaces directly (e.g., Freas 2010).

*Figure 5.7:*
*SEM image of bone captured as part of a saw mark analysis [image courtesy of Laurel Freas]*

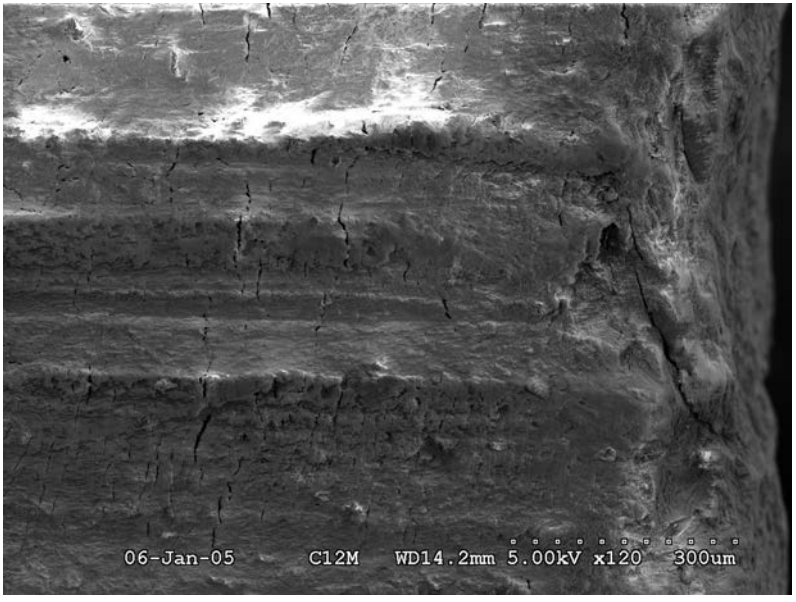

SEM has various applications in forensic trauma analysis including assessment of toolmarks (e.g., Alunni-Perret et al. 2005; Bartelink et al. 2001; Freas 2010; Saville 2007), direction of bullet travel (e.g., Rickman & Smith 2014), effects of thermal alteration (e.g., Herrmann & Bennett 1999; Quatrehomme et al. 1998), and differences between perimortem and postmortem fractures (e.g., Bradley et al. 2013). SEM has also been applied to the fractography of bone (e.g., Kimura et al. 1977; Koester et al. 2008; Martens et al. 1986; Wise et al. 2007,). These studies provide important information about bone microstructure and the mechanical properties of bone; however, the high level of magnification obtained in SEM may not be necessary or even optimal for studying forensically relevant fracture patterns in bone (Christensen et al. 2018a). This, in addition to the expense and time involved in preparing and analyzing samples, makes SEM largely impractical for standard fractographic analysis of bone.

### *5.4.5 Atomic force microscopy (AFM)*

Atomic force microscopy (AFM) is a type of scanning probe microscopy that uses a small cantilever with a sharp tip to physically probe the surface of a material. The position of the sample relative to the tip and recording height of the probe is used to generate information about the topography of the sample surface at very high (nanometer) resolutions. In biology and biophysics, AFM has been used to image and mechanically probe biomaterials such as DNA, proteins, and tissues (Thurner 2009). Atomic force microscopes are useful for characterizing the topography of very smooth surfaces, which are ill-suited to SEM. In addition to an image mode, most AFMs have a force mode that uses the AFM cantilever to measure force-distance curves, allowing for measurement of Young's moduli and other mechanical properties in very small structures (Griepentrog et al. 2013).

AFM has been used to investigate the structure of bone on a nanoscale, structure-function relationships, and differences

in mechanical properties between structures such as interstitial lamellae and osteons (Thurner 2009). Like SEM, the cost, logistical difficulties, and very high resolution of AFM make it impractical for standard fractographic analysis of bone in forensic casework.

## 5.5 Coatings

Coating fracture surfaces with contrast media can help to accentuate features or increase observable detail for fractographic examination, photography, and microscopy (Figure 5.8). Forensic fractography examinations of other materials commonly involves coating the surface to decrease reflection and increase contrast. Because of bone's light color, reflection in some cases may interfere with visualization of surface details. In forensic cases, easily reversible coatings are recommended to avoid making permanent changes to specimens.

*Figure 5.8:*
*Cast replicas of a bone fracture surface treated with various coatings; left to right: untreated, black fingerprint powder, dual contrast fingerprint powder, silver ink, gold sputter [from Christensen et al. 2018a]*

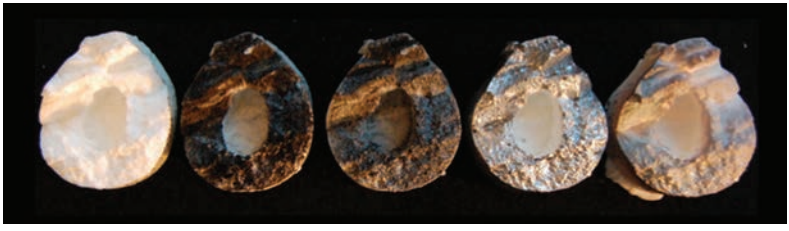

### *5.5.1. Fingerprint powders*

Fingerprint powders are typically used to develop latent prints, but can also be used to coat fracture surfaces for fractographic examination. The application of powder helps to reduce reflection and enhance contrast of fracture surface details. Black or dual contrast (silver or gray) fingerprint powder can be used for this purpose. Both types of powder reduce reflection, but black powder creates a matte effect that decreases contrast in photographs. Dual

contrast powder (Figure 5.9), which is designed to contrast with both dark and light surfaces, is recommended for use on bone because it enhances surface features without negatively affecting contrast (Christensen et al. 2018a).

*Figure 5.9:*
*Bone fracture surfaces that have been treated with dual-contrast fingerprint powder to enhance surface details*

Fingerprint powder is inexpensive, widely accessible, easy to apply, and easy to remove. A fingerprint powder brush can first be used to apply the powder loosely to the fracture surface, followed by using a nylon bristled brush (e.g., a toothbrush) to brush the powder into the surface. This step removes excess powder and ensures thorough coverage. After analysis is complete, a wet nylon brush and any common cleanser or detergent can be used to remove the fingerprint powder (Figure 5.10).

*Figure 5.10:*
*Bone surfaces that previously were treated with fingerprint powder from which the powder was later removed*

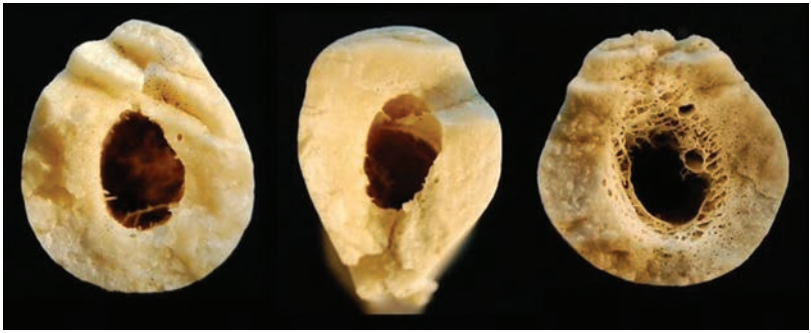

### *5.5.2 Inks*

Coating fracture surfaces with silver metallic ink (Pilot Corporation of America, Trumbull CT) also enhances details and increases contrast for visual examination (Christensen et al. 2018a). Due to the reflective nature of metallic ink, however, it may be more difficult to photograph (Quinn 2020). Ink treatments are not easily reversible and are therefore not recommended for use on bone in forensic cases. A safer alternative is to create a replica of the fracture surface (see section 5.8.) and apply the ink treatment to the replica to avoid permanent changes to the original specimen.

### *5.5.3 Dye penetration and staining*

Inks and dyes are also useful for visualizing incomplete or "hairline" cracks. Dye penetration is a form of nondestructive testing often used to search for hidden cracks in ceramics as part of fractographic analysis (Quinn 2020). The same principle can be applied to examine hairline cracks in bone. Green felt tip pens are commonly used for ceramics because the eye is most sensitive to green wavelengths and because these dyes can be easily removed with ethanol or, in persistent cases, with a 30% solution of hydrogen peroxide (Quinn 2020).

While more research is needed to understand the most appropriate penetrating inks to use on bone, some types of inks may be more effective than others at visualizing hairline cracks. Acrylic and water-based inks, for example, can effectively highlight hairline cracks in bone (Figure 5.11). Ink can be applied using a small paint brush to a small portion of the area containing fractures, with excess ink immediately wiped away with a damp paper towel. This procedure can be repeated until all hairline cracks are highlighted. Working on a small area at a time is recommended because acrylic ink is difficult to remove once dry. Felt tip pens tend to be less effective on bone, especially if the surface is slightly greasy, and more effort is required to apply the ink to large surface areas. Most inks applied to bone will be difficult to remove once dry. While some stains may be removable from smooth surfaces, inks will persist within hairline cracks and on fracture surfaces. Dye penetration should therefore be considered a non-reversible process in bone.

*Figure 5.11:*
*Bone fractures before (top) and after (bottom) treatment with acrylic ink to enhance the appearance of hairline cracks*

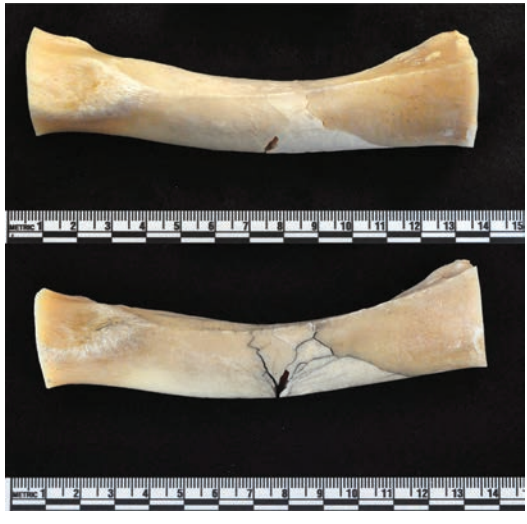

### *5.5.4. Sputter-coating*

Sputter coating is a process that uses specialized equipment to apply a thin (5-40 nm) layer of metal or another substance onto the surface of a specimen within a small vacuum chamber. Certain types of SEM require preparation of specimens with conductive gold, gold-palladium, platinum, or carbon sputter coating. The conductive coating eliminates the buildup of surface charges generated as electrons bombard the sample surface. In addition to its use in SEM, sputter coating also enhances contrast in reflected light and can aid examination with the unaided eye or optical microscopes (Christensen et al. 2018a; Quinn 2020). Sputter coat can be removed with aqua regia, but there is still a risk of damaging bone. It is therefore considered an irreversible process. As with other non-reversable coatings, it is recommended to apply sputter coat to replicas rather than original specimens.

## 5.6 Illumination sources

The angle and source of illumination are important factors to consider when observing and documenting fractures and fracture surfaces. Any visual analysis requires adequate general illumination to observe features of interest. Additionally, oblique or low angle, grazing illumination is often used to examine and photograph objects during forensic assessment (Christensen et al. 2018a). This technique positions a shallow-angled light source close to the surface under observation to accentuate texture and depth. Oblique lighting can be accomplished using a variety of light sources and can significantly enhance visualization of bone fracture surface details (Figure 5.12). Because bone is often translucent, oblique lighting can transmit light through the side of a bone, which can obscure the features on the fracture surface. Masking tape on the side of the bone closest to the light source can be used to block this effect. It is important to completely rotate the specimen when using adjusted illumination, as the light will bring out certain features better from different illumination angles. Lighting can also help to

reveal cracks that may otherwise be difficult to detect visually. For example, cracks like those discussed in Section 3 that are formed and close very quickly, or those in the vicinity of sharp impact sites. This section discusses various illumination sources suitable for use in fractography. Every sample will have its own unique lighting challenges. Users are encouraged to experiment with different lighting sources and angles before choosing a specific setup.

*Figure 5.12:*
*Bone fracture surfaces with various lighting treatments; left to right: untreated and unlit, illuminated with oblique lighting, treated with fingerprint powder and unlit, treated with fingerprint powder and illuminated with oblique lighting [from Christensen et al. 2018a]*

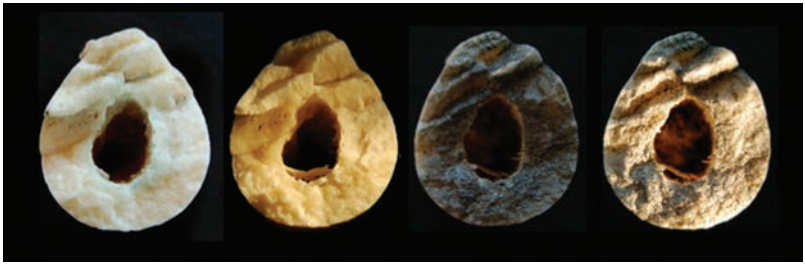

### *5.6.1. Light rings*

Light rings can be stand-alone magnifying lamps or can be a microscope accessory. Lamps are typically constructed on a floor stand, leaving the user's hand free, and also have adjustable arms for easy positioning (Figure 5.13). Microscope light rings clamp to the objective lens of the microscope and provide direct illumination to the object under observation. Both provide uniform lighting of the entire surface under observation. Unlike oblique lighting, uniform lighting on its own is not typically conducive to emphasizing texture and depth (Quinn 2020). In examinations of bone, they may not enhance visualization of surface features but may be useful for illuminating small cracks. Magnifying lamps are also not ideal for photography since the magnifier will reflect objects behind the lamp (including the user).

*Figure 5.13:*
*Light ring used to examine a fractured bone surface*

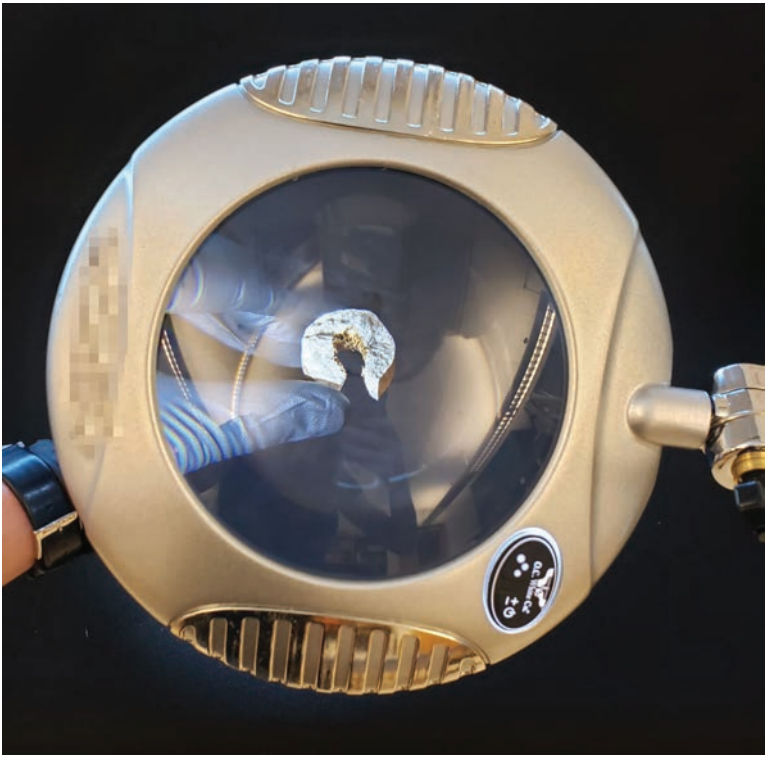

### *5.6.2. Fiberoptic lights*

Gooseneck fiberoptic lights are easily angled and adjusted and are therefore useful in producing oblique lighting (see Figure 5.3). The ability to adjust the light source is an advantage because different illumination angles will highlight different features of interest. Light sources with dual gooseneck lights are especially helpful, where one light provides general illumination while the other is used to produce low angle grazing light emphasizing surface topography (Quinn 2020). Adjustable holders can be used to adjust and secure the guides in place during analysis.

### *5.6.3. Other lights*

Other small lights (including flashlights or LED lights) may also be used as illumination sources. On most cell phones, for example, the LED light used in flash photography doubles as a flashlight. Cell phone lights can be used to provide general or angled illumination of fracture surfaces. During the examination, a stand or holder is useful to position the phone and free hands for other tasks. Because the flashlight is powered by the phone's battery, constant use will drain the battery more quickly than typical use.

## 5.7 Imaging and documentation

Technical notes for forensic anthropology casework should include sufficient information such that another practitioner could reach the same conclusions independently (SWGANTH 2012). It is therefore important to document the features that form the basis of fractographic analysis and subsequent conclusions throughout the examination. Documentation should include both written notes and visual records. Visual documentation can take a variety of forms including sketches, fracture maps, photography, and radiology. Images should be labeled such that the bone, fragment or fragments, and anatomical orientation are clear. Images should also contain a scale (e.g., a ruler or a common object of known dimensions and, if relevant, a magnification marker) to demonstrate the size of the element and/or feature under analysis.

As discussed in section 5.1, elements under investigation should be documented before cleaning and processing, and it is recommended that the overall fracture pattern – and as practical, individual fragments to be examined – also be documented after processing but before analysis. If fragments are damaged or lost, or if they are treated or altered for further examination, this record preserves their original appearance. Additionally, sketches or photographs of the overall fracture pattern are useful to reference during analysis. These images can help orient fragments relative

to the whole and can be marked up to aid in note taking during analysis. This is particularly useful in cases involving complex fractures where the analyst must examine multiple components to locate the fracture origin or establish the direction of cracking (Quinn 2020).

Documentation also plays an important role in communicating findings to other analysts, in case reports, and in the courtroom. An overall sketch or photograph demonstrates the context and orientation of a fracture pattern or fracture origin and helps others understand the analysis (Quinn 2020). Images are also useful for demonstrating the presence of and relationships between fractographic features relevant to the analysis.

### *5.7.1 Sketches*

Hand-drawn sketches aid both documentation and interpretation of fractures (Figure 5.14). Sketching is a useful exercise because it requires the interpretation of fracture patterns as they are reproduced in the sketch. Sketches are also an effective means of communicating overall fracture pattern and the orientation of fragments under analysis. They can be used to highlight features of interest in greater detail or to show the fracture origin, direction of cracking, and other relevant information. Sketches can be labeled and marked with notes to justify interpretations of features. Sketches can also be useful in large case studies and experimental research involving examination of multiple similar fractured bones. Sketching fracture patterns onto a baseline image of an unbroken bone helps standardize recording. If sketches are made it should be noted if they were made to scale and if so, what scale was used.

*Figure 5.14:*
*Fracture pattern sketch; hairline cracks are represented with dashed lines and arrows reflect the direction of fracture propagation*

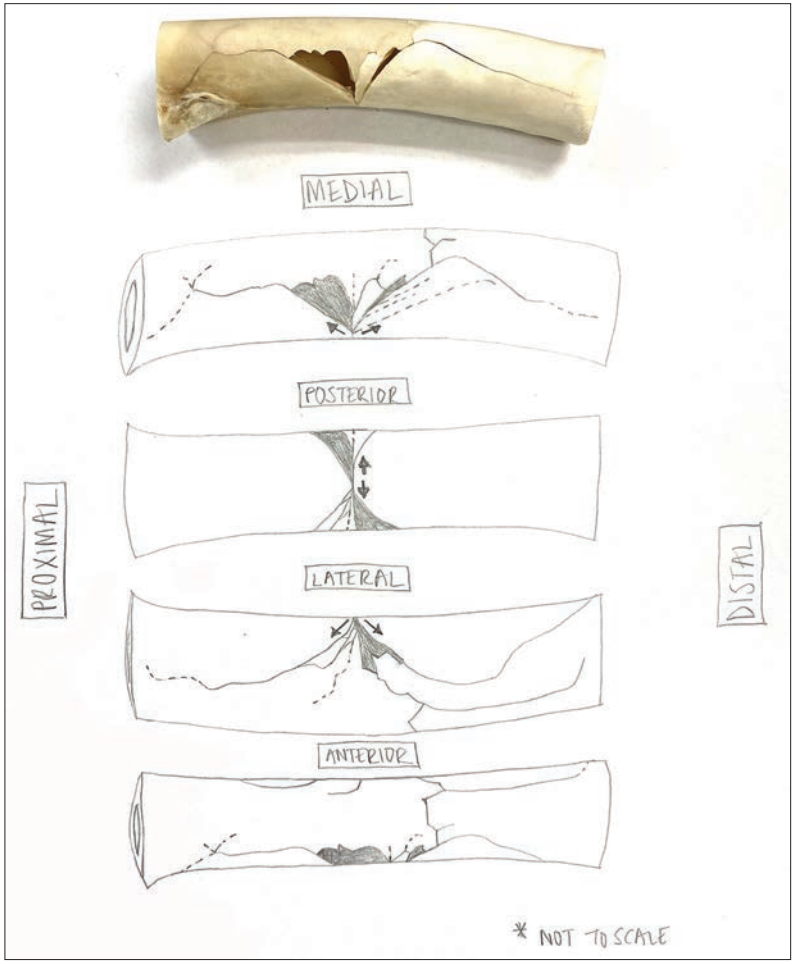


### *5.7.2 Fracture maps*

A **fracture map** (Figure 5.15) is a montage composed of local images showing small fracture details organized systematically

around an overall image (Quinn 2020). Overall images of a fracture pattern or surface are important for orienting viewers but may not communicate smaller fractographic features effectively. A fracture map addresses this by connecting local information with a global interpretation (Quinn 2020).

*Figure 5.15:*
*Example of a fracture map of a femur broken in experimental 4-point bending [from Isa et al. 2021]; solid arrow indicates loading direction and dashed arrows indicate crack propagation direction; the middle image depicting the overall fracture pattern is surrounded by images depicting more specific details from certain locations (this case is further discussed in Section 7)*

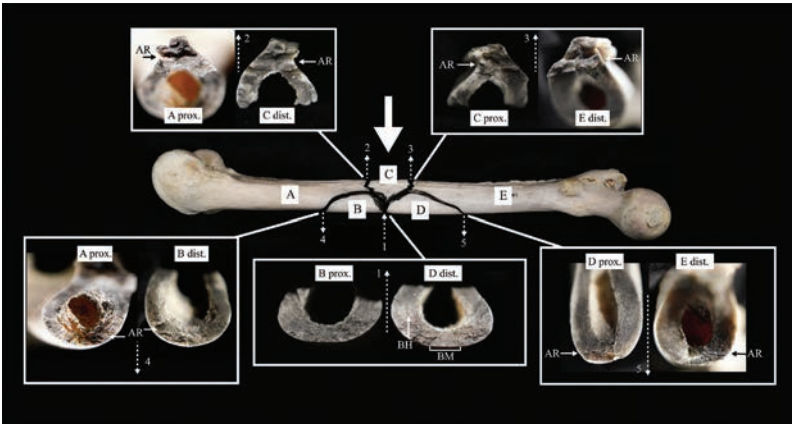


The first step in creating a fracture map is to obtain an image of the overall (global) fracture pattern or surface of interest. Each fragment or area of interest should be labeled according to the established system. Next, close-up (local) images are taken showing the features of interest. Each of these images should be labeled with the fragment or area number/letter, anatomical orientation, and features of interest such as the fracture origin and crack propagation direction. Finally, a program such as Adobe Photoshop can be used to arrange the local images around the global image to create a montage. To maximize clarity, the local images should be arranged close to their corresponding location on the global image.

A fracture map helps orient viewers to the larger fracture pattern and provides a reference for the location of each fragment and feature such that another person can easily understand the relationship between the local features and the global interpretation. This makes the analysis more transparent, demonstrates the work that has gone into the analysis, and allows others to come to independent conclusions (Quinn 2020).

### *5.7.3 Photography*

Photography is an efficient method of documenting overall fracture patterns and more detailed features of interest. Photographing against a neutral, non-reflective background and including a scale to show the size of the element or feature being photographed is recommended. Illumination is also important, and oblique lighting often helps emphasize texture and create contrast. Moving the light source relative to the subject will highlight different features, and therefore taking multiple photographs of the same element with different lighting to produce an optimal image or images is often useful.

Various types of cameras can be used to document fractographic analyses. Digital cameras and cellphone cameras create high-quality images of features easily visible with the naked eye, while microscope cameras capture smaller features in greater detail. While camera resolution (i.e. the number of megapixels in the sensor) used to be an important consideration, modern cameras, including those on cell phones, all contain sufficient resolution for all but the most specialized applications. Proper lighting and focus are more important concerns.

A typical fractographic analysis involves multiple photographs. It is important to follow a standard protocol for saving and labeling images so they are not lost and remain organized and accessible. Original files should be maintained, and file size reduced only in copies to preserve original image quality. Original files should be

labeled with information such as case number, fragment number/letter, anatomical orientation, and magnification to aid location and retrieval of specific images.

#### 5.7.3.1 Digital cameras

Digital single lens reflex (DSLR) cameras, digital single lens mirrorless (DSLM) cameras, and even simple consumer digital cameras can produce high-quality images to be used in fractographic analysis. Macro lenses produce sharp, highly detailed, close-up images of small features at close focusing distances. A 1:1 magnification ratio produces a life-size reproduction of the subject, but some macro lenses can deliver even higher magnification ratios, allowing for closer, larger-than-life shots.

#### 5.7.3.2 Cell phone cameras

Built-in cell phone cameras are easy and convenient to use and can produce quality images for use in fractography (Quinn 2020). Newer models offer high megapixel sensors and optical and digital zoom capabilities. Various magnifier apps and accessories (such as macro lens attachments) are available and can further increase magnification capabilities. It is also possible to use phone cameras to take photos through one eyepiece of a stereo microscope (Figure 5.16).

*Figure 5.16:*
*Image of a fractured ceramic bend bar, taken by holding a cell phone camera lens to one eyepiece of a stereo microscope; oblique lighting is also used here to enhance surface details*

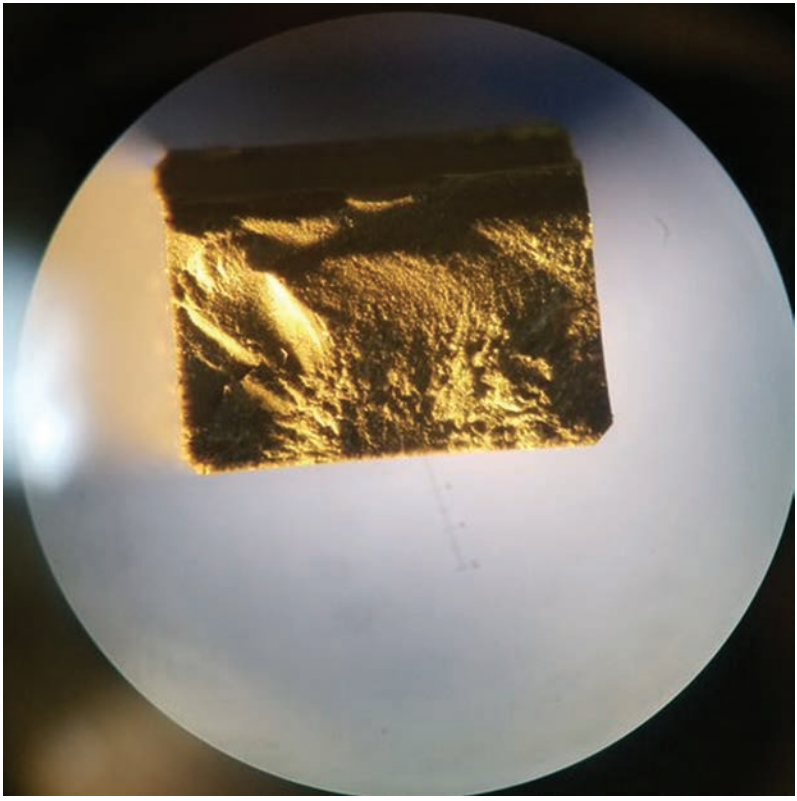

There are, however, some caveats to phone cameras. Even with higher megapixel ratings, cell phone cameras may not be able to achieve the same quality of image as DSLR or DSLM cameras. Although cell phone cameras have sufficient resolution, the automatic focus and lighting adjustments built into the software can make it a challenge to optimize the image. In addition to technical considerations, the use of personal cell phones could

present complications regarding chain of evidence in forensic cases. Analysts should also consider laboratory protocols for taking and storing images on cellular devices.

#### 5.7.3.3 Microscope cameras

Digital (USB) microscopes (such as those discussed in Section 5.4.3) have built-in camera capabilities, making it possible to easily record, store, and even annotate still images and videos. Optical microscopes are available with built-in digital camera capabilities, but these are often expensive. Attaching a digital microscope camera to a standard optical microscope may present a more affordable option. Digital microscope cameras attach to a mount or adapter on an optical microscope and connect to a USB port to display "live" images on an external monitor. These images can be acquired and saved. Standard software commonly includes robust image capture, documentation, and measuring capabilities. Magnification should be labeled on the image and/or in the file name to avoid later confusion.

### *5.7.4 Radiology*

Radiologic imaging is a non-destructive and non-invasive method of examining internal structures of many materials, including bone. Two-dimensional radiology ("x-rays") can be useful for detecting fractures as well as foreign objects in bone and other materials (Figures 5.17 and 5.18). Traditional 2D radiology (film or digital) is more widely available and more frequently utilized in postmortem examinations than 3D imaging. 2D radiology, however, has the disadvantages of silhouette effects and structure superimposition, which can make it difficult to determine the actual location of fractures or items of interest within 3-dimensional space.

*Figure 5.17:*
*2-D radiographs of a cranium (left) and partial pelvis (right); although fractures and missing bone can be seen, it is difficult to appreciate their position and orientation in two dimensions*

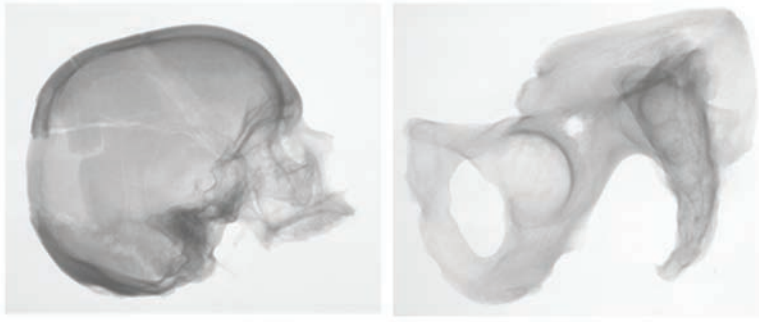

*Figure 5.18:*
*Radiology can reveal fractures in many materials including wood; an x-ray of a baseball bat reveals the presence of a fracture (white arrows). Also visible are two nails (solid black arrows), as well as the voids where two previous nails have been removed (dashed black arrows)*

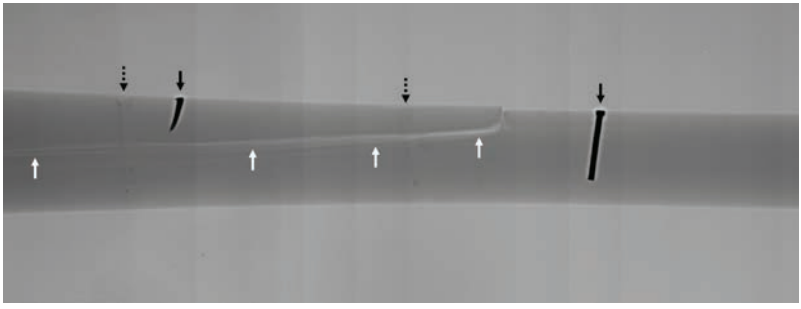

X-ray computed tomography (CT) is a particularly useful radiologic tool for examining skeletal trauma and conducting non-destructive analyses of the internal and external structures of fractured bone. CT has the advantage of allowing the analyst to reconstruct the bone or item of interest in 3 dimensions, and therefore is ideal for accurately locating and assessing fractures and other features (Figure 5.19). CT imaging also allows for the

nondestructive inspection of internal regions of bones, for example the endocranial aspect of a cranium (without having to, for example, remove part of the cranium to view the inside), as well as slice views that can be very informative (for example, see Figure 3.11). CT imaging is becoming more frequently used in medical diagnostics as well as postmortem examinations. Several types of CT systems are available, including traditional medical or clinical scanners, submicron and nano CT scanners (also referred to as 3D x-ray microscopes), and industrial CT scanners (Christensen et al. 2018b). They all use the same technology, but x-ray microscopes are typically used to analyze very small objects (usually less than 20mm). Industrial CT systems can be used for examination of whole bones with much greater penetration of dense materials, increased spatial and contrast resolution and better image quality than medical CT systems, but cannot be used to image entire bodies. Industrial CT scanners are able to image bone fracture surfaces with considerable resolution and detail (Figure 5.20).

*Figure 5.19:*
*3D reconstructions from industrial CT scans of a cranium with fractures (left) and an ulna with surgical devices (right)*

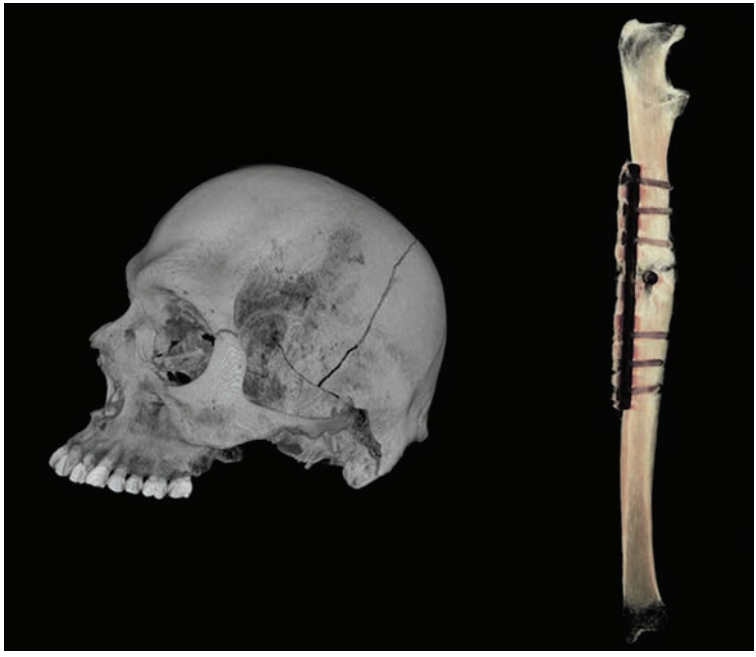

*Figure 5.20:*
*Industrial CT scans of bone fracture surfaces*

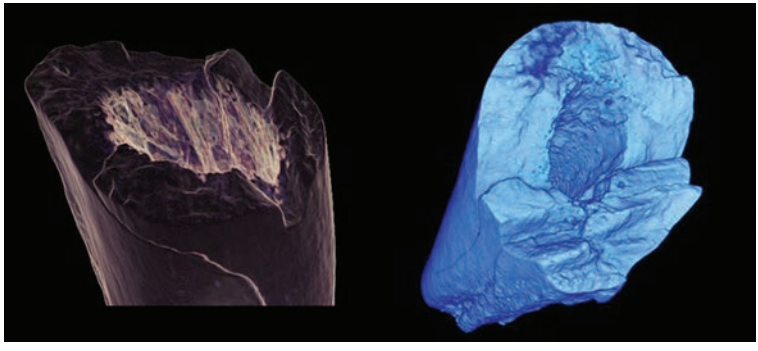

Medical CT systems have the ability to capture scans of whole/complete bodies. This potentially allows for examination and measurement of bone without the need to modify (i.e., sample and/or macerate) remains. This is useful in cases where there is significant adhering soft tissue, where remains cannot be modified, and potentially for examination of skeletal trauma in living patients (Figure 5.21). Although industrial CT scanners can produce high-resolution imaging of fracture surfaces and can be used for visualizing fractographic features (Christensen et al. 2018a) fractographic features are also visible in reconstructions generated from traditional medical CT scans, despite the lower resolution of these images.

*Figure 5.21:*
*Bone fracture surface of a trauma patient reconstructed from a medical CT scan [modified from Christensen & Decker 2021]*

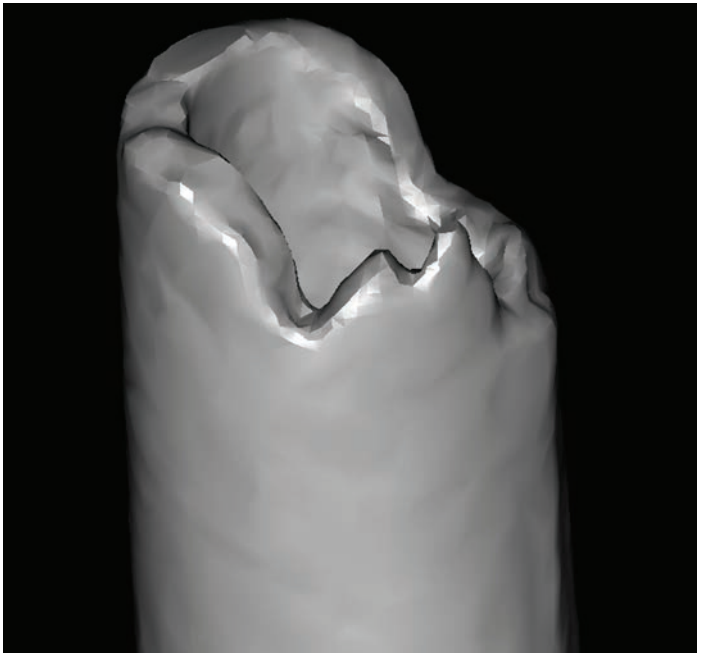

### *5.7.5 Photogrammetry and surface scanning*

Photogrammetry and surface scanners, including laser and structured light scanners can also be used for 3-dimensional documentation of broken bones and fractured surfaces (Obertová et al. 2019), though accuracy and quality depend on the method of acquisition and the settings applied (Edwards & Rogers 2018).

Photogrammetry uses mathematical methods to obtain information about the dimensions and location of an object from photographs, and can be applied to skeletal material (Lussu & Marini 2020). Two-dimensional digital photographs are taken of an object from different viewpoints (Figure 5.22). Next, structure-from-motion algorithms are applied to match corresponding features between the images and calculate angles and distances from the camera. This data is used to generate a point cloud representing the surface of the photographed object. Additional algorithms are applied to create a textured mesh that is used to create a photorealistic 3D model (Figure 5.23).

*Figure 5.22:*
*General photogrammetry set-up, including camera, light source, non-reflecting background, turntable, and calibrated photogrammetric scale bars*

*Figure 5.23:*
*An image of a bone used to create a photogrammetry model, and (inset) a screen capture of the final 3D model assembled from 160 images creating approximately 500,000 faces and 250,000 vertices [scan courtesy of Rachel Radandt]*

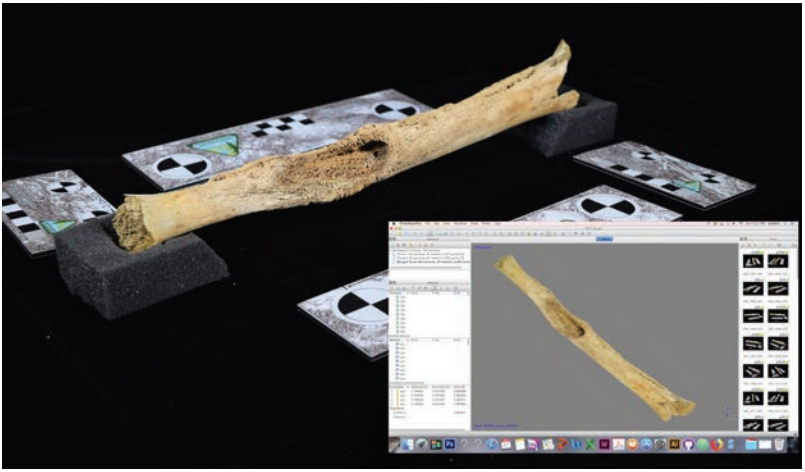

Surface scanners can also be used to create 3D images of fractured bones. Laser scanners project a laser point or line onto an object and capture the reflection of the laser with sensors (Figures 5.24 and 5.25). Trigonometric triangulation is applied to map the object's surface. Because the object is located at a known distance from the source of the laser, it is possible to calculate measurements using the reflection angle of the laser light. Structured light scanners use a combination of projectors and cameras to project and record a pattern of light on an object. Documentation of surface topography is based on the distortion of the light pattern on the object.

*Figure 5.24:*
*Handheld, high precision metrological 3D scanner using blue-light technology to capture intricate details of a bone surface; resolution up to 0.1mm, volume capture of 2000 cm3, and real time fusion of 7.5 frames per second*

*Figure 5.25:*
*A screen capture following 3D surface scanning; this is the first scan of a human tibia; multiple scans will provide more detail*

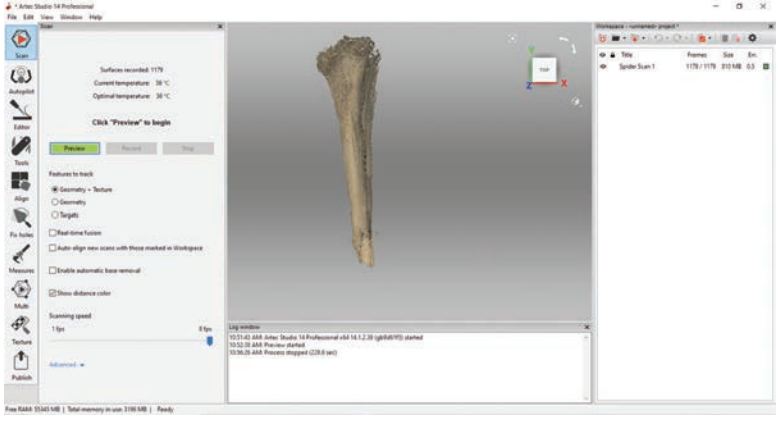

### *5.7.6 Reflectance Transformation Imaging*

Reflectance Transformation Imaging (RTI) is a photographic method that combines a series of variably-lighted photographs, enhancing surface details in an interactive digital image (Cultural Heritage Imaging 2011; Mudge 2008; Newman 2014; Schroer 2012), and has been shown to be a very effective method of examining bone surface features (Clarke & Christensen 2016). A series of flashes are reflected off black spherical balls into the camera lens, and the reflectance is encoded in each pixel of the image. These images, combined with associated software, facilitate enhancement of the surface details of an object (Figure 5.26). The ability to capture subtle surface variation details makes it particularly appealing for fractography analyses and documentation. Time and file storage may be minor limitations, but overall RTI is relatively inexpensive, easy to perform, and effective for imaging surface details on bones.

*Figure 5.26:*
*Bones with saw marks, with surface details enhanced using RTI software adjustments; default images are depicted on the left; the top right image is adjusted using specular enhancement, and the bottom right is adjusted using diffuse gain [modified from Clarke & Christensen 2016]*

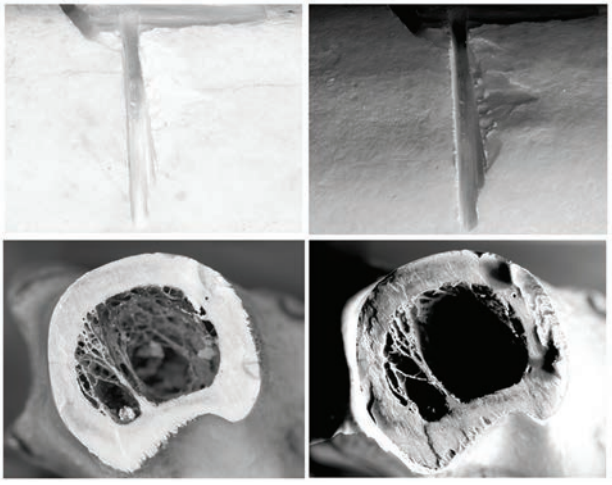

### *5.7.7 Rulers and scales*

Scales include rulers and objects of known dimensions that are included in fractographic analyses (and other forms of forensic documentation) to show the size of the element and features under investigation. While it is possible to add a scale to an image after the fact, setting the scale early helps avoid guesswork and mistakes. These can be replaced with marker bars in subsequent reports. Photographs should be taken with the scale next to the bone, fragment, or surface. Software for some microscope digital cameras make it possible to add scale bars and magnification markers to an image; it is important that the microscope and scale are appropriately calibrated.

## 5.8 Replication

Replication of fracture surfaces and other features may be useful in a fractographic analysis (Fréchette 1990; Varner 2012). In some cases, it may be impossible or impractical to examine or manipulate larger specimens under a microscope. Rather than cutting the original specimen to fit, a low-profile replica can be created as a way of examining small areas of larger pieces (Varner 2012). Replicas also preserve a 3-dimensional record of fracture surface information in the event that the original specimen is lost or damaged, or if destructive analysis is required. Replicas can also be used in the courtroom, for teaching, and potentially, for analysis. Analyses requiring permanent treatments can be performed on replicas instead of bone (Christensen et al. 2018a; Quinn 2020). For example, gold or carbon sputter coating can be applied to replicas in preparation for SEM or to enhance viewing in reflected light. In some cases, fracture surface features may be more easily observed in replicas than on the original fracture surface (Quinn 2020). Conversely, replicas may not capture fine details of the original.

### *5.8.1 Molding and casting*

Molding and casting represent one option for replicating fractures and fracture features (Figure 5.27). Molding creates a "negative" (or "reversed") replica of a fracture surface. To make

a mold, the replica material is applied over a fracture surface and then removed once dry. An impression of the mirror image of the fracture surface is preserved in the material. An advantage of a negative replica is that some depressed features like pores and cracks become raised on the replica, which make these features easier to visualize and image using SEM (Varner 2012). Casting creates a positive replica, an exact reproduction of the original fracture surface. Casting requires multiple steps. First, the negative (mold) is made. Then, casting materials are poured into the mold to produce the positive replica. Once a mold is made it can be used to make multiple positive replicas.

*Figure 5.27:*
*Silicone mold created from a fractured femur (left) which was then used to create a replica of the bone portion using a casting resin (middle and right)*

Silicone-based products are typically used to make negative replicas (Varner 2012). Filled and unfilled silicone rubber are typically used in the fractography of ceramics and glass. Filled silicone rubber is opaque. Replicas are fast and easy to make, relatively inexpensive, and set quickly at room temperature. Unfilled silicone rubber is transparent and is therefore useful for examining fractures with transmitted light. It is less viscous than filled silicone rubber and flows easily into pores and tight spaces, reducing the production of artifacts. Unfilled silicone rubber is more expensive than filled silicone rubber and sets slowly (about 24 hours) at room temperature (Varner 2012). In most cases, filled silicone rubber is likely sufficient for the fractography of bone.

When choosing a molding material, it is important to consider possible alterations to the original specimen. For example, some materials may penetrate areas of significant exposed trabecular bone, making it difficult or impossible to remove from the original specimen (Christensen et al. 2018a). Several silicone-based molding materials have been applied to well-preserved archaeological bone samples, though with some products (particularly, Xantopren and Mikrosil) leaving stains and residues on cortical bone (Dittmar et al. 2005). This may be a factor to consider when selecting molding materials. Care should also be taken to minimize or prevent the introduction of artifacts when creating a mold, for example inadequate contact between the replica material and the bone, or inclusions such as air bubbles (Varner 2012).

Once a mold is made, casting material is poured into the mold and allowed to dry. Polyurethane and epoxy resins are typically used to make positive cast replicas. Resins can be difficult to remove from fracture surfaces (Varner 2012), therefore they should be used only to create casts and should not be applied directly to bone. When the mold is removed, the cast represents a copy of the original bone and features of interest.

Many of the materials and products used in dental/tooth casting are also suitable for fractographic applications (Quinn 2020). Polyvinylsiloxane (PVS) is one material used to take impressions (negative replicas) of teeth. PVS replicas are relatively inexpensive, produce good replication of surface details, and set within minutes (Varner 2012). These impressions can then be filled with resin or plaster to produce casts.

### *5.8.2 Digital replication methods*

Fractographic details can also be captured digitally and used to make replicas (Figure 5.28). Surface or CT scan data can be used to create 3D point clouds or mesh model files. These files can be shared and/or exported to a 3D printer. An advantage of 3D printing is that it is possible to easily produce multiple life-sized positive replicas. 3D replicas based on CT images include both internal and external bone structures. These prints can be sectioned to examine the internal structure without damaging the original bone. In contrast, surface scanners collect data only on external surfaces. Therefore, the resulting 3D models will only replicate the external surface.

*Figure 5.28:*
*Fracture surface of original bone (top left), CT scan of fractured femur (top right) and 3D printed replica created from 3D CT files (bottom)*

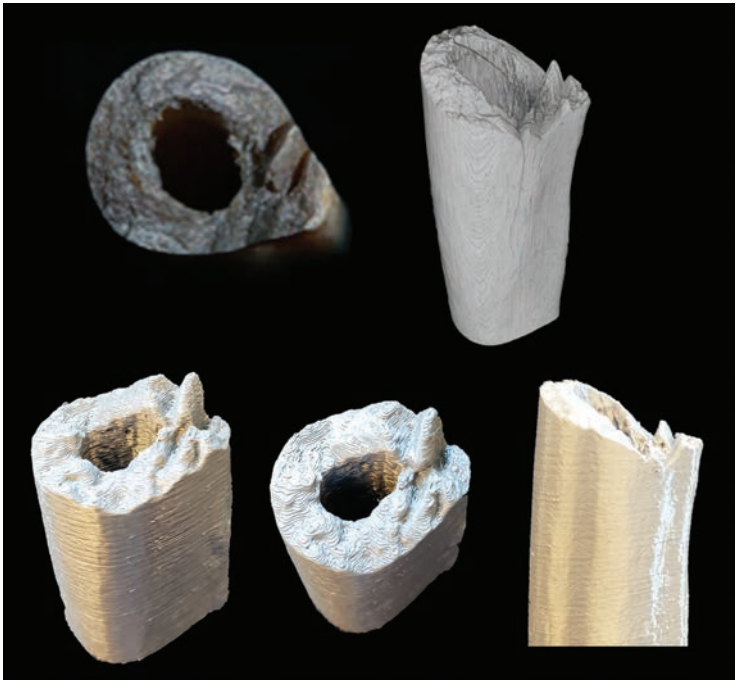

Although useful for visual demonstrations of fracture patterns, measurements of fractures taken from 3D models based on photogrammetry, laser scanning and structured light scanning may be smaller than measurements taken from bone, and fine fracture lines including fracture termini may not be reproduced in the model (Edwards & Rogers 2018).

### 5.9 Specimen reconstruction

Reconstructing fractured specimens may help clarify the fracture event, for example allowing the assessment of branching and cracking patterns, documenting the overall fracture pattern, and understand relationships between fragments. The extent of reconstruction required may be related to the energy involved in the fracture event; low energy fractures involve less branching and therefore fewer fragments while high energy fractures can involve many branching events and therefore significantly more fragments. Fragment reconstruction is a common practice in trauma analysis, and it is often tempting to immediately refit the bone fragments into their original anatomic position to visualize overall fracture patterns. Reconstruction, however, should only be performed when necessary to gain additional information, and fragments should be affixed very carefully. Attempts to physically refit fracture surfaces may alter them through abrasion or chipping. These alterations could mask fracture features or preclude accurate assessment of the fracture surface, or even damage the fracture surfaces to the extent that they no longer fit together. Reconstruction of fragments is in fact discouraged for certain materials such as metals, where bringing fracture surfaces together tends to obliterate fine details on the surface that may prevent diagnosing the fracture cause. When it needs to be performed, another material is commonly placed in between, with the pieces brought into close proximity while avoiding actual surface contact. It is currently unknown whether similar measures should be used for bone, but in any case, reconstruction of bone fragments should be performed with great care. Bone quality and the integrity of the fracture surfaces should

be considered before attempting reconstruction. When performed, reconstruction methods that are reversible without damaging the bone should be used. Fragments may need to be separated later for subsequent examination or due to unintentional errors in reconstruction.

Fragments should only be affixed when it is certain that they are correctly associated along a fracture margin. The use of a microscope may be useful in confirming the association of small fragments or in cases where the surface area joining fragments is very small. The anatomical and physical properties of the fragments and fracture surface should be given greater consideration than other factors such as color or condition since such differences may be the result of taphonomic processes or may represent evidence of trauma or other alterations. In some cases, reconstruction can reveal patterns that would be difficult to detect by examining isolated fragments (Figure 5.29). Labeling bone fragments with a numbering or lettering system can also be helpful in expediting examination and minimizing fragment-to-fragment refitting attempts. Pencils or fine-tipped markers are suggested. It is best to avoid marking on fracture surfaces or the fracture origin.

*Figure 5.29:*
*Partially reconstructed skull with thermal alterations of the cranium and mandible, especially the cranial vault; a burn pattern near the left mastoid process (right) reveals that the fracture occurred prior to the thermal event; several of the fragment labels are also seen (left)*

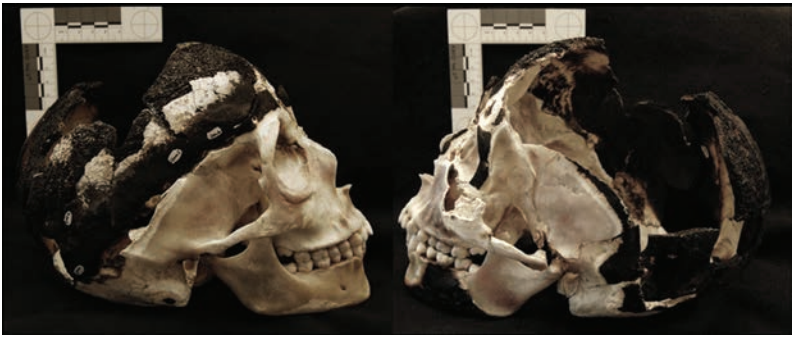

Complete reconstruction may not always be possible. In some cases, the fracture energy may be great, such that so many fragments are created that reconstruction may be impractical. Fragments that would join two other fragments may be missing, or bones may be warped due to taphonomic alterations or plastic deformation. This can be especially apparent on the skull. Since bone is more brittle in response to rapid loading, reconstruction may be easier for high-velocity impacts versus lower velocity where the bone is more likely to bend. Reconstruction should never be forced in order to correct for warping of the bone since this can lead to further damage. Bone fragment shape dictates the sequential order that fragments can be affixed; incorrect consideration of this order can result in voids that prevent additional fragments from being joined. Fragment reconstruction requires thoughtful patience; depending on the condition of the remains and the level of fragmentation, the process of locating associated fragments, affixing supports, and allowing adhesives to dry can be repetitive, tedious, and time-consuming.

### *5.9.1 Temporary reconstruction*

In some cases, it may only be necessary to hold fragments in place temporarily. This can be accomplished using adhesive tapes, wax, or clay. Bracing and stabilizing methods can also be used, for example using wooden struts or small pieces of metal to hold fragments together (Jayaprakash et al. 2017). Ideally, these should only be applied on external surfaces to avoid contamination of fracture surfaces and to avoid damaging fragile trabecular bone. Adhesives should not generally be applied to bone with friable surfaces, such as in cases involving burned remains (Galloway et al. 2014) since their removal can result in damage to the bone. Elements held together using these temporary methods are typically fragile and unwieldy, so caution should be used when moving or manipulating temporarily reconstructed bones.

### *5.9.2. Permanent or semi-permanent reconstruction*

If fragments need to be more permanently or rigidly affixed, this can be accomplished using glue or other adhesives. This should be done sparingly and using reversible adhesives (i.e., those that can be dissolved using water or acetone). Consideration should be given to forensic goals (such as examination time) as well as long term storage plans.

Paraloid B-72® is an acrylic resin commonly used in archaeological and other conservation reconstructions and is soluble in acetone. Nitrocellulose adhesives such as Duco Cement ® are easily removed with acetone but take time to dry and may also alter tissue composition, potentially affecting subsequent examination such as elemental analysis. Cyanoacrylate adhesives ("superglues") dry quickly and bond strongly (including when bones are still oily) but are nonreversible.

If glue is used, it can be helpful to stabilize the bones while the glue dries, which can be accomplished with the use of a small sandbox. Attaching smaller pieces to larger pieces first may be helpful (Galloway et al. 2014). Any application (including tapes or glues) should be used sparingly and on external surfaces only when possible. Applying glue to the fracture surface should be avoided if possible. If necessary, it is preferable to avoid applying glue to fracture origin regions, and glue should be used sparingly to avoid build up, which can lead to misfitting.

### *5.9.3. Digital reconstruction*

It is also possible to digitally reconstruct fractured bones, which is noninvasive and minimizes handling (Jani et al. 2020; Mahfouz et al. 2016). This can be accomplished using either 3D surface scanners or CT scans. Specialized software can be used to digitally process these scans, separate and label fragments, and create surface models for each. An algorithm can then be applied to align and merge

the fragmentary elements. In cases involving crushed or highly fragmented bones, CT scans taken prior to cleaning and processing preserve the presence and location of small fragments. (Mahfouz et al. 2016). The reconstructed models can then even be 3D printed for further analysis (Jani et al. 2020). CT scans can also be used to document and preserve fragile or complex, manually reconstructed bones (Christensen et al. 2018b) (Figures 5.30 and 5.31).

*Figure 5.30:*
*3D printed replica of a cranium created from a CT scan showing external (left) and internal (right) views [modified from Christensen et al. 2018b]*

*Figure 5.31:*
*CT scan of reconstructed cranium with thermal alterations; top images show the skull as received, and the bottom images show the skull following processing and reconstruction (note: this is the same cranium pictured in Figure 5.29)*

## 5.10 Summary

In bone, features relevant to fractographic analysis are often visible without magnification, though some level of magnification may help visualize some features. Simple methods including the application of oblique lighting and coating with contrast media can enhance these features. Microscopes allow for examination of features not visible with the naked eye, including those at the microstructural and even the atomic level. Documentation is an

important part of fractographic analysis. Traditional documentation methods, including notes, sketches, and photographs, are sufficient for recording fractures in bone. It is also possible to capture fracture surfaces in 3D using digital methods such as photogrammetry, surface scanning, and CT scanning. In some cases, it may be useful to produce physical replicas or 3D models for use in courtroom settings, teaching, or destructive analyses. The physical properties of trauma cases vary considerably, and it is the careful consideration of these properties that dictate which of the methods or tools described in this section will be used.

# Future Directions

## 6. Future directions

We are gaining a better understanding of bone failure and how fractography can be applied to answer forensic questions about it, but there is still much to be learned. This section discusses various paths forward, including suggestions for future research approaches and new technologies that may further enhance the application of forensic bone fractography.

### 6.1 Research approaches

Although case reports and other retrospective studies involving fractography of bone may be informative (and we encourage practitioners to publish them!), research involving controlled laboratory tests is the best approach to understanding how bone fails. In laboratory tests, the cause of the fracture is known, extrinsic factors such as impact location and applied force can be directly controlled, and intrinsic factors such as bone density and geometry can be directly measured. Several considerations for bone fractography testing are discussed here.

#### *6.1.1 Human versus nonhuman bone*

Many studies of bone fractography have involved non-human skeletal material, which may be appropriate for studying certain aspects of bone failure as a material. Human bone, however, differs in many significant ways from non-human bone, particularly in the arrangement of the microstructure as well as bone geometry, both of which can significantly influence failure. For example, the osteonal structure of human bone plays a major role in its biomechanical properties (Kimura et al. 1977), and non-human bones may behave differently due to the absence of (or different sizes or arrangements of) Haversian systems (e.g., Clifton et al. 2008). Bone geometry, for example differences in long bone curvature, have been noted to potentially affect fracture patterns (Reber & Simmons 2015). The use of human bone samples is therefore ideal in most cases for studying and understanding the relationship between crack propagation and skeletal fracture features.

### *6.1.2 Fresh versus defleshed or dry bone*

Fresh and dry bone exhibit different biomechanical properties (Braidotti et al. 2000; Nyman et al. 2006; Rho & Pharr 1999; Sun et al. 2018) and, as discussed in section 1.3.1, macroscopic changes in fracture surface topography with increasing postmortem interval have been documented (e.g., Hentschel & Wescott 2015; Johnson 1985; Symes et al. 2014). The use of dry human bone in laboratory testing can provide important data regarding crack propagation and fracture features in the postmortem interval, but these results, although appropriate for taphonomic application, may not be applicable to fresh bone.

It may be desirable to approximate failure in living bone by using fresh bone samples. It is not always possible to test fresh bone samples immediately after procuring them. Usually, it is necessary to store samples prior to testing. Wrapping specimens in saline-soaked gauze, double bagging, and freezing them is recommended for storage (Belkhoff & Haut 2008). Storage of specimens at -20° C has been shown to have minimal effects on the biomechanical properties of bone over the course of short-term storage (Hamer et al. 1996; Kaye et al. 2012; Panjabi et al. 1985; Torimitsu et al. 2014; van Haaren et al. 2008). The use of previously frozen specimens is therefore appropriate for testing fresh bone failure. If tissue will be stored long term (more than 8 months), storage at -80° C is recommended to minimize enzymatic activity (Kang et al. 1997).

Various factors related to the preparation and storage of specimens may influence the mechanical properties of bone during testing. Readers are directed to sources such as The Bone Biomechanics Handbook (Cowin 2001) for a review of general considerations in the mechanical testing of bone. Hydration, in particular, influences various properties including Young's moduli, strength, and toughness; therefore, bone should be tested in its hydrated condition to approximate in vivo conditions (Turner & Burr

2001). Keeping specimens within physiological saline or wrapped in saline-soaked gauze during testing can help prevent degradation of bone due to dehydration (Turner & Burr 2001, Kaye et al. 2012).

### *6.1.3 Laboratory test considerations*

Laboratory testing can be conducted to investigate the mechanical behavior of bone. Bone can be described in terms of both material and structural properties. As a heterogenous, hierarchical material, the material properties of bone depend on the architectural level under consideration. Testing of bone material properties typically requires the use of small specimens to ensure that the bone being tested comprises a relatively uniform material throughout. In cortical bone testing, machined test specimens are often used to control for the influences of geometry. In mechanical testing of manufactured materials, machined specimens can be created that are uniform and/or configured for secure gripping in a loading device (Figure 6.1). Specimens are cut to uniform dimensions, ground to a standardized thickness, and/or polished to remove surface defects that may act as stress concentrators. The creation of uniform bone specimens is more complicated for several reasons. Morphological variation between subjects may affect the possible size and shape of specimens, and as a graded material, the composition, structure, and mechanical properties of bone may vary between and within elements (Sharir et al. 2008). Common loading regimes in mechanical testing of material bone include tension, compression, bending, and to a lesser extent, simple shear and torsion (e.g., Evans & Lissner 1957; McElhaney et al. 1970; Reilly et al. 1974, Reilly & Burstein 1975). Bone (like many other materials) typically fails under tension, and this loading regime is therefore desirable and common in laboratory tests. Direct tension is conceptually one of the simplest loading configurations, but in practice can be difficult to achieve and would not represent real-world circumstances of bone failure. Flexure/bending tests are typically easier to perform as well as more practical and realistic for bone.

*Figure 6.1:*
*Direct tension test*

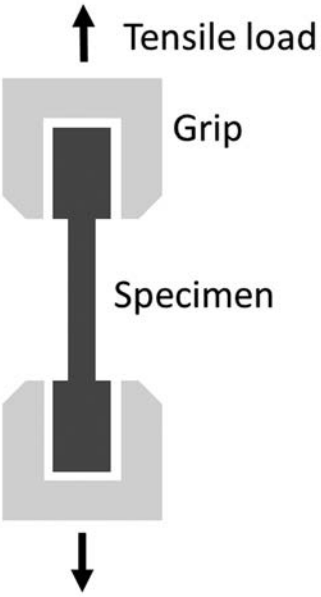


In addition to material properties, structural geometry plays an important role in the mechanical response of whole bones. Whole bone testing is used in mechanics to investigate the relationship between load and deformation, and in forensic research to investigate the relationship between known loading parameters and fracture patterns. Three-point and four-point bending are the most commonly used tests for whole bone specimens (Figure 6.2). In real-world failures, however, bones are typically subject to other and/or more complex loading regimes. In addition to bending, laboratory testing has been used to investigate various whole bone loading conditions including torsion (Frick 2003; Klenerman 1969), combined bending and axial compression (DeLand 2013; Ivarsson et al. 2009), combined bending and torsion (Frick 2003), and impact

testing (Isa et al. 2019; Kress et al. 1995; Kroman et al. 2011; Rabl et al. 1996; Yoganandan et al. 1995). To date, experimental studies of whole bones have largely described general fracture patterns while ignoring the fracture surfaces of bone. The application of fractography to fractures produced under experimental loading conditions may be of interest in future research.

*Figure 6.2:*
*Three-point (top) and four-point (bottom) bending tests*

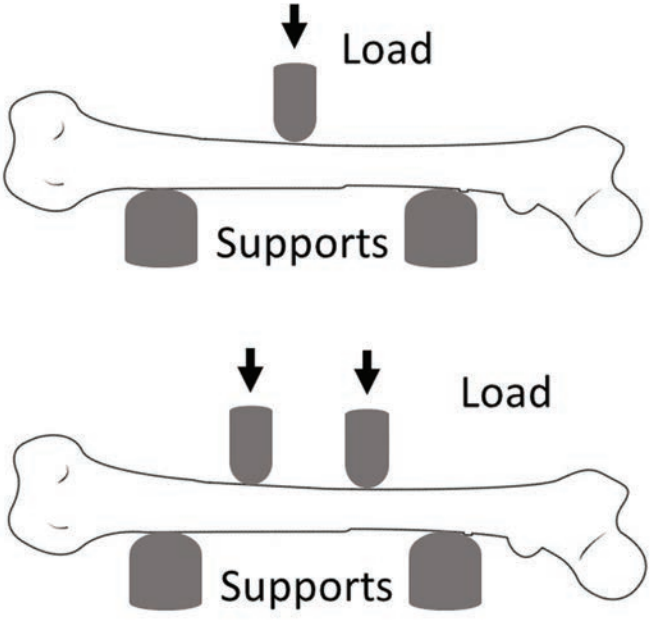


Fracture testing will often result in the creation of bone fragments. All of these fragments should be recovered, and the original conditions should be reconstructed or interpreted from these fragments. The use of a containment or shielding material around the bone can prevent the dispersion of fragments and

ensure a complete recovery. Orientation or location information such as loading points can also be marked on the bone prior to fragmentation/fracture. Such markings can help with later specimen orientation or reconstruction.

## 6.2 Research needs and ideas

Forensic bone fractography is a very new field. There is certain to be much more that will contribute to our understanding of bone failure in forensic contexts and how fractography can help to reconstruct the fracture event. In other materials, fractographic features have been shown to vary with several intrinsic and extrinsic factors. Forensic fractography of bone would benefit from qualitative and quantitative investigation of these relationships. Understanding these relationships represents an important first step for addressing forensic questions related to skeletal fracture including how and where force was applied and the properties of bone at the time of fracture. The following sections discuss some potential areas of study, which we hope will inspire and guide researchers and practitioners interested in learning more.

### *6.2.1 Visualization enhancements*

Various powders, inks, and dyes are discussed in Section 5 for enhancing the surface details of fracture bones. Many of these, such as ink penetration, may prove to be promising new methods for analyzing fractures, documenting evidence, and presenting results and conclusions to others. Application of acrylic or water-based ink has been shown to be a fast, effective, and inexpensive method for enhancing crack branching patterns in bone to aid in analysis and photography. A limitation of this method is that once dry, inks persist within hairline cracks and in the crevices of fracture surfaces. While removal methods are still being tested, initial results indicate inks cannot be entirely removed from bone even with chemicals (e.g., hydrogen peroxide, acetone, or ethanol). Additional research is needed to evaluate alternatives that perform similarly well but

are more easily removed than the inks already tested. There may also be other and perhaps better ways to facilitate visualization of fractographic features that have not yet been explored. Some of the techniques already discussed are non-reversible and potentially damaging to bone, so any new applications should be tested experimentally prior to use in casework. Additional research into advanced imaging technologies may also reveal new methods that do not involve the direct application of materials to the bone.

### *6.2.2 Other bone types and trauma mechanisms*

Much work on forensic fractography of bone has involved bending of long bones. Although there have been a handful of studies investigating fractography of projectile trauma and of other bone types (e.g., Lillard & Christensen 2020; Rickman & Shackel 2019a,b), more research is needed to better understand the applications of forensic fractography to other bone types (e.g., crania, ribs) as well as to other trauma mechanisms (e.g., projectile, sharp, thermal).

Research investigating fracture surface features has largely focused on long bones (Christensen et al. 2018a; Christensen and Hatch 2019; Isa et al. 2020; Lillard & Christensen 2020; Love & Christensen 2018). While long bones have relatively large proportions of cortical bone, a decrease in cortical area due to smaller overall bone size or a higher proportion of trabecular bone may limit the amount of information available on fracture surfaces (Christensen et al. 2018a, Love & Christensen 2018). Fracture surface features have not yet been studied from a forensic perspective in flat or irregular bones, which have significantly less cortical area than long bones. Conversely, cone cracks have primarily been investigated in sandwich bones (Rickman & Shackel 2019a,b). More research is necessary to clarify how these features and others form and appear in different bone types, and to determine the utility and/or possible anatomical limitations of fractography for bone.

Another area in need of exploration is the application of forensic bone fractography to different loading regimes (see section 6.1.3), including different trauma mechanisms. Research on the forensic fractography of bone has primarily focused within the spectrum of blunt trauma. One topic of interest is whether fractography features are also present in bones broken under other circumstances. For example, a recent study demonstrated that informative fracture surface features are also present in bones subjected to high-velocity projectile trauma (Lillard & Christensen 2020). Fractography has yet to be formally applied to the assessment of fractures associated with sharp or thermal trauma. Thermal fractures, in particular, are not yet well understood from a fractography perspective, and would benefit from additional study. Another topic of interest is the relationship between parameters such as the direction, angle, velocity, and surface area of loading and the appearance, frequency, location, and orientation of fractography features. This will require prospective, experimental studies in which extrinsic variables can be controlled and/or directly observed.

Additionally, while research has shown macroscopic and microscopic differences between perimortem and postmortem fracture surfaces (Wheatley 2008; Wieberg & Wescott 2008) as well as between traumatic and thermal fracture surfaces (Herrmann & Bennett 1999), forensic fractography of bone as presented in this guide has yet to be applied to investigate these differences.

### *6.2.3 Radial crack lengths*

There are many quantitative approaches to failure analysis in other materials. Although no quantification has yet been applied to forensic fractography of bone, it is possible that some of these calculations (or modifications thereof) may be applicable to forensic assessments of bone, but much more work is needed. In other brittle materials, for example, the lengths of radiating cracks are understood to have relationships to several intrinsic and extrinsic factors (see Section 3). Specifically, the sums of the lengths of

cracks radiating from an indentation site have been found to be correlated with the applied load as well as the material toughness.

The relationship between crack length and material toughness was first described by Palmqvist (1957); subsequently, a number of different formulae have been derived to relate crack length to toughness parameters. Typically, these tests are conducted using an indenter and a test force. For example, a Vickers hardness test is conducted using a Vickers indenter (Smith & Sandland 1922), which is a pyramid-shaped indenter with a square base and 136° between opposite faces (Figure 6.3). The resulting crack length tests are used to measure toughness in hard metallic materials. It has also been shown that for a material with a well-defined toughness and not displaying significant R-curve behavior, the surface crack length is proportional to the indenting force to the 2/3 power (Roebuck et al. 2008). Bone toughness is fairly well understood, so further investigation of radial cracks in bone may also reveal relationships between crack lengths and the applied load.

*Figure 6.3:*
*Cracks propagating from an impact site with a Vickers indenter; the sums of the lengths of the cracks are related to the indentor load and the material toughness*

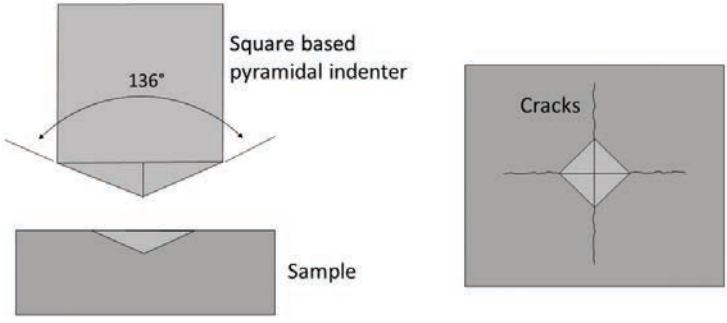


At present, radial cracks are used primarily in interpreting the impact location on bone, but this additional information may be

useful in understanding the amount of force/load required to create fracture patterns with given radial crack lengths, assuming a particular impactor geometry (indenters and impactors that occur in casework, of course, typically lack the well-defined geometry of hardness test indenters). A recent study using pig femora found that increased impact velocity resulted in a greater number, length, and degree of curvature of cracks produced (Cohen et al. 2016). Further research is needed to investigate these relationships in human bone.

### *6.2.4 Cone crack geometry*

Cone cracks can result from impacts (see Section 3), the angles of which vary depending on several factors including projectile velocity. In other materials, the relationship between projectile velocity and cone crack angles is known and therefore the velocity of the impactor can be estimated based on the cone angle. For example, a 0.8 to 1 mm steel ball traveling at 250 m/s creates 60 to 80-degree cone cracks in glass, and 70 to 90-degree cracks in silicon carbide (Akimune 1990; Chaudhri 1985; Knight et al. 1977).

Differences in projectile impact angle (specifically whether the projectile impacts the bone perpendicularly or tangentially) can affect the overall geometry of the defect (for example, a round defect versus a "keyhole" shaped defect). Little work has considered what factors might affect the angle of the cone or bevel produced by projectiles (Figure 6.4). One study of cone cracks in sandwich bones measured cone angles, finding that there was considerable overlap in angles across different projectile velocities (Rickman & Shackel 2019a). This suggests there may be significant contributions to cone angle from factors other than velocity, including intrinsic features of the material. Further experimental work is needed on the angle of beveled fractures in bone to establish the intrinsic and extrinsic factors that influence bevel geometry and angle.

*Figure 6.4:*
*Differences in cone angle (typically measured as the half-angle of the cone) in a sandwich bone*

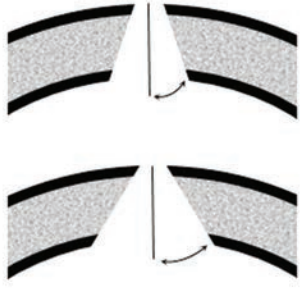

### *6.2.5 Mirror size*

There are a number of well-developed quantitative studies in the fractography of other brittle materials related to mirror size (e.g., Choi & Gyekenyesi 1998; Kirchner et al. 1976). In glasses and ceramics, for example, there is a relationship between the size of the mirror region and stress at the instant of fracture; the smaller the mirror, the larger the stress at the origin. This relationship is mathematically described using the equation:

$$\sigma\sqrt{(R)} = A$$

where σ is the tensile stress at the origin at the instant of fracture, R is the mirror radius, and A is the mirror constant (considered a material property), which can be either the mirror-mist boundary or inner mirror, $A_i$, or the mist-hackle boundary or outer mirror, $A_o$.

Mirror can be difficult to identify in bone (and quite possibly even more difficult to measure), and the mirror constant for bone is currently unknown. It is likely, however, that a better understanding of the relationship between mirror size and stress state in bone may help improve interpretations from bone fractography analyses by providing information on the absolute or at least relative stresses involved in an impact event.

### *6.2.6 Branching distance and angle*

Similarly, there is also a relationship between the distance a crack travels before branching and the stored energy of the structure; the greater the stored energy, the shorter the distance to branching. When the crack is traveling through a field of constant stress, the relationship is:

$$\sigma\sqrt{(R_b)} = A_b$$

where σ is the stress, $R_b$ is the branching distance (radius), and $A_b$ is a material constant called the fracture branching constant. A comprehensive list of mirror and branching constants for glasses and ceramics can be found in Quinn (2016). Fracture branching constants may depend on structure geometry and stress state (Hull 1996; Shetty et al. 1983).

Branching angles can vary with stress state, structure strength, structure geometry, loading configuration, and the number of branching events. Branching events are commonly seen in skeletal fractures (most notably, wedge or "butterfly" fractures often observed from bending in long bones – see Section 3) but little is known about how these might be interpreted in forensic contexts.

### *6.2.7 Effects of reconstruction*

For some materials including metals, physical reconstruction of fragments is discouraged because bringing fracture surfaces into direct contact risks obliterating fine details on the surface. Reconstruction is a common practice in forensic anthropology, and can be very useful in visualizing overall fracture patterns. While bone is harder and more brittle than many metals and perhaps less prone to such alterations, the effect of reconstruction on fracture surface features of bone is currently unknown. Studies investigating whether reconstruction significantly alters bone fracture surface details would be beneficial. In the event that such alterations are a risk, alternative methods of reconstruction could also be explored.

## 6.3 Technologies

Certain technological innovations may also facilitate forensic fractography research and application. Several are discussed here, though there are undoubtedly many others, which we encourage practitioners and researchers to explore.

### *6.3.1 High speed photography*

High speed photography (Field 1983) can be a very useful tool in studying fractures. The first extensive use of this approach in fractography was applied to glass and helped determine the terminal velocity of cracks in soda lime glass (Schardin & Struth 1937). More recent studies have used high speed photography to study the relationship between radial and circumferential fractures and the impact velocity and material thickness in laminated glass (Chen et al. 2013). Studies of impact fractures in bone have also benefited from high speed photographic techniques, clarifying issues such as remote crack initiation (Isa et al. 2019) (Figures 6.5 and 6.6) and the forming of cone cracks (Rickman & Shackel 2019 a,b). It is likely that high speed photography and videography have many other useful applications for the study of bone fractography.

*Figure 6.5.*
*Fracture origin in bent bone shown in still frames from a combined loading experiment (3-point bending with compressive axial loading) performed on a human femur; the impact anvil was applied posteriorly at the midshaft; Panel 1: initiation in tension, Panel 2: fracture branching, Panel 3: angulation of fracture branches along the longitudinal axis, Panel 4: fracture termination on the compression surface [modified from Isa et al. 2018]*

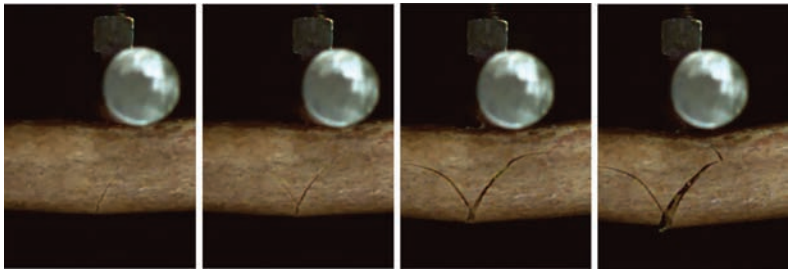

*Figure 6.6:*
*Remote crack origin in a cranium shown in still frames from an experimental cranial impact with a 1.125-inch diameter aluminum implement; Panel 1: a linear fracture originates in the inferior temporal (A) and propagates toward the impact site (B), Panel 2: a ring fracture encircles the impact site (A and B), Panel 3: the implement begins to penetrate the bone at the impact site, Panel 4: a linear fracture travels from the point of impact and propagates anteriorly (arrow) [modified from Isa et al. 2019]*

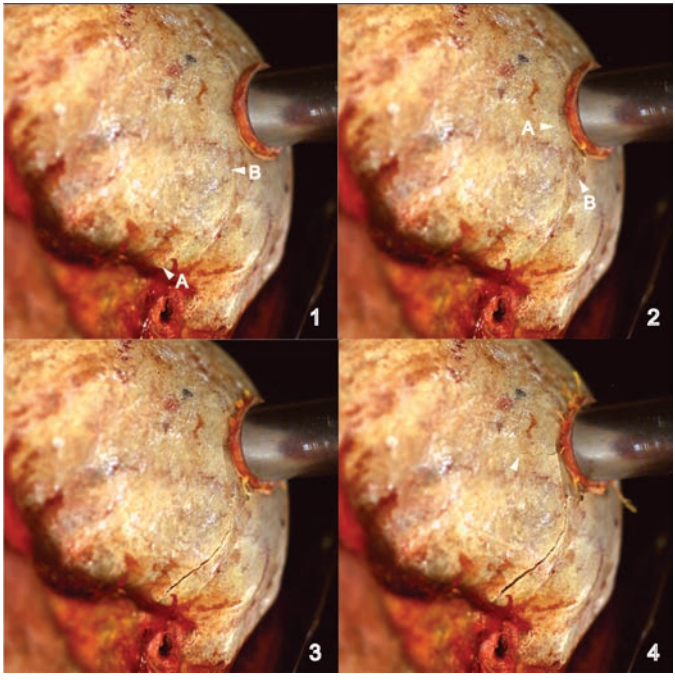


### *6.3.2 Imaging technologies*

Advanced imaging technologies have been used extensively to study bone and trauma, and have been applied in various anthropological studies and examinations. Some of these approaches have also been used in studies of bone fractography. For example, high resolution CT scanning has been shown to capture fracture surface features and cracks very well (Figure 6.7), and even traditional medical CT scans have been shown to reveal

fracture features that can be used to apply fractography (Figure 6.8). Because of the reduced resolution in postmortem and medical CT scans (compared with direct observation or microCT scans), some surface features may be more difficult to detect. If, however, it is known prior to the scan that the fracture surface will be assessed, it may be possible to increase the scan resolution in this region.

*Figure 6.7:*
*High resolution microCT scan of fractured femur surface; bone mirror, arrest ridges, cantilever curl, and crack branches are readily visible*

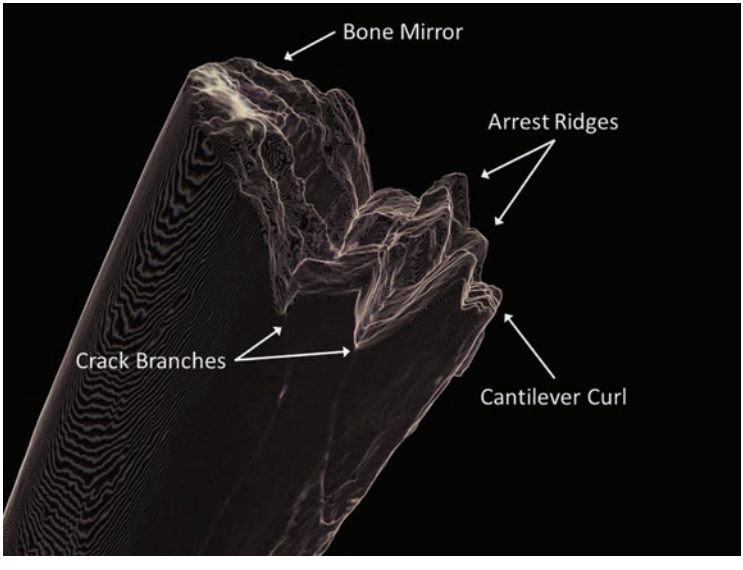

*Figure 6.8:*
*Postmortem CT scan of a fractured femur in a motor vehicle accident victim performed at a medical examiner's office as part of a routine forensic workup, with fracture surface isolated using proprietary software; bone mirror, arrest ridges, and cantilever curl (solid arrows) are readily visible, allowing an interpretation of crack propagation direction (dashed arrow) [modified from Christensen & Hatch 2019]*

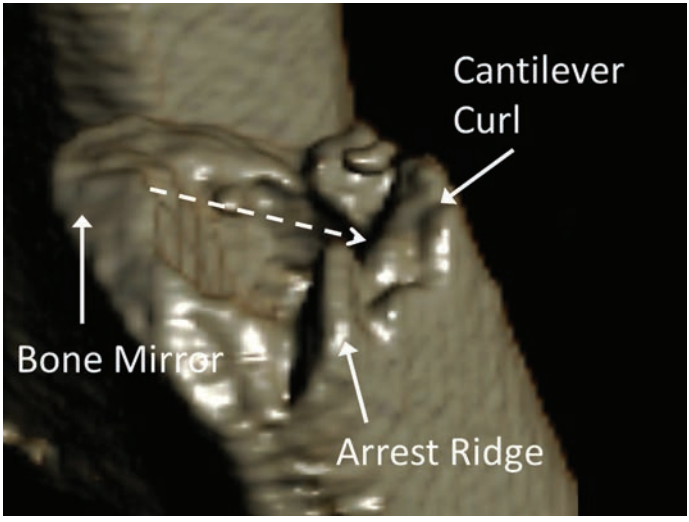


### *6.3.3. Digitization*

Digitization may aid in quantitative fractographic analysis of bone. Many forensic anthropology labs have access to a digitizer, a tool used to record the locations of landmark data in 3-dimensional space. While anthropologists primarily use digitizers to gather craniometric data, this technology can also be applied to record and measure fracture patterns (Cohen et al. 2016, 2017). Digitizers can be used to measure fracture lines directly on reassembled bones. This allows for the collection of 3D coordinates of deviation points along each segment of a fracture line. From this data it is possible to calculate parameters such as fracture segment lengths and total fracture length (Cohen et al. 2016, 2017), and may also be useful in calculating branching angles and distances.

### *6.3.4 Machine learning*

Recent advances in the field of fractography have involved the use of machine learning and artificial intelligence to automatically detect, classify, and quantify textures, defects, and other features from images of fracture surfaces. With machine learning, computer algorithms use sample data (a "training set") to build a model for making predictions or decisions. These models can then be applied to novel data to perform an intended task. Advantages of machine learning include the ability to automate tasks and reduce observer bias associated with visual inspection. In fractography, machine learning has been applied to various tasks including characterizing fracture types (Bastidas-Rodriguez et al. 2016) identifying, counting, and measuring dimples of viscous detachment (Konovalenko et al. 2018), and classifying crack growth mechanisms (Tsopanidis et al. 2020). Machine learning may also have applications for quantitative fractographic analysis of bone, such as identifying and counting particular features or flaws, classifying and measuring regions (e.g., mirror and hackle regions) of a fracture surface, characterizing branching events, and more.

While machine learning can remove observer bias and be an accurate classification tool, depending on the machine learning method used, the salient features that permitted it to be accurate may not be discoverable or revealed to the user. Nonetheless, a method with a very high correct classification rate indicates that there is information that was detected that would permit success and justify additional research.

## 6.4 Summary

Forensic fractography of bone is a new field that abounds with research possibilities. From studies to better understand how bone fractures initiate, to technologies to improve visualization and interpretation of fracture patterns, there are endless opportunities for research that could be applied to forensic fractography of bone.

We hope that the current limitations and suggestions provided in this section serve to inspire and motivate practitioners and researchers to explore this exciting new area.

# Conclusions and Case Examples

## 7 Conclusions and case examples

Brittle materials often display fracture patterns recognizable even to a relatively inexperienced analyst. While some patterns may be more subtle or require more sophisticated equipment or experience to identify and interpret, this guide makes it clear that with a little practice and a few basic tools, fractography can be used to examine and interpret skeletal fractures and improve the overall quality of the forensic anthropological analysis. This final section offers some summary thoughts and guidance and provides several case examples to illustrate some applications of fractography.

### 7.1 Suggestions for further practice and study

As with most things, the more fractography you do, the easier it becomes. Indeed, practitioners with more experience identify a greater number of overall fractographic features (Christensen et al. 2018a). Readers interested in improving their fractography skills are encouraged to examine as many fractured specimens as possible. This could include not only bone, but any fractured materials or structures. Self-guided hands-on experience can be quite valuable. A broken coffee mug or drinking glass can now become a great training opportunity! Take the broken pieces to your microscope and appreciate the patterns you now see! You can make tubular structure fractures by breaking large crayons, or curvilinear surface fractures by impacting a hardboiled egg (vary the size of the impacting surface or the rate of loading). If nonhuman bones are accessible, they can be broken and studied to try to identify the origin of the fracture. Several useful guides on fractography of ceramics are available and serve as a good introduction to the science, its nomenclature, and the application of fractography to fracture analysis. For example, the NIST Recommended Practice Guide (Quinn 2020) provides a very comprehensive resource to fractography of glass and ceramics. The study of these materials can provide a solid foundation for the fractography of other brittle materials.

Forensic fractography of bone involves an integration of knowledge from a variety of sources to determine how a fracture occurred. A fractographer should possess a strong working knowledge of the microstructure and mechanical properties of the material they are studying (in the case of forensic anthropologists, bone). This information is generally part of any thorough forensic anthropological training or education program. Additionally, some knowledge of fracture mechanics and other engineering fields is very useful. For anthropology students (or professionals seeking additional knowledge), this may require pursuing courses in engineering departments or other seminars, short courses, or self-study. Many of the engineering principles in this guide have been simplified, but resources are certainly available for those interested in learning more. In certain complex cases, consultation with an engineer may also be useful. An aptitude for problem and puzzle solving is also an asset.

It is hoped that this guide has demonstrated both the utility of fractography for forensic analysis of bone, as well as how readily it can be applied. Fractography-based assessments of bone should not replace other anthropological analyses of skeletal trauma, but rather should be used in conjunction with examination of other fracture characteristics such as missing bone, discoloration, measurements, and intrusive materials/substance/residues. The most thorough and accurate analysis of skeletal trauma will result from utilizing all available evidence relating to the bone's failure and considering the total bone trauma pattern within its recovery and anatomical contexts. Keep in mind that there is a triad composed of 1) fracture patterns and features, 2) intrinsic material properties, and 3) extrinsic factors of the failure event. Knowledge of two of these components can be used to reasonably infer the third.

### *7.1.1 Training exercise using broken glass*

A glass fractography training exercise was created by striking a glass vessel with a hammer (Figure 7.1). The glass fragments

were first laid out on brown paper and roughly traced. Each fragment was then examined using a stereomicroscope. The act of reconstruction can easily damage fracture surfaces and should not be done unless it is probative, and only after the fracture surfaces have been examined and documented; as a training exercise, however, reconstructing can be invaluable practice. After the fracture surfaces of this broken vessel were analyzed and labels added, the fragments were reconstructed and held in place using adhesive tape. Arrows indicate the direction of crack propagation, and letters indicate whether the crack initiated on the inside ("I") or outside ("O") of the vessel. The reconstructed fragments display a complex pattern that suggests significant secondary breakage (i.e., fractures not due to the initial impact).

*Figure 7.1:*
*Glass vessel that was broken and reconstructed as a training exercise*

The remainder of this section reviews several case studies and describes the utility of a fracture map that may facilitate interpretation and explanation (for example in a report or testimony) of fractographic analyses of bone.

## 7.2 Case examples

In this section, several case studies are presented in which fractography is used to assess and clarify a fracture or trauma event. While bone fractures are emphasized, examples from forensic contexts involving other materials are also presented.

### *7.2.1 Inclusion in glass*

A tempered glass window installed in a new building fractured (Figure 7.2). The window was quite high up and the cause of fracture was questioned, initially speculated to have resulted from a bb gun or wind-driven debris. The location of the origin fragments was easily identified by the fragment morphology (including its larger size and greater number of sides compared to the other fragments; see Section 2.1). Where the two fragments meet, a grey speck was identified in the middle of the tension layer. This speck was later confirmed to be a nickel sulfide inclusion in the glass and was determined to be the cause of the fracture.

*Figure 7.2:*
*Overview of fractured tempered glass window (left); the two origin fragments can be identified by their morphology (top right, origin fragments indicated with arrows), and the inclusion can be seen between them (bottom right, inclusion indicated with an arrow) [images courtesy of Mary K. Holden and Pepperdine University]*

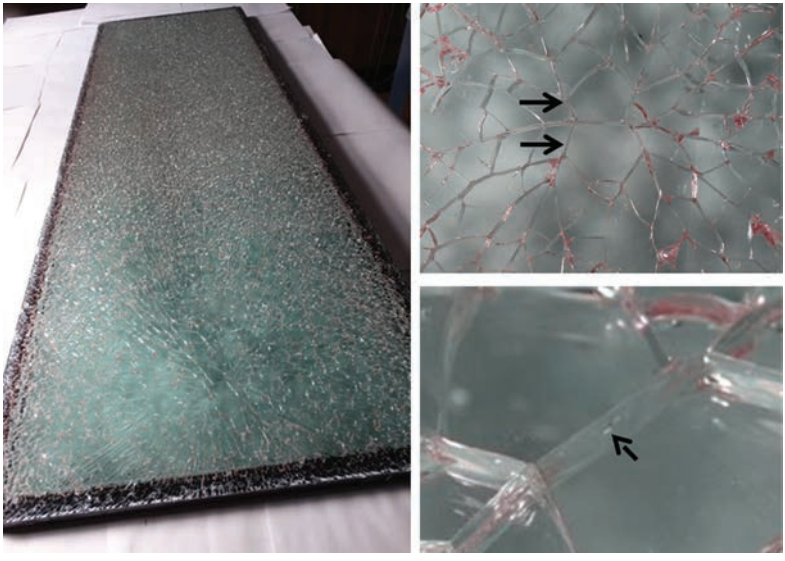

### *7.2.2 Comparison of fracture surface features with autopsy findings*

This case was reviewed as part of a case series aimed at comparing fracture surface features with autopsy findings and traditional forensic anthropology analyses including gross soft tissue, skeletal, and radiologic findings (Love & Christensen 2018). A six-year-old male was struck by a car after running into a roadway and was pronounced dead upon arrival at the hospital. The left femur was fractured, and a segment was retained following autopsy for anthropology consultation. Fractographic assessment by two anthropologists revealed a prominent cantilever curl on the lateral fracture surface, arrest ridges oriented anterior-to-posterior, and hackle oriented medial-to-lateral (Figure 7.3). These findings

indicate that the fracture initiated on the medial side, traveling from medial to lateral, suggesting that the bone was struck on the lateral side (impact direction from left to right). This finding was corroborated by the autopsy findings including abrasions on the left lateral leg and buttocks and pronounced subcutaneous hemorrhaging of the musculature of the left lateral thigh, leading to the conclusion of a left lateral leg impact. Previous anthropological analysis noted two branching ("butterfly") fractures (one complete, one incomplete) with apices on the medial surface indicating a medial side fracture initiation, consistent with the fracture surface findings (Figure 7.4). In this case, fresh and complete bone along with soft tissue presence makes the diagnosis somewhat straightforward, but also demonstrates how much of the same information can be gained by examination of the fracture surface. This is especially important given that many anthropological examinations do not have the benefit of soft tissue analysis (or sometimes even all bone fragments) to complement skeletal analysis.

*Figure 7.3:*
*Proximal surface of the left femoral shaft fragment in posterior-inferior view with the linea aspera at the top of the image (A) and inferior (B) views; solid arrows in A indicate arrest ridges, and the circle marks the cantilever curl; solid arrows in B indicate bone hackle; dashed arrows in both images indicate the direction of fracture propagation [from Love & Christensen 2018]*

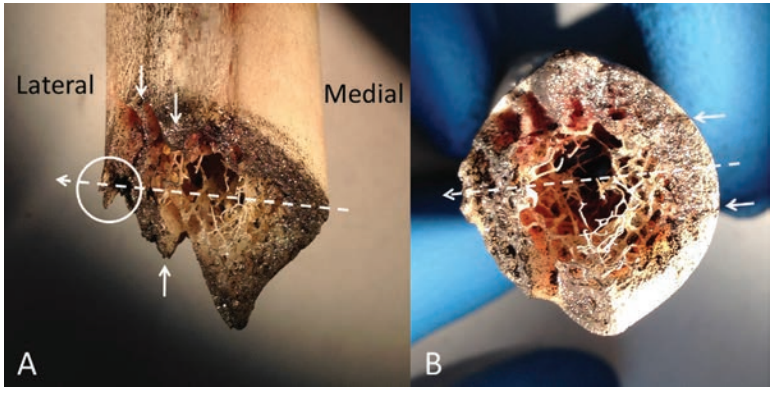

*Figure 7.4:*
*Posterior surface of the left femoral shaft, with proximal toward the top of the photo; the white arrow indicates an incomplete branching fracture with the apex toward the medial surface of the bone; the black arrow is marking an incomplete fracture that is part of the distal branching fracture pattern [from Love & Christensen 2018]*

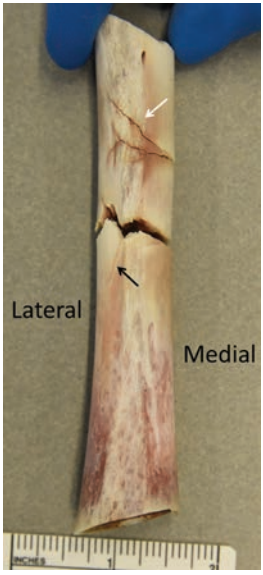


Of note here: For those practitioners working within medical examiner offices (or having access to their cases), such cases may also provide a training/education opportunity. If the trauma event is well understood based on other evidence (autopsy, context, etc.), the bones can be examined from a fractography perspective to understand how these features are associated with the details of the known trauma event.

### *7.2.3 Cranial blunt trauma with radial and circumferential cracks*

In this case a blunt impact resulted in significant comminution of the posterior cranium and numerous associated fractures

including radial and circumferential (Figure 7.5). In cases where the impacting object has a large surface area, radial cracks may not necessarily lead back to a central location/point, but following the radial cracks will still lead back to the impact region. Arc-shaped cracks near the point of impact may be an incomplete ring crack, as portions are internally beveled as observed on a CT scan, but other circumferential and concentric fractures can be seen more remote from the impact region (Figure 7.6). In this case, CT scanning played a significant role in both interpreting the fracture patterns (from both ectocranial and endocranial views) as well as preserving the reconstruction of the bone fragments. Plane slice views seen in the CT scan also revealed fracture patterns that could not have been appreciated visually or using 2D radiology (Figure 7.7).

*Figure 7.5:*
*Blunt impact with a large surface area object to the posterior cranium; a CT scan of the cranium as received and prior to fragment reconstruction (left); photo of posterior cranium following reconstruction (middle); while radial cracks (right, white dashed lines) do not meet together at a singular point, they lead back to the impacted area where the cracks began, and circumferential (or possibly ring) cracking roughly follows the margin of the impacted area (right, black dashed line)*

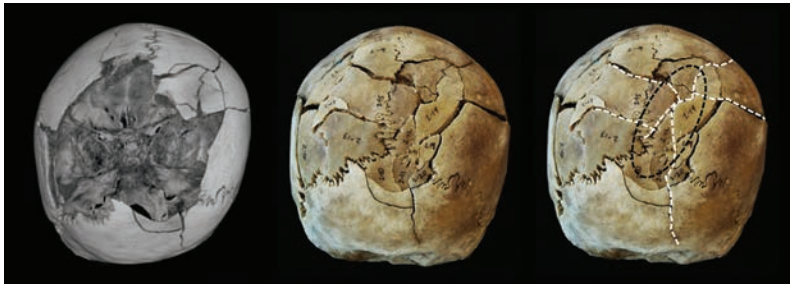

*Figure 7.6:*
*A CT scan of the reconstructed cranium helps in visualizing fractures (left), including concentric fractures (middle) as well as allowing visualization of the fracture pattern from the endocranial surface (right)*

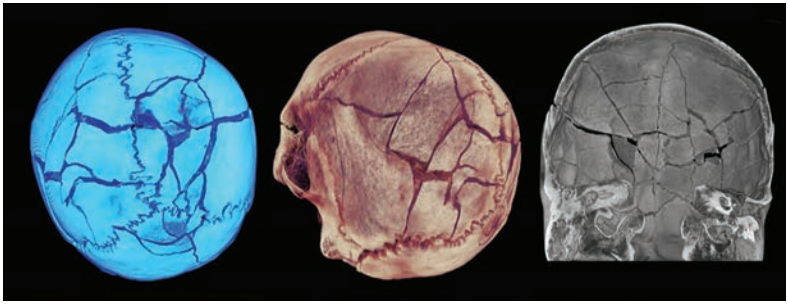

*Figure 7.7:*
*A plane slice view of a section of the trauma region reveals fracture patterns that could not be appreciated with a visual examination; posterior view of reconstructed cranium showing slice location (left); slice view (middle), and closeup of one section showing a series of angled/beveled fracture lines (right)*

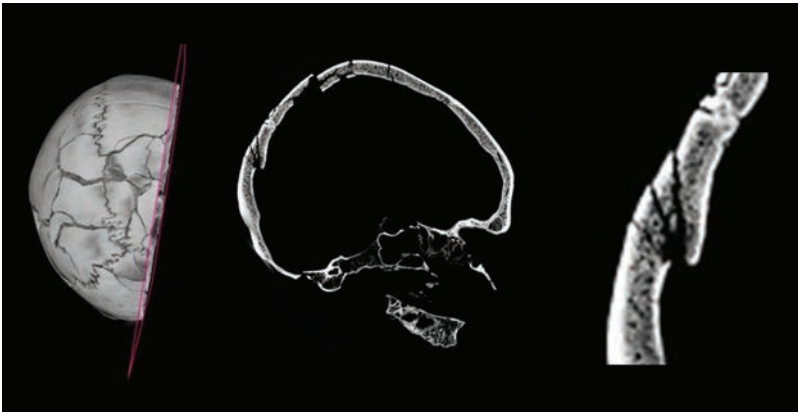

### *7.2.4 Cranial blunt trauma with endocranial fracture initiation*

In this case, assessment of the endocranial surfaces of the cranium was necessary to visualize all of the associated fractures and interpret the cause. Ectocranially, fractures are noted on both the left and right lower cranial vault involving the left temporal

and parietal, and right temporal, parietal, and zygomatic (Figure 7.8). There are also fractures associated with the foramen magnum that involve the occipital squama, pars basilaris, and right occipital condyle. CT scanning provided an opportunity to view the internal surfaces without cutting the cranium open.

*Figure 7.8:*
*Left lateral (left), inferior (center), and right lateral (right) images showing fractures of the lower cranial vault and cranial base; an impact site is not identified*

The ectocranial fractures are all appreciated on the exterior views of the CT scan images (Figure 7.9). Endocranially, the scan also revealed bilateral fractures that initiated on the endocranial surfaces of the parietal bones but never propagated through the thickness of the bones to the ectocranial surface and therefore could not be seen on external examination (Figure 7.10). In this case, compression can be concluded, causing the bilateral inward bending of the lateral cranial vault. The major fractures appreciated ectocranially likely resulted from the compression forces experienced at the cranial base.

*Figure 7.9:*
*CT scan showing ectocranial fractures*

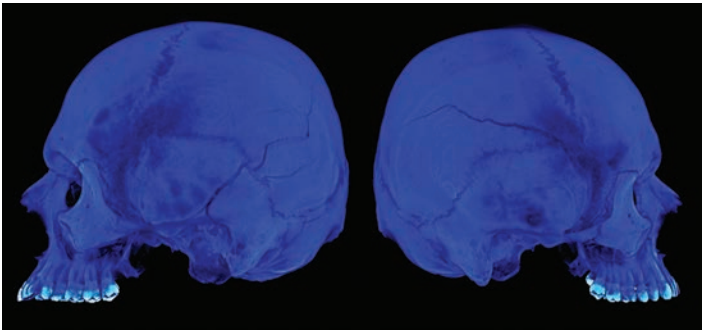

*Figure 7.10:*
*CT scan showing cut-away views with radiating fractures (top); close-ups of the boxed regions show fractures that initiated on the endocranial surface (fracture initiation marked with white arrows) but did not propagate to the external surface.*

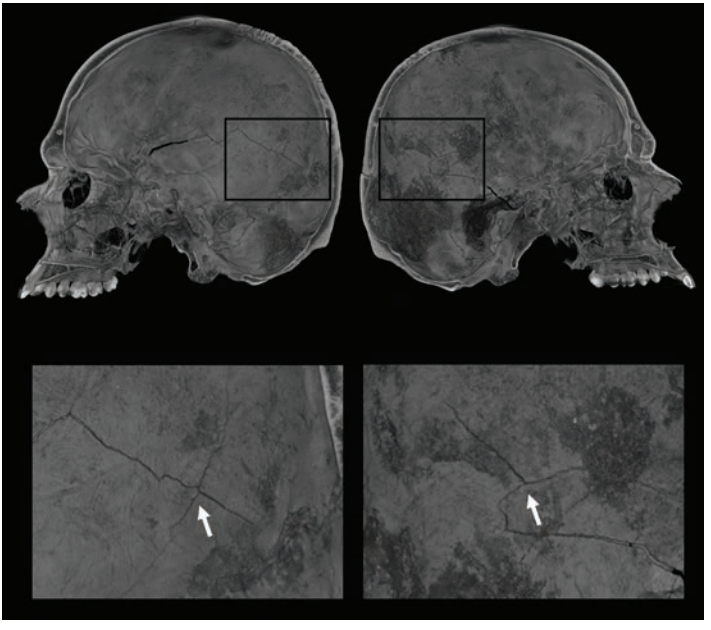

### *7.2.5. Cone crack in glass with window tint*

In this case, a victim was found in the driver's seat of a vehicle with projectile wounds, but it was initially unclear from which direction the projectile originated. (As with impacts to bones, the term "projectile" is preferable to "bullet" when referring to impacts to glass, since other fast-moving objects may cause similar cracking patterns, and the fracture pattern alone cannot be used to identify the impactor.) The front passenger's side window was missing from the vehicle but was later discovered on the side of the road and displayed a perforating cone crack (Figure 7.11). Typically, tempered glass shatters into many small fragments, but in this case the fragments were held together by an after-market window tint that had been applied. Due to the shape and curvature of the window, it was clear that the tint had been applied to the interior side of the window. The perforating cone crack was smaller on the tint side of the glass, and beveled outward toward the non-tint side, indicating that the impact was on the tint side.

*Figure 7.11:*
*Perforating cone crack in a tempered vehicle window with after-market tint*

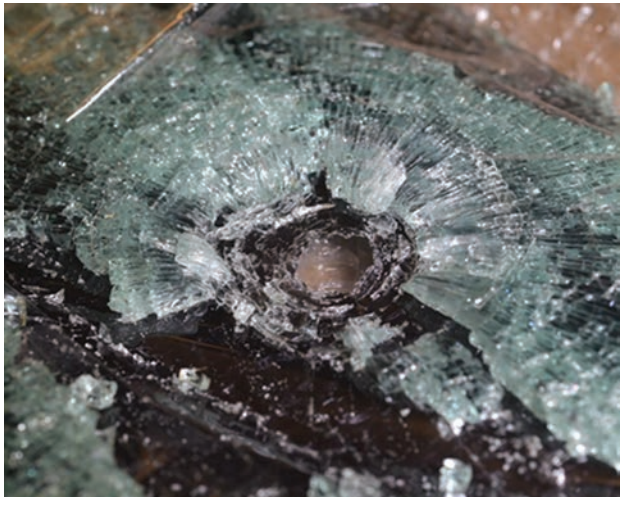

### *7.2.6 Reconstructed partial cranium with cone crack*

Multiple skeletonized cranial bone fragments were received from a medical examiner who suspected projectile trauma due to autopsy findings on the torso. Beveled margins were noted on several of the fragments, and upon reconstruction an internally-beveled circular alteration is noted in the occipital (Figure 7.12). The cranium is only partially present, with the facial skeleton and cranial base being absent. Fracture patterns including a cone crack, radial, and circumferential fractures are easily visualized in a CT scan (Figure 7.13). Radial cracks extend from the circular alteration, and circumferential cracks intersect and terminate into them, indicating that the radial cracks occurred first. A plane slice view in the region of the circular alteration confirms a cone crack that flares internally, and also shows that a circumferential crack is angled outward relative to the projectile impact site, indicating a likely ectocranial crack initiation (Figure 7.14). Taken together, it is apparent that the projectile impacted here ectocranially.

*Figure 7.12:*
*Cranial bones as received (upper left) and cranium as reconstructed in anterior (middle) and superior (right) views*

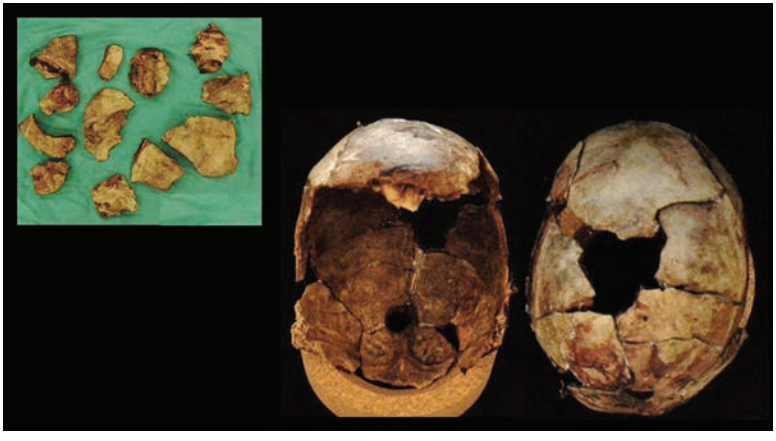

*Figure 7.13:*
*CT scan showing reconstructed partial cranium in posterior (left), superior (middle) and inferior (right) views; radial and circumferential cracks are easily visualized, as is the circular alteration in the occipital which is internally-beveled*

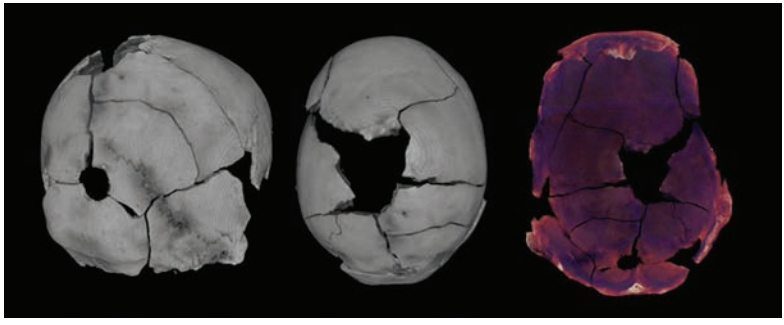

*Figure 7.14:*
*Plane slice view of the region including the circular alteration; overview of the slice region (left), sliced plane (middle), and close-up of cone crack (right); the middle image also captures one of the angled circumferential cracks which suggests ectocranial crack initiation*

### *7.2.7 Cranial blunt trauma with cone crack*

In this case, a cranial impact produced a circular defect resulting from a large cone crack as evidenced by the ring crack being continuous (i.e., not interrupted by radiating cracks) as well as the fact that the defect is internally beveled (Figure 7.15). There are several fractures radiating away from the impact location, as well as fractures that radiate within the boundaries of the cone crack,

resulting in comminution (Figure 7.16). In this case, blunt impact is concluded, with the contact surface being moderately large, likely just smaller than the cone crack. Several of the fragments from within the cone crack could be reconstructed and the cracks do not line up with the radial cracks, indicating that the cone crack occurred first, and comminution of the fragments after.

*Figure 7.15:*
*Impact with ring crack shown photographically as received (left); a CT scan view of the ectocranial surface shows the margins of the cone crack (middle) and internal beveling can be seen on a close-up endocranial view (right)*

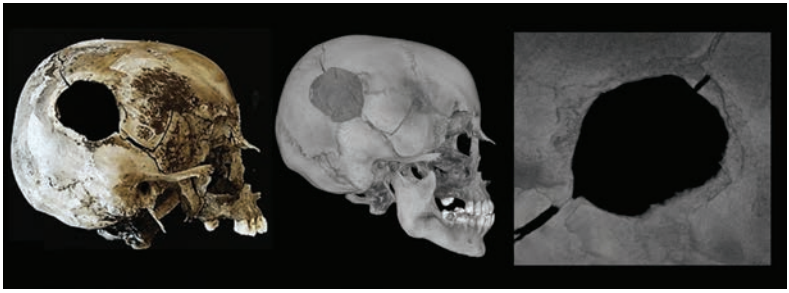

*Figure 7.16:*
*Reconstructed comminuted fragments within the cone crack*

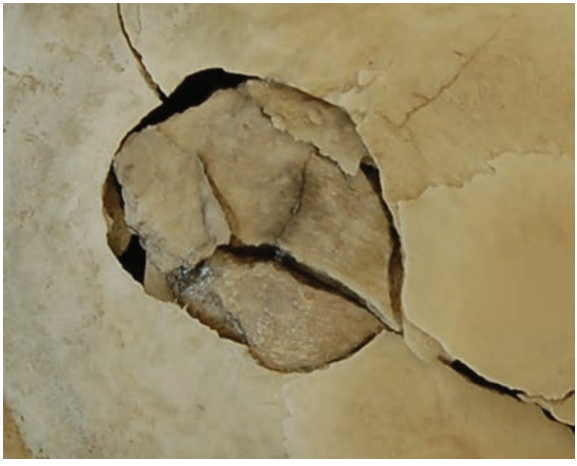

This pattern is similar to findings in experimental impacts with a 1.125-inch (2.858 cm) diameter circular impactor and where fracture initiation and propagation were captured using high-speed video (Figure 7.17). In these cases, ring cracks formed just outside of the radius of the impactor. Fractures then radiated from the edge of the ring crack away from the impact site as well as within the boundaries of the ring crack, including from the edge of the ring crack toward the center of impact, and endocranially, from the center of impact outward. The continuous nature of the fracture as well as internal beveling confirms that this is a ring crack and that it occurred prior to the radiating fractures which are not continuous across the ring crack.

*Figure 7.17:*
*Experimental impacts (including one with penetration of the cranial vault, right) resulting in ring cracks and subsequent inward and outwardly radiating fractures (note: the left fractures resulted from the impact sequence shown in Figure 6.6)*

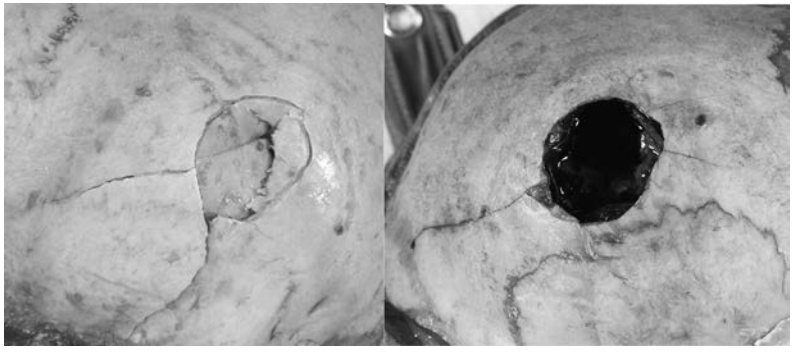

### *7.2.8 Intersecting cracks from projectile entrance and exit*

A projectile entered the left temporal creating a single radial crack that extends across the left and right parietals, terminating in the right squamosal suture (Figures 7.18 and 7.19). The projectile exited the right parietal bone. Entrance and exit locations are confirmed by internal beveling of the left temporal defect and external beveling of the right parietal defect. Three radiating

fractures are associated with the exit defect in the right parietal, one of which terminates into the radiating fracture associated with the entrance impact. The intersecting crack indicates that the radial cracks from the exit impact are subsequent to the radial crack from the entrance impact. In this case, the radial crack from the entrance impact traveled across the cranium prior to the projectile impacting the exit site. A second exit defect is present in the right anterior frontal squama, with a radiating fracture that terminates into one of the radiating fractures from the other exit defect, indicating that this exit occurred subsequently; a second entrance defect was not located.

*Figure 7.18: Radiating and intersecting fractures in left lateral (left) and right lateral (right) views*

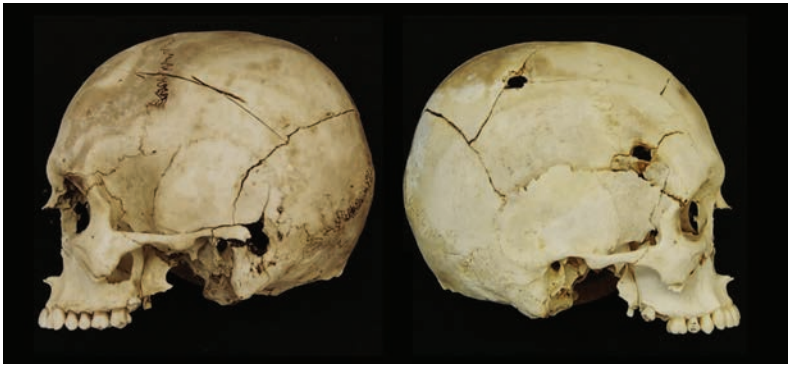

*Figure 7.19:*
*Radiating fractures shown on external (left) and cutaway endocranial (right) views of a CT scan; three radial fractures (dashed white arrows) extend from a projectile exit impact (black arrow) in the right parietal bone; one of the radiating fractures terminates into a previous fracture (solid white arrow) that is associated with the projectile entry impact in the left temporal bone*

### *7.2.9 Fractography of femur trauma from a medical CT scan*

Removal of soft tissue from more complete remains may be impractical in some cases, and assessments can be expedited by assessing fracture surfaces from CT scans. In this case, a motorcyclist struck by a car presented to a Level 1 trauma hospital, and was CT scanned upon arrival to the emergency department (Christensen & Decker 2020, 2021). The scan was performed with a Philips Brilliance 64 slice CT scanner using a standard trauma scan protocol. Thin slice data sets of the lower extremities were acquired using bone and soft tissue algorithms. The fracture surfaces were visualized as 3D computational models using volume rendering software (Figure 7.20). Even using a traditional medical CT scanner, fracture surface features including bone mirror, arrest ridges and cantilever curl are seen, and the direction of crack propagation (and therefore the direction of impact or loading) can be interpreted.

*Figure 7.20:*
*Fractography features as seen on 3D renderings of fracture surfaces; volumetric rendering (top left), combined volumetric and surface rendering (middle), and surface rendering (bottom left); fracture surface features are shown right on the surface rendering, with the direction of crack propagation indicated by the dashed arrow and the general direction of impact or loading (not necessarily a specific impact location or angle) shown by the solid arrow [from Christensen & Decker 2021]*

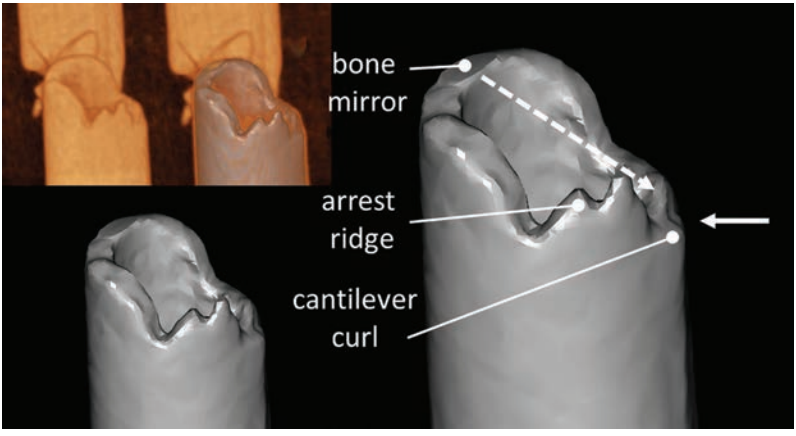


### *7.2.10 Direction and sequence of impacts in a train windshield*

The derailment of a local commuter train that resulted in 8 deaths and more than 200 injuries led to rampant media speculation about the cause. A witness statement indicated that the train may have been hit with a projectile (i.e., a bullet) prior to the derailment. There were numerous fractures to the train's windshield, but fractographic analysis was able to clarify the sequence of events and exclude the bullet theory. The initial break was caused by a large force acting on the windshield, likely from the cab impacting the ground on its side, bending under its weight until the window failed in tension. This caused a large V-shaped fracture, consisting of radial fractures emanating from the impact site (Figure 7.21). All other fractures terminate into this fracture, indicating that it occurred first. One of these fractures is a cone crack (Figure 7.22) that is beveled inwardly,

and likely occurred from a small object striking (but not penetrating) the outside of the windshield at a moderate velocity.

*Figure 7.21:*
*Fractures in the windshield of a derailed train (left); a V-shaped fracture (right) occurred first, with all other fractures terminating into this fracture*

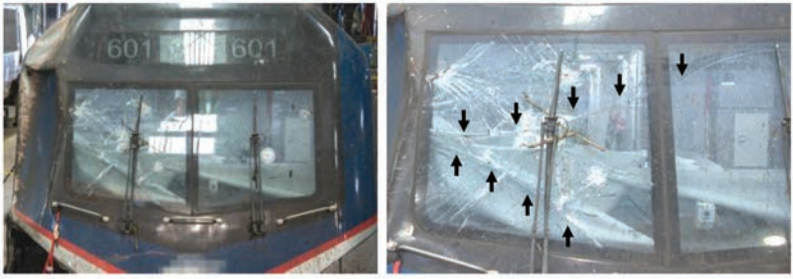


*Figure 7.22:*
*Cone crack in a train windshield; the direction of beveling indicates that the window was struck from the outside, and intersection/superimposition of the cone crack with part of the V-shaped crack (shown with arrows) indicates that the cone crack occurred after the initial windshield fracture*

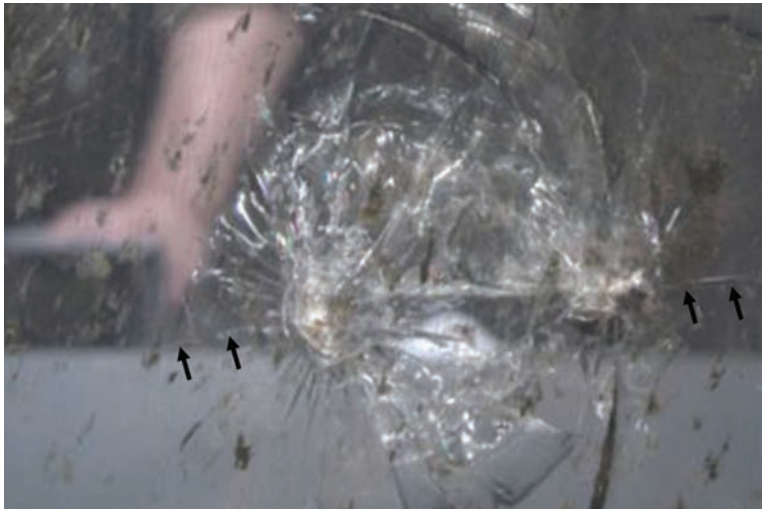

### *7.2.11 Fracture sketch of a clavicle and rib with projectile impact fractures*

A 28-year-old male sustained fatal projectile trauma during an argument. At autopsy, the left clavicle and left 4th rib were retained along with associated bone fragments, which were processed to remove soft tissue to facilitate reconstruction and examination. Sketches of the fracture patterns were included as part of the anthropologist's bench notes, which involved sketching each fracture and alteration exactly as it appeared on the bone. This allowed the documentation of details needed to interpret the fracture event and answer the forensic question of interest, in this case the direction of the projectile. Additionally, the sketching of each individual fracture (as compared to simply taking photographs) requires the analyst to consider fracture relationships and provides insight as to how the bone was affected by intrinsic factors, such as cortical thickness, anatomic feature, and bone morphology. Observations of beveling, inclusions such as projectile remnants, and measurements of the fractures also serve to help understand the fracture event. In this case, the sketches and other case documentation allowed the interpretations below.

The medial end of the left clavicle (Figure 7.23) was fractured. The sternal surface exhibits a cone-shape defect that expands from .32" at the center of the joint surface to .73" on the posterior shaft. A longitudinal fracture is also associated with the posterior fracture. When the bone fragment created by the impact is removed, the path of the projectile can be visualized. The projectile direction was anterior to posterior and slightly right to left.

*Figure 7.23:*
*Sketch of fractures to clavicle; patterns of fractures and missing bone indicate that the projectile direction was anterior to posterior and slightly right to left*

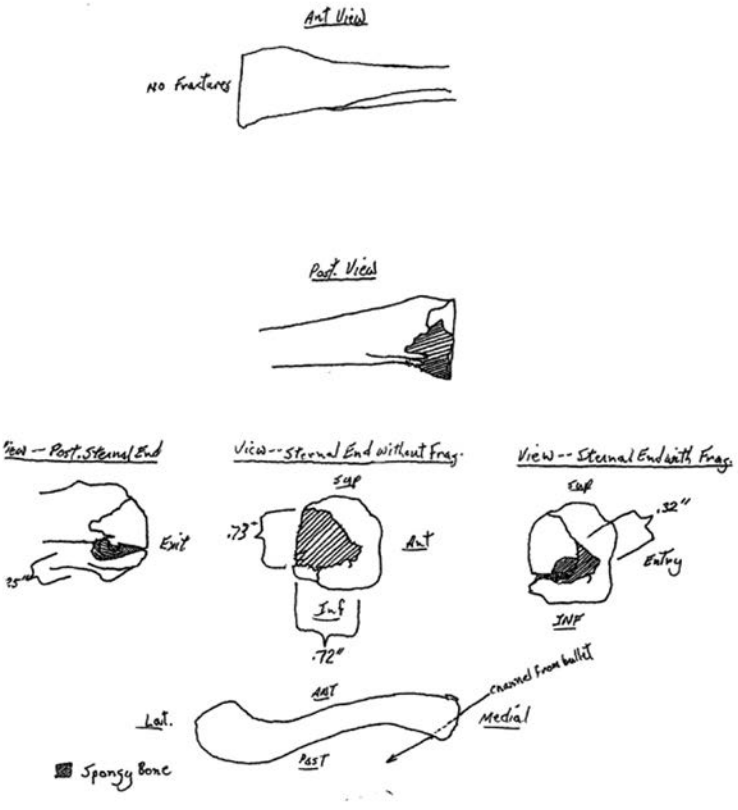


There was extensive fracturing of the angle of the left 4th rib (Figure 7.24). The fragments were reconstructed to reveal a .19" by .43" defect in the internal surface with depressed bone as well as metal inclusions along its margin. The external surface of the rib has bone fragments missing from the inferior border just lateral to the internal surface defect. This also indicates a projectile direction

anterior to posterior and right to left. The relationship between the clavicle defect and the 4th rib defect indicates that both fracture events were created by the same projectile, with a slight superior to inferior directionality.

*Figure 7.24: Sketch of fractures to rib; patterns of fractures, missing bone, and inclusions indicate that the projectile direction was anterior to posterior and right to left*

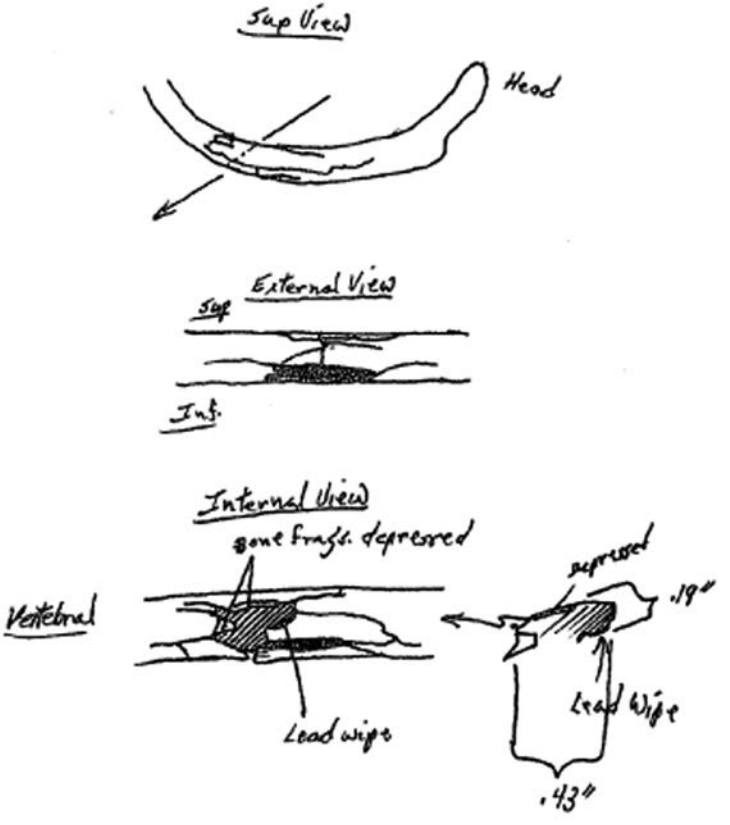

### *7.2.12 Analysis of ceramic fractures from impact*

FBI Laboratory Interns tasked with research-related duties were provided a ceramic mug and instructed to create fragments for a fractographic analysis (note: interns love breaking things!). Analysts were not informed of how the samples were created, but the Interns provided a collection of fragments to the fractographers. The fragments were reconstructed to clarify fracture patterns (Figure 7.25). Based on intersecting cracks, it is apparent that the first fracture to occur was one that circumscribes the base of the mug, since other fractures terminate at this crack. From the fracture pattern on the base of the mug, the fracture originates where the inside edge of the handle attaches to the base where a flaw (a bubble/void) is found in the ceramic (Figure 7.26). The meandering path of the fracture is often associated with low energy such as cases of thermal shock, but in this case may have resulted from a low energy impact on the handle.

*Figure 7.25:*
*Ceramic fragments prior to reconstruction (left) and following reconstruction (right)*

*Figure 7.26:*
*The crack that circumscribes the bottom of the mug (left) occurred first, with the crack initiating at a flaw near the handle (right, showing the boxed region on the left)*

Subsequent to this initial fracture, an impact was experienced on one side of the mug which resulted in damage at the impact site, radiating fractures, and a cone crack at the origin (Figure 7.27). The orientation of the cone indicates that the impact was on the external surface of the mug. Fracture surfaces were also examined, and Wallner lines on the fragment with the star logo showed the direction of fracture propagation and indicated that the fracture originated on the inside curve of the mug (Figure 7.27). The degree of damage and number of fractures can be an indication of the relative intensity of an impact. The multiple radiating fractures and focused damage at the second impact site indicates it contained more energy than the first. Overall, it is concluded that there were two distinct impact events. The first was likely a lower energy impact that was just strong enough to sever the base without shattering the rest of the mug. The second was a much higher energy impact which created the Hertzian cone and radiating fractures that terminated into the initial fracture.

*Figure 7.27:*
*The second impact site (arrow, left) produced a cone crack at the origin (middle); Wallner lines on one of the other fragments (right) indicates that the fracture here propagated from the inside curve of the mug*

### *7.2.13 Fracture fit of art frame fragments*

A home invasion homicide occurred in which the only objects missing were seven paintings worth approximately $500,000. Surveillance video showed a truck leaving the neighborhood the night of the theft and homicide, including grainy images thought to be one of the paintings on the seat. Approximately one month later, a suspect was identified and his vehicle (which was identified from the surveillance video) was searched. Several fragments of debris were recovered from the back of the truck which turned out to be fractured portions of art frames (Figure 7.28). The stolen art in this case involved Victorian-era frames which were constructed primarily of wood, Gesso (a calcium carbonate primer), and silver or gold leaf, consistent in composition with the recovered fragments.

*Figure 7.28:*
*Examples of debris recovered from the truck*

Several months later, a storage space was discovered containing the stolen paintings, some of which had fragments missing from their frames (Figure 7.29). Pieces of frame debris recovered from the truck could be physically reconstructed to fractured portions of the frames (Figure 7.30), confirming that they were once part of the same frame, and associating the debris from the suspect's truck to the stolen frames.

*Figure 7.29:*
*One of the recovered paintings (left), and two regions with part of the frame missing (right)*

*Figure 7.30:*
*Recovered fragments are shown left; the fragments are also shown partially (middle) and fully (right) refitted into the frame (right)*

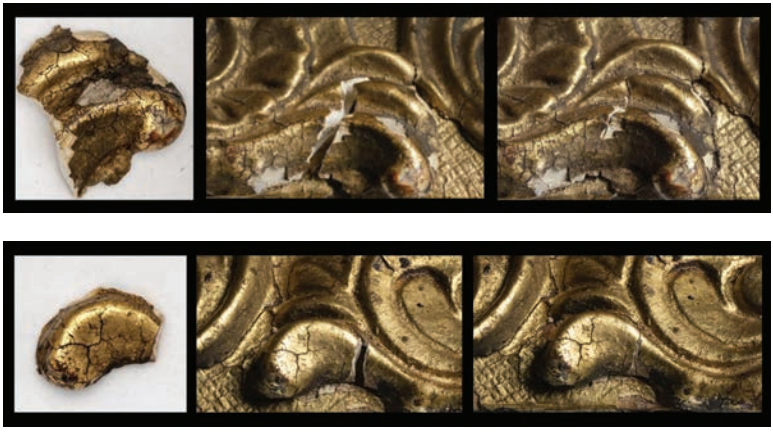

### *7.3 Fracture maps*

One useful way to document fractographic analysis (for case records and/or for later presentation, for example in a trial) is through a **fracture map** (see also Section 5.7.2). Fracture maps consist of a central image showing the overall fracture pattern or surface under consideration, along with a montage of local images showing smaller details. This provides context and helps orient viewers to the location of features being demonstrated. It is also an effective visual means of communicating all steps of the analysis from identification of features to interpretation. Fracture maps are especially useful in cases involving multiple fragments or in cases in which close-up images of different areas of a fracture surface are needed.

#### *7.3.1 Fracture map of an experimentally-fractured femur*

This case involves a femur that was fractured experimentally in 4-point bending (Isa et al. 2021), with the fracture event captured using high-speed videography (which can be used to confirm fracture propagation direction). The event resulted in five separate

fragments, all of which were retrieved, assembled, photographed, and incorporated into a fracture map (Figure 7.31). To create the map, the fragments were loosely articulated and photographed to show the overall fracture pattern. Each fragment was labeled A through E on this central image. Next, local photographs were taken of each fracture surface. These were placed as close to their corresponding location on the central image as possible. Each local image was labeled with the fragment letter and anatomical orientation of the fracture surface (for example, "C proximal" refers to the proximal surface of fragment C). Complementary fracture surfaces were displayed together for clarity. While including both surfaces may provide redundant information (for example, arrest ridges on both articulating surfaces), it can be useful to show both surfaces as some features (particularly bone mirror) may be more prominent on one surface than the other. Arrows, brackets, and labels were used to highlight features of interest, as well as crack propagation and force directions.

*Figure 7.31:*
*Fracture map depicting images of femur fragments and fracture surfaces, along with interpretation [from Isa et al. 2021]; the solid arrow indicates the loading direction, dashed arrows indicate the direction of fracture propagation, and several features are also labeled including bone mirror (BM), bone hackle (BH), and arrest ridge (AR)*

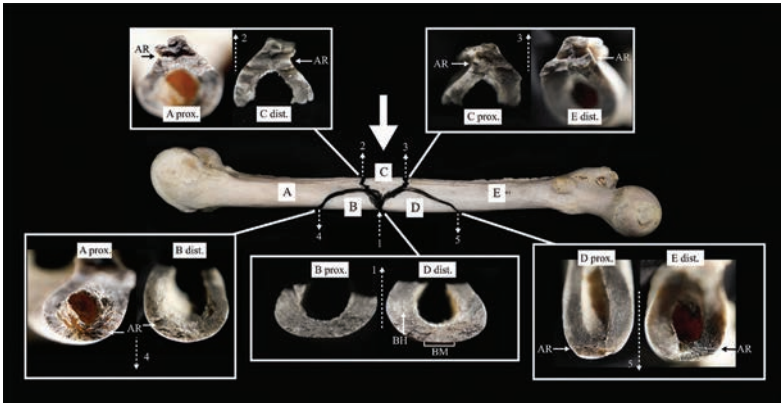

### *7.3.2 Practice fracture map*

The femur presented in this example was fractured under similar experimental loading conditions to the previous example. The overall image of the reconstructed bone fragments as well as local images of fracture surfaces have been arranged in a montage (Figure 7.32). Readers are encouraged to complete the labels and interpretations on the fracture map. A suggested "solution" is provided at the end of this guide.

*Figure 7.32:*
*Image montage of fractured femur. Readers wanting practice mapping and interpreting are encouraged to label the figure with surface features, crack propagation direction, and interpretation of force direction.*

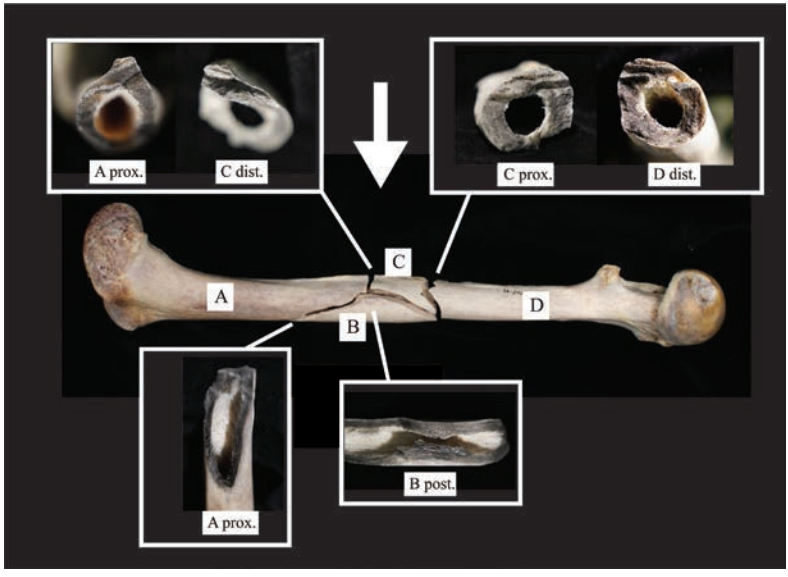


A suggested solution is provided on the following pages.

## A suggested solution for Figure 7.32:

*Figure 7.33:*
*Suggested solution to the fracture map depicted in Figure 7.32*

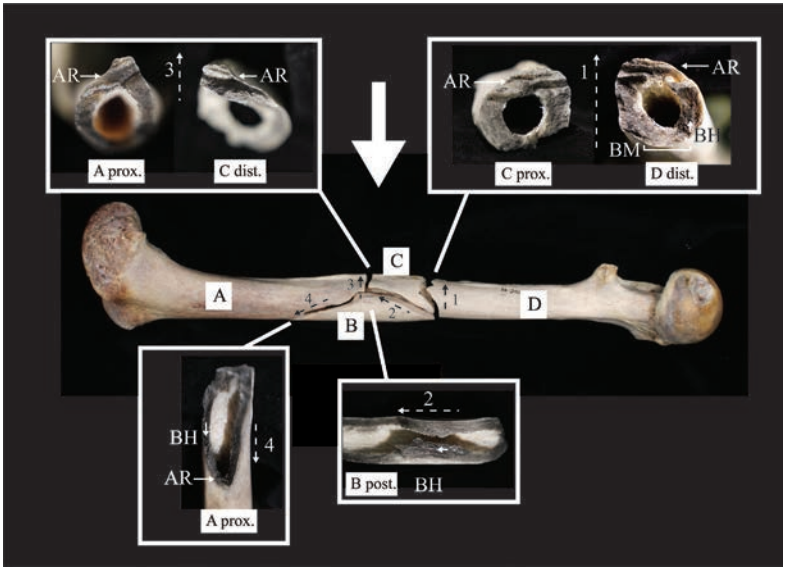


**For the fracture labeled 1**, the distal surface of fragment D exhibits bone mirror (BM) on the anterior surface, bone hackle oriented anterior-to-posterior, and arrest ridges (AR) oriented medial-to-lateral on the posterior surface. The proximal surface of fragment C (which is the complement to fragment D), also exhibits arrest ridges oriented medial-to-lateral on the posterior surface. The orientation of these features indicates that the fracture initiated anteriorly and traveled posteriorly at this location.

**For the fracture labeled 2**, the posterior surface of fragment B exhibits bone hackle (BH) oriented proximal-to-distal on the posterior fracture surface, indicating that the fracture traveled proximal to distal.

**For the fracture labeled 3**, complementary fracture surfaces on the proximal surface of fragment A and the distal surface of fragment C exhibit medial-to-lateral oriented arrest ridges posteriorly, indicating fracture propagated posteriorly at this location.

**For the fracture labeled 4**, the proximal surface of fragment A exhibits bone hackle oriented proximal-to-distal and an arrest ridge oriented medial-to-lateral on the anterior surface, indicating the fracture traveled from posterior to anterior at this location.

The black dashed arrows in the overall image and the white dashed arrows in the local images show the direction of propagation. Based on these fractures, the load can be determined to have been applied from posterior to anterior (solid white arrow).

# Glossary

## 8. Glossary of fractography-related terms

This section provides definitions to fractography and mechanics-related terms used in this guide. It is recognized that terms may have varied meanings depending on the specific field and context in which they are applied.

**anisotropic** – having different mechanical properties in different directions

**arrest lines** – sharp curved or straight lines on a fracture surface resulting from an arrested (or momentarily hesitated) crack

**arrest ridges** – pronounced peaks on a fractured bone surface aligned approximately perpendicular to the direction of crack propagation and resulting from drastic changes in crack propagation velocity on the compressive side of the fracture

**axial stress** – in a cylinder, stress parallel to the axis of cylindrical symmetry; stress acting in the lengthwise direction of a structure

**bending** – a loading mode that causes a structure to flex, creating internal stresses that vary from compression on one side of the structure to tension on the other

**beveling** – angling of an impact alteration such that it is larger on one surface of the structure than the other, usually in reference to fractured bone

**biomechanics** – field concerned with the study of mechanical laws relating to structure, function, and motion of biological systems

**bone hackle** – angular or rounded hackle on a bone fracture surface produced by increased crack speed and instability

**bone mirror** – a region at the fracture origin in bone that is relatively flat or featureless compared to the rest of the fracture surface

**branching** – the splitting of a single crack into two (or more) cracks due to the inability to dissipate the strain energy with a single crack; often associated with impacts or other dynamic events

**brittle** – characteristic of a material that undergoes little plastic deformation and has low energy absorption before failure
**buttressing** – the reinforcement of parts of the skeleton (typically the facial skeleton or proximal femur) in order to transfer and dissipate forces
**cantilever curl** – a curved lip just before terminal fracture of a body loaded in bending; also called compression curl; the positive portion is sometimes referred to as a breakaway spur in earlier anthropological literature
**chipping** – the fracture of a small piece of material from the edge of a structure; also called edge chipping
**circumferential fractures** – semi-circular cracks surrounding an impact site as a result of inward bending
**comminution** – the breaking up of bone into smaller pieces; in ceramics, concrete, and glass, the fragmentation that occurs from impact, compression, or grinding
**compression** – a load or stress that acts to decrease the dimension of (squeeze) a structure in the direction of the applied force
**concentric fractures** – two or more semi-circular cracks sharing a common center
**cone crack** – a conoidal fracture resulting from an object impacting or passing through a brittle material; also called Hertzian cone crack
**corner hackle** – a fan-like array of hackle that is created when a crack goes around a curve
**crack** – a plane of separation within an intact body
**ductile** – characteristic of a material that undergoes extensive plastic deformation and has high energy absorption before failure
**dynamic load** – load that is applied suddenly and at relatively high speed
**elastic deformation** – temporary deformation in response to a force

**failure** – fracture of a material as a result of applied stress.
**fatigue failure** – fracture occurring due to repetitive, subcritical loads
**fatigue striations** – lines produced by stepwise crack growth due to repetitive loading
**flaw** – a strength limiting irregularity from which a fracture may originate
**force** – the action of one object on another
**fractography** – field concerned with the study of fractured material in order to understand the cause of material failure
**fracture** – the separation of an object or material into two or more pieces under the action of stress
**fracture map** – a montage of fragments from a fractured structure, composed of an overall image surrounded by systematically organized local images showing smaller fracture details; also called a fracture montage, fractographic map, or fractographic montage
**fracture mechanics** – field of engineering mechanics concerned with the study of crack propagation in materials
**fracture origin** – the location as well as the flaw or discontinuity at which a fracture began
**fracture surface** – the surface created by the separation of two portions of a material as a result of a propagating crack front
**fracture toughness** – the critical stress intensity factor of a sharp crack where propagation of the crack suddenly becomes rapid and unlimited; a quantitative expression of a material's resistance to crack propagation
**grain boundary** – the interface between two crystallites in a polycrystalline material
**hackle** – lines or ridges on a fracture surface elongated in the direction of local crack propagation
**hoop stress** – stress exerted circumferentially in a cylinder
**impression** – alteration imparted when two objects come into contact; also called a tool impression

**inclusion** – a flaw consisting of a foreign body with a composition different than the normal composition of the structure in which it is embedded
**isotropic** – having the same mechanical properties in all directions
**kerf** – the notch or groove made by a cutting tool, typically a saw
**load** – the force(s) applied to an object
**magnitude** – the amount of force applied
**manufacturing defect** – a departure from the intended design of a product which may hinder its usability for the purpose for which it was intended
**microcrack** – a very small crack in a material that may not be visible with the unaided eye
**microdamage** – diffuse damage and microcracks in bone caused by normal physiological loading
**microstructural hackle** – broad lines on a fracture surface that are attributed to microstructural or geometric irregularity
**mirror** – smooth regions surrounding and centered on a fracture origin
**mist** – region adjacent to the mirror where micro-steps in the fracture surface become optically discernible; also called mist hackle
**moment of force** – turning effect of a force applied at a distance from the axis of rotation, with units of force·distance
**neutral axis** – the plane in the cross section of a structure in bending along which no tension or compression is experienced
**normal** – at a right angle (perpendicular) to a line or surface
**origin** – initiation point of a crack
**pattern** – identifiable information within an impression
**plastic deformation** – deformation of a material that is not recovered when the force applied is removed; permanent deformation
**quasi-static load** – a load that increases slowly with time

**radial crack** – crack extending outward from a point of impact
**R-curve** – the plot of the resistance to fracture versus crack extension; also called the crack growth resistance curve
**residual stress** – stress remaining or present in a material after the removal of or in the absence of an external load
**ring crack** – the circular-shaped origin associated with a cone crack
**sandwich structure** – a material configuration involving stiff faces separated by a lightweight core; an efficient way to resist mechanical loads with the least amount of material possible since this configuration has a large moment of inertia and high bending stiffness for the material's weight; also called sandwich-structured composite
**scarps** – curved lines on a fracture surface caused by the interaction of a propagating crack and a liquid
**shear** – a mode of loading that results from adjacent forces working in opposite directions across a plane
**shear hackle** – a variant of twist hackle that may appear on a hollow specimen
**static load** – load that is constant with time
**strain** – the change in dimension of a loaded body relative to its initial length, with units of length/length and as such is dimensionless
**strain energy** – a type of stored energy in a structure undergoing deformation
**step hackle** – a form of twist hackle that occurs as a single arc-shaped line as a result of bending and twisting of the crack front
**strength** – characteristic of a material that is related to the load or stress required to reach the failure point
**strength-limiting flaw** – a feature of a structure that acts as a stress concentrator
**stress** – load per unit area, with units of force/area, e.g., lbs/in$^2$ or N/m$^2$

**stress concentrator** – a feature within a structure that results in greater stresses in its vicinity than are present in areas more remote from it

**stress intensity factor** – a value used in mechanics to predict the stress state ("stress intensity") near a crack tip caused by a remote load or residual stresses; a theoretical construct usually applied to a homogeneous, linear elastic material, and useful for providing a failure criterion for brittle materials

**tension** – a load or stress that acts to increase the dimension of (stretch) a structure in the direction of the force

**thermal shock** – a load caused by a rapid change in temperature

**tool impression** – alteration imparted on an impacted structure that reflects the shape or other properties of the impacting object

**torsion** – a load or stress that involves rotation or twisting, creating shear stresses that vary with location in the structure

**toughness** – a measure of the energy absorption capability of a material before failure, with units of energy per unit volume

**trauma** – disruption of living tissue by an outside force

**trauma mechanism** – a forensic categorization of the way a fracture occurred, typically blunt, sharp, high-velocity, or thermal

**twist hackle** – hackle resulting from lateral rotation in the axis of principle tension, caused when the crack passes a microstructural or geometric feature, creating a localized series of roughly parallel ridges radiating at an angle to the main crack front

**velocity branching** – the splitting of a crack which has reach its terminal velocity into two cracks

**velocity hackle** – hackle markings formed on the surface of a crack that is propagating at close to its terminal velocity and appearing as discrete elongated steps aligned with the direction of crack propagation

**viscoelastic** – exhibiting both viscous and elastic properties when undergoing deformation
**wake features** – the offset alignment of features on the following side of a large inclusion
**wake hackle** – a line extending from a discontinuity such as an inclusion or pore that is aligned with the direction of crack propagation
**Wallner lines** – curved lines on a crack surface, that are bowed in the direction of crack propagation and are the product of an expanding crack front intersecting an expanding elastic wave; also called rib marks
**witness mark** – mark on the surface of a structure due to contact with a foreign body, usually in reference to ceramics and glass

# References

## References


Akimune Y. Hertzian cone crack in SiC caused by spherical particle impact. *Journal of Materials Science Letters* 1990;9:659-662.

Alunni-Perret V, Muller-Bolla M, Laugier JP, Lupi-Pégurier L, Bertrand MF, Staccini P, Bolla M, Quatrehomme G. Scanning electron microscopy analysis of experimental bone hacking trauma of the mandible. *Journal of Forensic Sciences* 2005;50(4):796-801.

American Society for Materials (ASM). *Failure Analysis and Prevention*, ASM Handbook, Vol. 11, Materials Park, OH; 2002.

American Society for Testing and Materials (ASTM) C 1322-15. *Standard Practice for Fractography and Characterization of Fracture Origins in Advanced Ceramics*" Annual Book of Standards, Vol. 15.01, ASTM Int., West Conshohocken, PA; 2015.

Anderson, TL. *Fracture Mechanic: Fundamentals and Applications*, 3rd ed. Boca Raton: CRC Press, Taylor and Francis Group; 2005.

Ashby MF. *Materials Selection in Mechanical Design*, 4th ed., Burlington: Butterworth – Heinemann; 2011.

Bajaj D, Arola DD. On the R-curve behavior of human tooth enamel. *Biomaterials*, 2009;30:4037-4046.

Bajaj D, Park S, Quinn GD, Arola DD. Fracture processes and mechanisms of crack growth resistance in human enamel. *Journal of Materials* 2010;62(7):76-82.

Bartelink EJ, Wiersema JM, Demaree RS. Quantitative analysis of sharp-force trauma: an application of scanning electron microscopy in forensic anthropology. *Journal of Forensic Sciences* 2001;46(6):1288-1293.

Bastidas-Rodriguez MX, Prieto-Ortiz FA, Espejo E. Fractographic classification in metallic materials by using computer vision. *Engineering Failure Analysis* 2016;59:237-252.

Beauchamp EK. *Fracture Branching and Dicing in Stressed Glass*. Sandia Laboratories Research Report, SC-RR-70-766, Jan; 1971.

Beauchamp EK. Mechanisms of hackle formation and crack branching. In Varner J, Fréchette VD, Quinn GD, Eds: *Fractography of Glasses and Ceramics*, 3rd edition. Ceramic Transactions, Vol. 64, Westerfield OH: American Ceramic Society; 1996:409-466.

Behiri JC, Bonfield W. Crack velocity dependence of longitudinal fracture in bone. *Journal of Materials Science* 1980;15(7):1841-1849.

Belkoff SM, Haut RC. Experimental methods in biological tissue testing. In Sharpe WN, Ed: *Springer Handbook of Experimental Solid Mechanics*. New York: Springer Science+Business Media; 2008:870-891.

Benninghof A. Spaltlinien am Knochen, eine Methode zur Ermittlung der Architektur platter Knochen. *Verhandlungen der Anatomische Gesellschaft* 1925;34:189-206.

Berryman HE, Berryman JF, Saul TB. Bone trauma analysis in a forensic setting—theoretical basis and a practical approach for evaluation. In Boyd CC, Boyd DC, editors. *Forensic Anthropology: Theoretical Framework and Scientific Basis*. Hoboken: John Wiley & Sons Limited, 2017:213-234.

Berryman HE, Kutyla AK, Davis JR. Detection of gunshot primer residue on bone in an experimental setting – an unexpected finding. *Journal of Forensic Sciences* 2010;55(2):488-491.

Berryman HE, Symes SA. Recognizing gunshot and blunt cranial trauma through fracture interpretation. In Reichs KJ, editor: *Forensic Osteology: Advances in the Identification of Human Remains*. Springfield: Charles C. Thomas, 1998:333-352.

Biringuccio V. *De La Pirotechnia*. Venice, 1540. Translation by Smith CS and Gnudi MT: The 'Pirotechnia' of Vannoccio Biringuccio, AIME, New York; 1942.

Bradley AL, Swain MV, Waddel JN, Das R, Athens J, Kieser JA. A comparison between rib fracture patterns in peri- and post-mortem compressive injury in a piglet model. *Journal of the Mechanical Behavior of Biomedical Materials* 2013;33(1):67-75.

Bradt RC. The fractography and crack patterns of broken glass. *Journal of Failure Analysis and Prevention* 2011;11(2):79-96.

Braidotti P, Bemporad E, D'Alessio T, Sciuto SA, Stagni L. Tensile experiments and SEM fractography on bovine subchondral bone. *Journal of Biomechanics* 2000;33(9):1153-1157.

Brogdon BG, Messmer JM. Forensic radiology of gunshot wounds. In: Thali MJ, Viner MD, Brogdon BG, Editors: *Brogdon's Forensic Radiology*, 2nd edition. Boca Raton: CRC Press, 2011:211-240.

Bullock RE, Kaae JL. Size effect on the strength of glassy carbon. *Journal of Materials Science* 1979;14:920–930.

Burr DB. Schaffler MB, Frederickson RG. Composition of the cement line and its possible mechanical role as a local interface in human compact bone. *Journal of Biomechanics* 1988;21(11):939-945.

Burstein A, Reilly D, Martens M. Aging of bone tissue: mechanical properties. *Journal of Bone and Joint Surgery American Volume* 1976;58:82–86.

Carter DR, Spengler DM. Mechanical properties and composition of cortical bone. *Clinical Orthopaedics and Related Research* 1978;135:192-217.

Chaudhri MM. High-speed photographic investigations of the dynamic localized loading of some oxide glasses. In: Kurkjian C, Ed. *Strength of Inorganic Glass*, Plenum: New York, 1985:87-113.

Chaudhri MM. Dynamic fracture of inorganic glasses by hard spherical and conical projectiles. *Philosophical Transactions* R 2015;373: 20140135. http://dx.doi.org/10.1098/rsta.2014.0135

Chen J, Xu J, Yao X, Liu B, Xu X, Xhang Y, Li Y. Experimental investigation on the radial and circular crack propagation of PVB laminated glass subject to dynamic out-of-plane loading. *Engineering Fracture Mechanics* 2013;112-113:26-40.

Chiang SS, Marshall DB and Evans AG. The response of solids to elastic/plastic indentation: I. Stresses and residual stresses. *Journal of Applied Physics* 1982;53(1):298-311.

Choi S, Gyekenyesi J. *Crack Branching and Fracture Mirror Data of Glasses and Advanced Ceramics*. National Aeronautics and Space

Administration, NASA/TM-199-206536; 1998

Christensen AM, Decker SJ. Forensic fractography of bone using CT scans: A case review series. *Forensic Anthropology* 2021; In Press.

Christensen AM, Decker SJ. Forensic fractography of bone using CT scans. *Proceedings of the 72nd Annual Meeting of the American Academy of Forensic Sciences*, February 17-22, 2020; Anaheim, CA.

Christensen AM, Hatch GM. Forensic fractography of bone using CT scans. *Journal of Forensic Radiology and Imaging* 2019;18:37-39.

Christensen AM, Hefner JT, Smith MA, Webb JB, Bottrell MC, Fenton TW. Forensic fractography of bone: A new approach to skeletal trauma analysis. *Forensic Anthropology* 2018a;1(1):32-51.

Christensen AM, Passalacqua NV. *A Laboratory Manual for Forensic Anthropology*. Elsevier-Academic Press: San Diego CA; 2018.

Christensen AM, Passalacqua NV, Bartelink EJ. *Forensic Anthropology: Current Methods and Practice*, 2nd Ed. San Diego: Academic Press; 2019.

Christensen AM, Rickman JM, Berryman HE. Forensic fractography of bone: fracture origins from impacts, and an improved understanding of the failure mechanism involved in beveling. *Forensic Anthropology* 2021;4(1):57-69.

Christensen AM, Smith VA. Rib butterfly fractures as a possible indicator of blast trauma. *Journal of Forensic Sciences* 2013;58(S1):S15-S19.

Christensen AM, Smith MA, Gleiber DS, Cunningham DL, Wescott, DJ. The use of x-ray computed tomography technologies in forensic anthropology. *Forensic Anthropology* 2018b;1(2):124-140.

Clarke S, Christensen AM. Reflectance Transformation Imaging (RTI) of saw marks on bones. *Journal of Forensic Radiology and Imaging* 2016;7:33-37.

Clifton KB, Reep RL, Mecholsky JJ. Quantitative fractography for estimating whole bone properties of manatee rib bones. *Journal of Materials Science* 2008;43(6):2026-2034.

Cohen H, Kugel C, May H, Medlej B, Stein D, Slon V, Hershkovitz I, Brosh T. The impact velocity and bone fracture pattern: Forensic perspective. *Forensic Science International* 2016;266:54-62.

Cohen H, Kugel C, May H, Medlej B, Stein D, Slon V, Hershkovitz I, Brosh T. The influence of impact direction and axial loading on the bone fracture pattern. *Forensic Science International* 2017;277:197-206.

Corondan G, Haworth WL. A fractographic study of human long bone. *Journal of Biomechanics* 1986;19(3):207-218.

Cowin SC, Editor: *Bone Biomechanics Handbook*. Boca Raton: CRC Press; 2001.

Cultural Heritage Imaging, *Reflectance Transformation Imaging: Guide to Highlight Image Processing*, (http://culturalheritageimaging.org/What_We_ Downloads/rtibuilde/RTI_hlt_Processing_Guide_v14_beta.pdf), 2011.

Currey JD. Strength of bone. *Nature* 1962;195:513-514.

Currey JD: The mechanical properties of bone. *Clinical Orthopaedics* 1970;73:21—231.

Currey JD: *Bones: Structure and Mechanics*. Princeton: Princeton University Press; 2013.

Daegling DJ, Warren MW, Hotzman JL, Self CJ. Structural analysis of human rib fracture and implications for forensic interpretation. *Journal of Forensic Sciences* 2008;53(6): 1301-1307.

DeLand TS. *Studies on the development and fracture mechanics of cortical bone* [Master's Thesis]. East Lansing: Michigan State University; 2013.

Dempster WT. Correlation of types of cortical grain structure with architectural features of the human skull. *American Journal of Anatomy* 1967;120:7-32.

DiMaio VJ. *Gunshot Wounds: Practical Aspects of Firearms, Ballistics, and Forensic Techniques* 2nd edition. New York: Elsevier Science publishing Company; 1993.

DiMaio D, DiMaio V. *Forensic Pathology*, second ed. Boca Raton: CRC Press; 2001.

Dittmar JM, Errickson D, Caffell A. The comparison and application of silicone casting material for trauma analysis on well preserved archaeological skeletal remains. *Journal of Archaeological Science: Reports* 2015;4:559-564.

Edwards J, Rogers T. The accuracy and applicability of 3D modeling and printing blunt force cranial injuries. *Journal of Forensic Sciences* 2018;63(3):683-691.

Emanovsky P. Low-velocity impact trauma: An illustrative selection of cases from the Joint POW/MIA Accounting Command – Central Identification Laboratory. In: Passalaqua, NV, Rainwater CW, eds. *Skeletal Trauma Analysis: Case Studies in Context*. Boca Raton, FL: CRC Press; 2015:156-166.

Emrith TS, Mole CG, Heyns M. Interpreting impact direction: applying fractography to the analysis of butterfly fractures produced by blunt force trauma. *Australian Journal of Forensic Sciences 2020*; Early View: https://doi-org.mutex.gmu.edu/10.1080/00450618.2020.1781252.

Evans FG. *Mechanical Properties of Bone*. Springfield, IL: Thomas;1973.

Evans FG, Lissner HR. Tensile and compressive strength of human parietal bone. *Journal of Applied Physiology* 1957;10:493-497.

Evans FG, Riolo ML. Relations between the fatigue life and histology of adult human cortical bone. *The Journal of Bone & Joint Surgery* (A) 1970;52(8):1579-1586.

Fenton TW, Birkby WH, Cornelison J. A fast and safe non-bleaching method for forensic skeletal preparation. *Journal of Forensic Sciences* 2003;48(1):1-3.

Fenton TW, Haut RC, Wei F. *Building a Science of Adult Cranial Fracture*. U.S. Department of Justice Document Number 300668, National Institute of Justice Award Number 2015-DN-BX-K013; 2021.

Fenton TW, Isa MI, Vaughan PE, Haut RC. (2015) Experimental and computational validations of the initiation and propagation of cranial

fractures in the adult skull. *Proceedings of the 67th annual meeting of the American Academy of Forensic Sciences*; February 16–21, 2015; Orlando, FL.

Field JE. Brittle fracture: its study and application. *Contemporary Physics* 1971;12(1):1-31.

Field JE. High-speed photography. *Contemporary Physics*. 1983;24(5):439-459.

Fischer-Cripps AC. *Introduction to Contact Mechanics*. Mechanical Engineering Series. Boston: Springer, 2007.

Freas LE. Assessment of wear-related features of the kerf wall from saw marks in bone. *Journal of Forensic Sciences* 2010;55(6):1561-1569.

Fréchette VD. *Failure Analysis of Brittle Materials*. Advances in Ceramics, Vol. 28, Westerville, OH: American Ceramic Society; 1990.

Frick SJ. *The effects of combined torsion and bending loads on fresh human cadaver femurs* [Master's Thesis]. Louisville: University of Louisville; 2003.

Galloway A. The biomechanics of fracture production. In Galloway A, editor: *Broken Bones: Anthropological Analysis of Blunt Force Trauma*. Springfield: Charles C. Thomas, 1999:35-62.

Galloway A, Wedel VL, Zephro L. Processes and procedures for trauma analysis. In Wedel VL, Galloway A, editors: *Broken Bones: Anthropological Analysis of Blunt Force Trauma*, 2nd edition. Springfield: Charles C. Thomas; 2014:11-32.

Galloway A, Zephro L. Skeletal trauma analysis of the lower extremity. In: Rich J, Dean DE, Powers RH, eds. *Forensic Medicine of the Lower Extremity: Human Identification and Trauma Analysis of the Thigh, Leg and Foot*. Totowa: Humana Press Inc.; 2005:253-277.

Gibelli D, Mazzarelli D, Porta D, Cattaneo C. Detection of metal residues on bone using SEM-EDS – part II: sharp force injury. *Forensic Science International* 2012;223:91-96.

Gozna ER. *Biomechanics of Musculoskeletal Injury*. Baltimore Williams & Wilkins, 1982.

Griepentrog M, Krämer G, Cappella B. Comparison of nanoindentation and AFM methods for the determination of mechanical properties of polymers. *Polymer Testing* 2013;32(3):455-460.

Griffith AA. The Phenomena of Rupture and Flow in Solids. *Philosophical Transactions Series A* 1920;221:163-198.

Gurdjian ES, Lissner HR, Webster JE. The mechanism of production of linear skull fracture; further studies on deformation of the skull by the stresscoat technique. *Surgery, Gynecology, & Obstetrics* 1947;85:195-210.

Gurdjian ES, Webster JE, Lissner HR. The mechanism of skull fracture. *Radiology* 1950;54:313-339.

Hamer AJ, Strachan JR, Black MM, Ibbotson CJ, Stockley I, Elson RA. Biomechanical properties of cortical allograft bone using a new method of bone strength measurement: A comparison of fresh, fresh-frozen and irradiated bone. *Journal of Bone and Joint Surgery* 1996;78(3):363-368.

Hentschel K, Wescott DJ. Differentiating peri-mortem from postmortem blunt force trauma by evaluating fracture tension surface topography using geographic information systems. *Proceedings of the 67th annual meeting of the American Academy of Forensic Sciences*; February 16–21, 2015; Orlando, FL.

Herrmann NP, Bennett JL. The differentiation of traumatic and heat-related fractures in burned bone. *Journal of Forensic Sciences* 1999;44(3):461-469.

Hertz H. *Miscellaneous Papers*, 1896. Translation by Jones DE, Schott GH. London: Macmillan and Co. Ltd.

Hull D. Influence of stress intensity and crack speed on the fracture surface topography: mirror to mist to macroscopic bifurcation. *Journal of Materials Science* 1996;31:4483-4492.

Hull D. Fractography: *Observing, Measuring and Interpreting Fracture Surface Topography*. Cambridge: Cambridge University Press; 1999.

Isa MI. *Experimental Investigations of Blunt Force Trauma in the Human Skeleton* [PhD dissertation]. East Lansing: Michigan State University; 2020.

Isa MI, Fenton TW, Deland T, Haut RC. Assessing impact direction in 3-point bending of human femora: Incomplete butterfly fractures and fracture surfaces. *Journal of Forensic Sciences* 2018; 63(1):38-46.

Isa MI, Fenton TW, Goots AC, Watson EO, Vaughan PE, Wei F. Experimental investigation of cranial fracture initiation in blunt human head impacts. *Forensic Science International* 2019;300:51-62.

Isa MI, Fenton TW, Antonelli L, Vaughan PE, Wei F. The application of fractography in trauma analysis of complex long bone fractures. *Proceedings of the 72nd Annual Meeting of the American Academy of Forensic Sciences*, February 17-22, 2020; Anaheim, CA.

Isa MI, Fenton TW, Antonelli L, Vaughan PE, Wei F. Investigating reverse butterfly fractures: An experimental approach and application of fractography. *Forensic Science International* 2021; 325:110899.

Ivarsson BJ, Genovese D, Crandall JR, Bolton JR, Untaroiu CD, Bose D. The Tolerance of the Femoral Shaft in Combined Axial Compression and Bending Loading. *Stapp Car Crash Journal* 2009;53:251-290.

James SP, Jasty M, Davies J, Piehler H, Harris WH. A fractographic investigation of PMMA bone cement focusing on the relationship between porosity reduction and increased fatigue life. *Journal of Biomedical Materials Research* 1992;26(5):651-662.

Jani G, Johnson A, Belcher W. Case report: Digital restoration of fragmented non-human skull. *Forensic Science International: Reports* 2020;2:100070.

Jaslow CR. Mechanical properties of cranial sutures. *Journal of Biomechanics* 1990; 23(4):313-321.

Jayaprakash PT, Alarmelmangai S, Pushparani C, Helmi H. Copper brace method: a new technique for reconstructing broken bone fragments. *Journal of Forensic Identification* 2017;67(2):180-189.

Jepsen KJ, Davy DT, Krzypow DJ. The role of the lamellar interface during torsional yielding of human cortical bone. *Journal of Biomechanics* 1999;32:303-10.

Johanns KE, Lee JH, Gao YF, Pharr GM. An evaluation of the advantages and limitations in simulating indentation cracking with cohesive zone finite elements. *Modelling and Simulation in Materials Science and Engineering* 2014;22:015011.

Johnson E. Current developments in bone technology. *Advances in Archeological Method and Theory* 1985;8:157-235.

Kadin Y, Mazaheri M, Zolotarevskiy V, Vieillard C, Hadfield M. Finite elements based approaches for the modelling of radial crack formation upon Vickers indentation in silicon nitride ceramics. *Journal of the European Ceramic Society* 2019;39:4011-4022.

Kang Q, An YH, Friedman RJ. Effects of multiple freezing-thawing cycles on ultimate indentation load and stiffness of bovine cancellous bone. *American Journal of Veterinary Research* 1997;58:1171-1173.

Kaufmann C, Cronin D, Worswick M, Pageau G, Beth A. Influence of material properties on the ballistic performance of ceramics for personal body armour. *Shock and Vibration* 2003;10:51-58.

Kaye B, Randall C, Walsh D, Hansma P. The effects of freezing on the mechanical properties of bone. *Open Bone Journal* 2012;4(1):14-19.

Kieser JA, Tahere J, Agnew C, Kieser DC, Duncan W, Swain MV, Reeves MT. Morphoscopic analysis of experimentally produced bony wounds from low velocity ballistic impact. *Forensic Science, Medicine and Pathology* 2011;7:322-332.

Kimura T, Ogawa K, Kamiya M. Fractography of human intact long bone by bending. *Zeitschrift Rechtsmedizin* 1977;79:301-310.

King C, Birch W. Assessment of maceration techniques used to remove soft tissue from bone in cut mark analysis. *Journal of Forensic Sciences* 2015;60(1):124-135.

Kirchner HP, Gruver RM, Sotter WA. Fracture stress-mirror size relations for polycrystalline ceramics. *Philosophical Magazine* 1976;33(5):775-780.

Klenerman L. Experimental fractures of the adult humerus. *Medical and Biological Engineering* 1969;7:357-364.

Knight CG, Swain MV, Chaudhri MM. Impact of small steel spheres on glass surfaces. *Journal of Materials Science* 1977;12:1573-1586.

Kocer C, Collins RE. Angle of Hertzian cone cracks. *Journal of the American Ceramic Society* 1998;81(7):1736-1742.

Koester KJ, Barth HD, Ritchie RO. Effect of aging on the transverse toughness of human cortical bone: evaluation by R-curves. *Journal of Mechanical Behavior of Biomedical Materials* 2011;4:1504-13.

Koester KJ, Ager JW, Ritchie RO. The True Toughness of Human Cortical Bone Measured with Realistically Short Cracks. *Nature Materials* 2008;7(8):672-77.

Kolsky H. The waves generated by brittle fracture in glass. *Transactions of the Society of Rheology* 1976;20(3):441-454.

Komo L, Grassberger M. Experimental sharp force injuries to ribs: Multimodal morphological and geometric morphometric analyses using micro-CT, macro photography and SEM. *Forensic Science International* 2018;288:189-200.

Konovalenko I, Maruschak P, Prentkovskis O, Junevičius R. Investigation of the rupture surface of the titanium alloy using convolutional neural networks. *Materials* 2018;11:2467.

Kranioti EF. Forensic investigation of cranial injuries due to blunt force trauma: current best practices. *Research and Reports in Forensic Medical* Science 2015;5:25-37.

Kress TA, Porta DJ, Snider JN, et al. Fracture patterns of human cadaver long bones. In: *Proceedings of the International Research Council on the Biomechanics of Impact* (IRCOBI). 1995:155-169.

Kroman AM. *Fracture Biomechanics of the Human Skeleton*. Dissertation. The University of Tennessee, Knoxville [PhD Dissertation], 2007.

Kroman A, Kress T, Porta D. Fracture propagation in the human cranium: a re-testing of popular theories. *Clinical Anatomy* 2011;24:308-318.

L'Abbé, EN, Symes SA, Raymond DE, Ubelaker DH. The Rorschach Butterfly: Understanding Bone Biomechanics Prior to Using Nomenclature in Bone Trauma Interpretations. *Forensic Science International* 2019;299:187-94.

Lankford J. 1982 Indentation microfracture in the Palmqvist crack regime: implications for fracture toughness evaluation by the indentation method. *Journal of Materials Science Letters* 1982;1:493-495.

Lawn BR. Indentation of ceramics with spheres: a century after Hertz. *Journal of the American Ceramics Society* 1998;81(8):1977-1994.

Lawn B, Wilshaw R. Indentation fracture: principles and applications *Journal of Materials Science* 1975;10:1049-1081.

Lillard K, Christensen AM. Fractography of long bones with high velocity projectile trauma. *Forensic Anthropology* 2020;3(3):135-138.

Love JC, Christensen AM. Application of bone fractography to a medical examiner sample: A case series. *Forensic Anthropology* 2018;1(4):221-227.

Love JC, Sanchez LA. Recognition of skeletal fractures in infants: An autopsy technique. *Journal of Forensic Sciences* 2009;54(6):1443-1446.

Lussu P, Marini E. Ultra close-range digital photogrammetry in skeletal anthropology: A systematic review. *PLoS ONE* 2020;15(4):1-29.

Lynch SP, Moutsos S. A brief history of fractography. *Journal of Failure Analysis and Prevention* 2006;6(6):54-69.

Machin R, Biggs M, Brough A, Morgan B. Imaging impact: Can computed tomography fractography determine direction of fracture propagation? *Proceedings of the 73rd annual meeting of the American Academy of Forensic Sciences*; February 15-19, 2021; virtual event.

Madea B, Staak M. Determination of the sequence of gunshot wounds of the skull. *Journal of the Forensic Science Society* 1988;28(5-6):321-328.

Mahfouz MR, Langley NR, Herrmann N, Fatah EEA. Computerized reconstruction of fragmentary skeletal remains for purposes of extracting

osteometric measurements and estimating MNI. *National Institute of Justice Report 2016*-DN-BX-K537; 2016.

Maloul A, Fialkov J, Whyne CM. Characterization of the bending strength of craniofacial sutures. *Journal of Biomechanics* 2013; 46(5):912-917.

Martens M, van Audekercke R, de Meester P, Mulier JC. Mechanical behavior of femoral bones in bending loading. *Journal of Biomechanics* 1986;19(6):443-454.

Martin RB, Burr DB, Sharkey NA. *Skeletal Tissue Mechanics*. New York: Springer; 1998.

McElhaney JH, Fogle JL, Melvin JW, Haynes RR, Roberts VL, Alem NM. Mechanical properties of cranial bone. *Journal of Biomechanics* 1970;3:495-511.

Meadows Jantz L. Skeletal examination and documentation. In Langley NR, Tersigni-Tarrant MA, editors: *Forensic Anthropology: A Comprehensive Introduction*, 2nd edition. Boca Raton: CRC Press; 2017:125-139.

Miyamoto A, Murakami Y. The morphology of the Hertzian cone in plate glass. *Journal of the Society of Materials Science, Japan* 2000;49(8):867-872.

Morgan EF, Unnikrisnan GU, Hussein AI. Bone mechanical properties in healthy and diseased states. *Annual Review of Biomedical Engineering* 2018;20:119-143.

Mudge M, Image-based empirical information acquisition, scientific reliability, and long-term digital preservation for the natural sciences and cultural heritage. Eurographics tutorial, *Cultural Heritage Imaging*, Crete, Greece, 2008: 1-26.

Nalla RK, Kruzic JJ, Kinney JH, Ritchie RO. Effect of aging on the toughness of human cortical bone: evaluation by R-curves. *Bone* 2004;35:1240-1246.

Nalla RK, Kruzic JJ, Kinney JH, Ritchie RO. Mechanistic aspects of fracture and R-curve behavior in human cortical bone. *Biomaterials* 2005a;26:217-231.

Nalla RK, Stolken JS, Kinney JH, Ritchie RO. Fracture in human cortical bone: local fracture criteria and toughening mechanisms. *Journal of Biomechanics* 2005b;38:1517-1525.

National Park Service. *Archaeology Program, Collections Management*. https://www.nps.gov/archeology/collections/mgt_01a.htm. Accessed 18 December 2020.

Nazari A, Bajaj D, Zhang D, Romberg E, Arola D. Aging and the reduction in fracture toughness of human dentin. *Journal of the Mechanical Behavior of Biomedical Materials* 2009;2(5):550-559.

Newman S, Applications of reflectance transformation imaging (RTI) to the study of bone surface modifications, *Journal of Archaeological Science* 2014;53:536-549.

Nyman JS, Roy A, Shen X, Acuna RL, Tyler JH, Wang X. The influence of water removal on the strength and toughness of cortical bone. *Journal of Biomechanics* 2006;39(5):931-938.

Nyman JS, Gorochow LE, Horch A, Uppuganti S, Zein-Sabatto A, Manhard MK, Does MD. Partial removal of pore and loosely bound water by low-energy drying decreases cortical bone toughness in young and old donors. *Journal of the Mechanical Behavior of Biomedical Materials* 2013;22:136-145.

Obertová Z, Leipner A, Messina C, Vanzulli A, Fliss B, Cattaneo C, Sconfienza LM. Postmortem imaging of perimortem skeletal trauma. *Forensic Science International* 2019;302:109921.

Öchner A, Ahmed W (Eds). *Biomechanics of Hard Tissues: Modeling, Testing, and Materials*. Wiley; 2011.

Øilo M, Hardang AD, Ulsund AH, Gjerdet NR. Fractographic features of glass-ceramic and zirconia-based dental restorations fractured during clinical function. *European Journal of Oral Sciences* 2014;122(3):238-244.

Olszta MJ, Cheng X, Jee SS, Kumar R, Kim Y, Kaurman MG, Douglas EP, Gower LB. Bone structure and formation: a new perspective. *Materials Science and Engineering* R 2007;58:77-116.

Palmqvist S. Method att bestamma segheten hos sproda material, sarskilt hardmetaller. *Jernkontorets Annaler* 1957;141:300-307.

Panjabi MM, Krag M, Summers D, Videman T. Biomechanical time-tolerance of fresh cadaveric human spine specimens. *Journal of Orthopaedic Research* 1985;3(3):292-300.

Park J, Fertala A, Tomlinson RE. Naproxen impairs load-induced bone formation, reduces bone toughness, and diminishes woven bone formation following stress fracture in mice. *Bone* 2019;124:22-32.

Passalacqua NV, Fenton TW. Developments in skeletal trauma: blunt force trauma. In: Dirkmaat D, ed. *A Companion to Forensic Anthropology*. Chichester: John Wiley & Sons Ltd, 2012:400-412.

Pechníková M, Porta D, Cattaneo, C. Distinguishing between perimortem and postmortem fractures: Are osteons of any help? *International Journal of Legal Medicine* 2011;125(4), 591-595.

Pechníková M, Mazzarelli D, Poppa P, Gibelli D, Scossa Baggi E, Cattaneo C. Microscopic pattern of bone fractures as an indicator of blast trauma: a pilot study. *Journal of Forensic Sciences* 2015;60(5):1140-1145.

Peterson J, Dechow PC. Material properties of the human cranial vault and zygoma. *The Anatomical Record Part A: Discoveries in Molecular, Cellular, and Evolutionary Biology* 2003; 247A(1):785-797.

Piekarski K. Fracture of bone. *Journal of Applied Physics* 1970;41:215-223.

Pope MH, Outwater JO. The fracture characteristics of bone substance. *Journal of Biomechanics* 1972;5:457-465.

Poundarik AA, Diab T, Sroga GE, Ural A, Boskey AL, et al. Dilatational band formation in bone. *Proceedings of the National Academy of Sciences* 2012;109:19178-83.

Powell BJ, Passalacqua NV, Baumer TG, Fenton TW, Haut RC. Fracture patterns on the infant porcine skull following severe blunt impact. *Journal of Forensic Sciences* 2012;57(2):312-317.

Preston FW. The angle of forking of glass cracks as an indicator of the stress system. *Journal of the American Ceramics Society* 1935;18(6):175-176.

Puppe G. Traumatische todesursachen. In Kutner R. (ed) *Gerichtliche Medizin, Zwölf Vorträge*. Jena: Gustav Fischer, 1903:65-84.

Quatrehomme G, Bolla M, Muller M, Rocca J, Grévin G, Bailet P, Ollier A. Experimental single controlled study of burned bones: contribution of scanning electron microscopy. *Journal of Forensic Sciences* 1998;43(2):417-422.

Quatrehomme G, Piercecchi-Marti MD, Buchet L, Alunni V. Bone beveling cause by blunt trauma: a case report. *International Journal of Legal Medicine* 2016;130(3):771-775.

Quinn GD. *Recommended Practice Guide: Fractography of Ceramics and Glasses, 3rd Ed*. National Institute of Standards and Technology (NIST) Special Publication 960-16e3; 2007;2016;2020.

Quinn JB. Extrapolation of fracture mirror and crack-branch sizes to large dimensions in biaxial strength tests of glass. *Journal of the American Ceramics Society* 1999;82(8):2126-2132.

Quinn JB, Schultheis LW, Schumacher GE. A tooth broken after laryngoscopy: Unlikely to be caused by the force applied by the anesthesiologist. *Anesthesia and Analgesia* 2005;100: 594-596.

Rabl W, Haid C, Krismer M. Biomechanical properties of the human tibia: fracture behavior and morphology. *Forensic Science International* 1996;83(1):39-49.

Rainwater CW, Congram D, Symes SA, Passalacqua NV. Fracture surface characteristics for the interpretation of perimortem blunt force fractures in bone. *Proceedings of the 71st annual meeting of the American Academy of Forensic Sciences*. February 19-23, 2019; Baltimore, MD.

Réaumur de RA. *L'Art de Convertir le Fer Forgé en Acier, et L'Art d'Adocir le Fer Fondu*. Paris: Michel Brunet; 1722. Translation by Sisco AG: *Réaumur's Memoirs on Steel and Iron*. University of Chicago Press, 1956.

Reber SL, Simmons T. Interpreting injury mechanisms of blunt force trauma from butterfly fracture formation. *Journal of Forensic Sciences* 2015;60(6):1401-1411.

Reilly DT, Burstein AH. The elastic and ultimate properties of compact bone tissue. *Journal of Biomechanics* 1975; 8:393-405.

Reilly DT, Burstein AH, Frankel VH. The elastic modulus for bone. *Journal of Biomechanics* 1974;7: 271-275.

Rho JY, Pharr GM. Effects of drying on the mechanical properties of bovine femur measured by nanoindentation. *Journal of Materials Science: Materials in Medicine* 1999;10(8):485–488.

Rice RW. Fracture topography of ceramics. In: Fréchette V, LaCourse W, Burlick VL, eds, *Surface Interfaces of Glasses and Ceramics*. New York: Plenum; 1973:439-472.

Rice RW. Ceramic fracture features, observations, mechanism and uses. *Fractography of Ceramic and Metal Failures*, Special Technical Publication 827. West Conshohocken, PA: American Society for Testing and Materials, 1984:5-103.

Richter HG, Kerkhof F. Stress Wave Fractography. In Bradt RC, Tressler RE eds: *Fractography of Glass*. New York: Plenum; 1994:75-109.

Rickman JM, Smith MJ. Scanning electron microscope analysis of gunshot defects to bone: An underutilized source of information on ballistic trauma. *Journal of Forensic Sciences* 2014;59(6), 1473-1486.

Rickman JM, Shackel J. A novel hypothesis for the formation of conoidal projectile wounds in sandwich bones. *International Journal of Legal Medicine* 2019a;133:501-519.

Rickman JM, Shackel J. Crack propagation through sandwich bones due to low-velocity projectile impact. *International Journal of Legal Medicine* 2019b;133:1443-1459.

Ritchie RO, Koester KJ, Ionova S, Yao W, Lane NF, and Ager III, JW. Measurements of the toughness of bone: A tutorial with special reference to small animal studies. *Bone* 2008;43(5) 798-812. See also Erratum, *Bone* 2010;47(3):706.

Roebuck B, Bennett E., Lay L, Morrell R. *Palmqvist Toughness for Hard and Brittle Materials*. National Physical Laboratory Good Practice Guide No 9, Middlesex UK; 2008.

Saha S, Hayes WC. Relations between tensile impact properties and microstructure of compact bone. *Calcified Tissue Research* 1977;24(1):65-72.

Saville PA, Hainsworth SV, Rutty GN. Cutting crime: The analysis of the "uniqueness" of saw marks on bone. *International Journal of Legal Medicine* 2007;121(5):349–-57.

Schardin H, Struth W. Neuere Ergibnisse der Funken-kinemographie. *Zeitschrift Technisch Physik* 1937;18:474-477.

Scherrer SS, Quinn GD, Quinn JB. Fractographic failure analysis of a Procera AllCeram Crown using stereo and scanning electron microscopy. *Dental Materials* 2008;24(8):1107-1113.

Scherrer SS, Quinn JB, Quinn GD. Fractography of dental restorations. *Key Engineering Materials* 2009;409:72-80.

Schroer C, Advanced imaging tools for museum and library conservation and research, *American Society of Information Science and Technology* 2012;38(3):38-42.

Scientific Working Group for Forensic Anthropology (SWGANTH). *Documentation, Reporting and Testimony*; 2012:1-8.

Shah FA, Ruscsák K, Palmquist A. 50 years of scanning electron microscopy of bone—a comprehensive overview of the important discoveries made and insights gained into bone material properties in health, disease, and taphonomy. *Bone Research* 2019;7(1):1-15.

Sharir A, Barak MM, Shahar R. Whole Bone Mechanics and Mechanical Testing. *Veterinary Journal* 2008;177(1): 8-17.

Shetty D, Rosenfield A, Duckworth W. Crack branching in ceramic disks subjected to biaxial flexure. *Communications of the American Ceramics Society* 1983:C10-C12.

Smith RL, Sandland GE. An accurate method of determining the hardness of metals, with particular reference to those of a high degree of hardness. *Proceedings of the Institution of Mechanical Engineers* 1922;1:623-641.

Spatola BF. Atypical gunshot and blunt force injuries: Wounds along the biomechanical continuum. In Passalacqua NV, Rainwater CW: *Skeletal Trauma Analysis: Case Studies in Context*. New York: John Wiley and Sons, Ltd; 2015:7-26.

Spitz W. *Spitz and Fisher's Medicolegal Investigation of Death: Guidelines for the Application of Pathology to Crime Investigation*. Springfield: Charles C. Thomas, 1993.

Steadman DW, DiAntonio LL, Wilson JJ, Sheridan KE, Tammariello SP. The effects of chemical and heat maceration techniques on the recovery of nuclear and mitochondrial DNA from bone. *Journal of Forensic Sciences* 2006;51(1):11-17.

Sun X, Li L, Guo Y, Zhao H, Zhang S, Yu Y, Wu D, Liu H, Yu M, Shi D, Liu Z, Zhou M, Ren L, Fu L. Influences of organic component on mechanical property of cortical bone with different water content by nanoindentation. *AIP Advances* 2018;8(3):035003.

Symes SA, Berryman HE, Smith OC. Saw marks in bone: Introduction and examination of residual kerf contour. In Reichs KJ, editor: *Forensic Osteology: Advances in the Identification of Human Remains*. Springfield: Charles C. Thomas; 1998:389-409.

Symes SA, Williams JA, Murray EA, Hoffman JM, Holland TD, Saul JM. Taphonomic context of sharp-force trauma in suspected cases of human mutilation and dismemberment. In Haglund WD, Sorg M, editors, *Advances in Forensic Taphonomy: Method, Theory, and Archaeological Perspectives*. Boca Raton: CRC Press; 2002:403-434.

Symes SA, L'Abbe EN, Chapman EN, Wolff I, Dirkmaat DC. Interpreting traumatic injury to bone in medicolegal investigations. In: Dirkmaat DC, ed. *A Companion to Forensic Anthropology*. Chichester: John Wiley & Sons Ltd; 2012: 340-389.

Symes SA, L'Abbe EN, Stull KE, Lacroix M, Pokines JT. Taphonomy and the timing of bone fractures in trauma analysis. In: Pokines JT, ed. *Manual of Forensic Taphonomy*. Boca Raton, FL: CRC Press; 2014:341-366.

Thompson JY, Anusavice KJ, Naman A, Morris HE. Fracture surface characterization of clinically failed all-ceramic crowns. *Journal of Dental Research* 1994;73(12):1824–1832.

Thurner PJ. Atomic force microscopy and indentation force measurement of bone. *Wiley Interdisciplinary Reviews: Nanomedicine and Nanobiotechnology* 2009;1(6):624-649.

Topoleski LDT, Ducheyne P, Cukler JM. A fractographic analysis of in vivo poly(methylmethacrylate) bone cement failure mechanisms. *Journal of Biomedical Materials Research* 1990;24(2):135-154.

Torimitsu S, Nishida Y, Takano T, Koizumi Y, Hayakawa M, Yajima D, Inokuchi G, Makino Y, Motomura A, Chiba F, Iwase H. Effects of the freezing and thawing process on biomechanical properties of the human skull. *Legal Medicine* 2014;16(2):102-105.

Tsirk A. Fracture markings from flake splitting. *Journal of Archaeological Science* 2010;37(8):2061-2065.

Tsirk A, Parry WJ. Fractographic evidence for liquid on obsidian tools. *Journal of Archaeological Science* 2000;27(11): 987-991.

Tsopanidis S, Herrero Moreno R, Osovski S. Toward quantitative fractography using convolutional neural networks. *Engineering Fracture Mechanics* 2020;231:106992.

Turner CH, Burr DB. Experimental techniques for bone mechanics. In Cowin SC, editor: *Bone Mechanics Handbook*, 2nd edition. Boca Raton: CRC Press; 2001, 7-1—7-36.

van Haaren EH, van der Zwaard BC, van der Veen AJ, Heyligers IC, Wuisman PIJM, Smit TH. Effect of long-term preservation on the mechanical properties of cortical bone in goats. *Acta Orthopaedica* 2008;79(5):708-716.

Varner JR. Using replicas in fractography of glass and ceramics. In Varner J, Wightman M, editors: *Fractography of Glasses and Ceramics, 6th edition*. Ceramic Transactions, Vol. 230, Jacksonville FL: American Ceramic Society; 2012:299-308.

Varvani-Farahani A, Najmi H. A damage assessment model for cadaveric cortical bone subjected to fatigue cycles. *International Journal of Fatigue* 2010;32:420-27.

Vashishth D, Behiri J, Bonfield W. Crack growth resistance in cortical bone: concept of microcrack toughening. *Journal of Biomechanics* 1997;30:763-9.

Vashishth D, Tanner KE, Bonfield W. Contribution, development and morphology of microcracking in cortical bone during crack propagation. *Journal of Biomechanics* 2000;33(9): 1169-1174.

Vermeij EJ, Zoon PD, Chang SBCG, Chang SBCG, Keereweer I, Pieterman R, Gerretsen RRR. Analysis of microtraces in invasive traumas using SEM/EDS. *Forensic Science International* 2012;214(1):96-104.

Viel G, Gehl A, Sperhake JP. Intersecting fractures of the skull and gunshot wounds – Case reports and literature review. *Forensic Science, Medicine and Pathology* 2009;5(1):22-27.

Wang X, Shen X, Li X, Agrawal M. Age related changes in the collagen network and toughness of bone. *Bone* 2002;31(1):1-7.

Warren PD, Hills DA, Dai DN. Mechanics of Hertzian cracking. *Tribiology International* 1995;28(6):357-362.

Weiner S, Wagner HD. The material bone: structure-mechanical function relations. *Annual Review of Materials Science* 1998;28:271-298.

Wheatley BP. Perimortem or postmortem bone fractures? An experimental study of fracture patterns in deer femora. *Journal of Forensic Sciences* 2008;53(1):69-72.

Wieberg DAM, Wescott DJ. Estimating the timing of long bone fractures: Correlation between the postmortem interval, bone moisture content, and blunt force trauma fracture characteristics. *Journal of Forensic Sciences* 2008;53(5):1028-1034.

Wise LM, Wang Z, Grynpas. The use of fractography to supplement analysis of bone mechanical properties in different strains of mice. *Bone* 2007;41(4):620-630.

Yoganandan N, Pintar FA, Sances AJ, Walsh PR, Ewing CL, Thomas DJ, Synder RG. Biomechanics of skull fracture. *Journal of Neurotrauma* 1995;12(4):659-668.

Zaera R, Sánchez-Gálvez V. Analytical modelling of normal and oblique ballistic impact on ceramic/ metal lightweight armours. *International Journal of Impact Engineering* 1998;21 (3):133-148.

Zapffe CA, M. Clogg, Jr. M. Fractography—A new tool for metallurgical research. *Transactions of the American Society of Metals* 1945(34):71-107.

Zukas JA. Penetration and perforation of solids. In Zukas JA, Nicholas T, Swift HF, Greszczuk LB, Curran DR (eds): *Impact Dynamics*, John Wiley and Sons, Inc.; 1982:155-214.